DISSERTATION

THE ECOLOGICAL IMPACTS OF AGRIVOLTAICS IN SEMI-ARID GRASSLANDS

Submitted by

Christopher Ryan Toy

Department of Soil and Crop Science

In partial fulfillment of the requirements

For the Degree of Doctor of Philosophy

Colorado State University

Fort Collins, Colorado

Fall 2025

Doctoral Committee:

Advisor: Meagan E. Schipanski

Steve Fonte
Alan Knapp
Stephanie Malin

ABSTRACT

THE ECOLOGICAL IMPACTS OF AGRIVOLTAICS IN SEMI-ARID GRASSLANDS

The rapid expansion of solar energy infrastructure onto agricultural lands presents a critical challenge: how to meet renewable energy goals without compromising ecosystem integrity. While agrivoltaic systems theoretically enable multifunctional landscapes providing both energy and ecosystem services, comprehensive understanding of their ecological impacts remains limited. I conducted multi-scale assessments of ecosystem responses to single-axis tracking solar arrays in Colorado's semi-arid grasslands. Through controlled experiments at Jack's Solar Garden and landscape surveys across nine installations, I examined how solar infrastructure affects carbon cycling, plant communities, arthropod populations, and forage productivity and quality. In this dissertation I discuss how solar energy infrastructure and agrivoltaic management affect a variety of ecosystem functions and how these findings can inform land management, regulatory policies, solar array design, and future research.

My research revealed that solar arrays create distinct microclimates that spatially reorganize ecosystem functions at small scales. Beneath panels, reduced light availability and precipitation interception decreased soil water content relative to open areas, resulting in 27-30% lower aboveground productivity and 31% reduced soil CO_2 flux. However, carbon stocks in surface soils (0-15 cm) increased by 25% under panels three years post-installation, suggesting enhanced carbon stabilization despite lower productivity. Edge microclimates, receiving redistributed precipitation from panel runoff, showed higher soil moisture than open areas and maintained comparable productivity while supporting intermediate carbon cycling rates. Notably,

belowground net primary productivity in open areas between panels exceeded under microclimates by 59%, with roots shifting allocation patterns under panels to favor deeper soil layers (50% at 15-30 cm versus 30% in open areas).

Vegetation management strategies interacted strongly with solar microclimates to influence ecosystem service provision. While native seed mixes were intended to enhance pollinator habitat and biodiversity, establishment challenges led to dominance by non-native rhizomatous grasses (86% cover) across native treatments. Pasture vegetation produced 65-100% higher aboveground biomass than native treatments. Floral resources were concentrated in open areas between panels, which supported 2.7-fold more flowers than under-panel positions, though irrigation tripled flower production beneath panels. Forage quality showed complex spatial patterns: despite 30% lower forage production under panels, the quality of forage was higher due to greater concentrations of crude protein.

Landscape-scale surveys across nine commercial solar installations 5-8 years post-construction revealed a surprising disconnect between plant and arthropod communities. Despite 19-47% higher plant species richness, 21-37% greater Shannon diversity, and 1-15% higher total vegetative cover in solar arrays compared to adjacent control sites, arthropod communities showed consistent negative responses. Flying arthropod abundance declined by 48% overall, with Coleoptera (-65%) and pollinators (-50%) showing the strongest reductions. Ground-dwelling arthropods decreased by 27%, driven primarily by mixed feeders (-71%) and predators (-50%), while only Hymenoptera (primarily ants) showed a positive response (non-significant). This decoupling of plant diversity from arthropod abundance suggests that physical infrastructure effects and/or typical solar array management through mowing may override the benefits of enhanced plant resources.

These findings demonstrate that agrivoltaic systems create novel ecosystems characterized by spatial heterogeneity in resource availability and ecological processes. While solar infrastructure imposes clear constraints on certain ecosystem components—particularly mobile arthropod communities—the reorganization of plant productivity, carbon cycling, and forage resources suggests opportunities for management optimization. The persistence of ecosystem services depends critically on recognizing and working with the inherent spatial heterogeneity created by solar arrays rather than attempting to homogenize management across microclimates. Strategic approaches that leverage high-productivity edge zones for forage production, maintain open areas for pollinator resources, and utilize under-panel areas for carbon sequestration could optimize the multifunctional potential of grassland agrivoltaic landscapes. I hope that this work will help guide responsible stewardship of our working lands for future generations, ensuring that renewable energy expansion enhances rather than diminishes the ecological foundation upon which both human and natural communities depend.

ACKNOWLEDGEMENTS

First, I would like to thank my parents for supporting me throughout my life. I never would have been able to make it this far without the foundation they laid for me. Thank you to the InTERFEWS program and the Soil and Crop Science Department for introducing me to so many other amazing graduate students. My peers have easily taught me as much or more than I ever learned in classes. Thank you to the members of my graduate committee, Steve Fonte, Alan Knapp, and Stephanie Malin for exposing me to new ideas and broadening my idea of what my dissertation could entail. Thank you to all of the undergrads that contributed countless hours helping me collected the data presented here, especially Nelson Heider-Kuhn, Brittani Meis, and Nick Skaric. Thank you to everyone at Jack's Solar Garden and the Colorado Agrivoltaic Learning Center for helping get my research off the ground and giving me lots of opportunities to tell people about my work.

Thank you to Meagan, my advisor, for giving me the opportunity to pursue what must have by all means looked like a strange passion project when we started down this road. I hope that you had the opportunity to learn a bit from all our work together too. Thank you for guiding me through the maze of pitfalls I encountered from experimental design, to data collection, lab management, and statistical analysis. Thank you for creating a community in your lab where all of your students can collaborate and learn from each other. None of this happens in a vacuum, and I know I couldn't have done it without you.

This material is based upon work supported in part by the National Science Foundation under Grant No. 1828902. Any opinions, findings, and conclusions or recommendations

expressed in this material are those of the author(s) and do not necessarily reflect the views of the National Science Foundation.

This research was supported in part by the intramural research program of the U.S. Department of Agriculture, National Institute of Food and Agriculture, AFRI award number 2023-67011-40493. The findings and conclusions in this preliminary publication have not been formally disseminated by the U.S. Department of Agriculture and Should not be construed to represent any agency determination or policy.

To my Melissa, my wife, thank you for always walking by my side and sharing everything that God has given us. You have held me aloft countless times through struggles, taught me to be a better man, and made even the sweetest moments a little bit sweeter by being there to share them with me. To Valentine, my son, thank you for reminding me just how much beauty and love there really is in this life. This work is for you. I pray that I can make the world just a little bit more beautiful, the way you see it.

TABLE OF CONTENTS

CHAPTER 1: INTRODUCTION

The global transition to renewable energy represents one of humanity's most significant land use transformations of the 21st century. As solar photovoltaic capacity expands at approximately 73% annually, reaching 1,177 GW globally in 2022 (IRENA, 2023), vast areas of agricultural and natural lands are being converted to host energy infrastructure. In the United States alone, meeting decarbonization goals will require 5.7 million acres of solar development by 2035, with 70-80% expected on agricultural lands (DOE, 2021; Walston et al., 2022) which amounts to roughly 0.5% of the total area currently used for agriculture in the US. This unprecedented landscape transformation occurs at the intersection of two critical global challenges: climate change mitigation through renewable energy deployment and the biodiversity crisis threatening ecosystem functioning worldwide.

Semi-arid grasslands have emerged as focal points for solar development due to their high solar irradiance, relatively flat topography, and perceived low agricultural value. However, these ecosystems provide essential services including carbon sequestration, livestock forage, pollination biodiversity conservation, and nutrient cycling (Milne et al., 2015; Swinton et al., 2007). Grasslands cover 14% of Earth's terrestrial surface, account for about 16% of global net primary production (Wang et al., 2022), and support the majority of global livestock production. The rapid conversion of these working landscapes to energy production raises fundamental questions about trade-offs between climate mitigation strategies and ecosystem integrity.

Agrivoltaic systems—the co-location of solar photovoltaic panels with agricultural production—have emerged as a promising approach to address competing demands for land while potentially enhancing both energy and food security (Walston et al., 2022; Barron-Gafford

et al., 2019). By maintaining vegetation and potentially agricultural production beneath and between solar panels, these systems theoretically enable multifunctional landscapes that provide both renewable energy and ecosystem services. However, solar infrastructure fundamentally alters environmental conditions through multiple mechanisms: panels intercept and redistribute solar radiation creating light gradients from <10% to >90% of ambient conditions (Armstrong et al., 2016; Li et al., 2025), concentrate precipitation at drip edges while intercepting moisture beneath panels (Elamri et al., 2018; Lambert et al., 2021), and modify temperature and wind patterns (Marrou et al., 2013).

Early foundational work on the environmental impacts of solar energy identified potential habitat loss, soil erosion, and hydrological changes as challenges (Hernandez et al., 2014). Despite expanding research, critical knowledge gaps persist about how solar infrastructure affects ecosystem functioning. Most existing studies examine single ecosystem services or taxonomic groups in isolation, preventing understanding of system-level responses and cross-scale interactions (Bennun et al., 2023). The application of the ecosystem service bundle framework, which recognizes that services often show non-random associations across landscapes (Raudsepp-Hearne et al., 2010)—to agrivoltaic systems remains unexplored.

Furthermore, research has only recently begun to focus more on the role of single-axis tracking systems that now dominate utility-scale installations. Unlike fixed-tilt arrays that create static shade patterns, tracking systems produce dynamic light environments as panels rotate to follow the sun's path (Sturchio et al., 2022). In one example, researchers found that despite 38% light reduction, grassland productivity decreased only 6-7% due to photosynthetic plasticity of C3 grasses (Kannenberg et al., 2023). However, this research focused primarily on plant

physiological responses, leaving questions about community composition, multi-trophic interactions, and belowground processes largely unexplored.

This dissertation addresses these knowledge gaps through an integrated assessment of ecosystem responses to single-axis tracking solar arrays in Colorado's semi-arid grasslands, where 80,000 acres of solar development are projected by 2030 (Colorado Energy Office, 2023). By employing complementary approaches—from controlled experiments to landscape-level surveys with proper controls—this research provides comprehensive understanding of the ecological trade-offs and opportunities created by renewable energy infrastructure.

The dissertation comprises three interconnected studies:

Chapter 2 focuses specifically on carbon cycling dynamics at the same experimental site, quantifying how solar microclimates affect above and belowground net primary productivity, soil organic carbon stocks, and soil CO_2 flux across three years with varying precipitation. This chapter examines the mechanisms by which altered light and moisture regimes affect carbon inputs and outputs, testing whether agrivoltaic systems can maintain soil carbon sequestration services despite altered environmental conditions.

Chapter 3 evaluates trade-offs and synergies among six ecosystem services within an experimental agrivoltaic array at Jack's Solar Garden, examining how vegetation management (native species establishment versus existing pasture) and irrigation interact with solar-induced microclimates to affect pollinator resources, forage production, biodiversity, and carbon sequestration. Using the ecosystem service bundle framework (Bennett et al., 2009; Finney et al., 2017), this chapter tests whether active management can optimize multiple services simultaneously or whether spatial heterogeneity itself provides the key to multifunctionality.

Chapter 4 provides a landscape-scale assessment across nine solar installations 5-8 years post-construction, simultaneously examining plant communities, flying and ground-dwelling arthropod populations, root biomass, and soil properties. Using paired comparisons with control sites managed identically to pre-installation conditions, this chapter reveals how solar infrastructure affects multiple trophic levels and whether enhanced plant diversity translates to improved habitat for arthropod communities.

Together, these studies advance understanding of how renewable energy infrastructure transforms ecological systems in semi-arid grasslands, providing essential evidence for developing sustainable land use strategies. Society is accelerating toward renewable energy goals while facing a biodiversity crisis. Ensuring that solutions to climate change don't inadvertently compromise ecosystem integrity represents one of the defining challenges of our time.

LITERATURE CITED

Armstrong, A., Ostle, N. J., & Whitaker, J. (2016). Solar park microclimate and vegetation management effects on grassland carbon cycling. *Environmental Research Letters*, 11(7), 074016.

Barron-Gafford, G. A., Pavao-Zuckerman, M. A., Minor, R. L., Sutter, L. F., Barnett-Moreno, I., Blackett, D. T., Thompson, M., Dimond, K., Gerlak, A. K., Nabhan, G. P., & Macknick, J. E. (2019). Agrivoltaics provide mutual benefits across the food–energy–water nexus in drylands. *Nature Sustainability*, 2(9), 848–855.

Bennett, E. M., Peterson, G. D., & Gordon, L. J. (2009). Understanding relationships among multiple ecosystem services. *Ecology Letters*, 12(12), 1394–1404.

Bennun, L., van Bochove, J., Ng, C., Fletcher, C., Wilson, D., Phair, N., & Carbone, G. (2023). Existing evidence on the effects of photovoltaic panels on biodiversity: A systematic map with critical appraisal of study validity. *Environmental Evidence*, 12, 22.

Colorado Energy Office. (2023). *Colorado renewable energy outlook: Solar development projections 2030*. Colorado Energy Office, Denver, CO.

DOE (U.S. Department of Energy). (2021). *Solar Futures Study*. Office of Energy Efficiency and Renewable Energy, Washington, DC. DOE/EE-2310.

Elamri, Y., Cheviron, B., Lopez, J. M., Dejean, C., & Belaud, G. (2018). Water budget and crop modelling for agrivoltaic systems: Application to irrigated lettuces. *Agricultural Water Management*, 208, 440–453.

Finney, D. M., Murrell, E. G., White, C. M., Baraibar, B., Barbercheck, M. E., Bradley, B. A., Cornelisse, S., Hunter, M. C., Kaye, J. P., Mortensen, D. A., Mullen, C. A., & Schipanski, M. E. (2017). Ecosystem services and disservices are bundled in simple and diverse cover cropping systems. *Agricultural & Environmental Letters*, 2(1), 170033.

Hernandez, R. R., Easter, S. B., Murphy-Mariscal, M. L., Maestre, F. T., Tavassoli, M., Allen, E. B., Barrows, C. W., Belnap, J., Ochoa-Hueso, R., Ravi, S., & Allen, M. F. (2014). Environmental impacts of utility-scale solar energy. *Renewable and Sustainable Energy Reviews*, 29, 766–779.

IRENA (International Renewable Energy Agency). (2023). *Renewable capacity statistics 2023*. IRENA, Abu Dhabi.

Kannenberg, S. A., Sturchio, M. A., Venturas, M. D., & Knapp, A. K. (2023). Grassland carbon-water cycling is minimally impacted by a photovoltaic array. *Communications Earth & Environment*, 4(1), 238.

Lambert, Q., Bischoff, A., Cueff, S., Cluchier, A., & Gros, R. (2021). Effects of solar parks on soil quality, microclimate, CO2 effluxes, and vegetation under a Mediterranean climate. *Land Degradation & Development*, 32(18), 5190–5202.

Li, Y., Armstrong, A., Simmons, C., Krasner, N. Z., & Hernandez, R. R. (2025). Ecological impacts of single-axis photovoltaic solar energy with periodic mowing on microclimate and vegetation. *Frontiers in Sustainability*, 6, 1497256.

Marrou, H., Guilioni, L., Dufour, L., Dupraz, C., & Wery, J. (2013). Microclimate under agrivoltaic systems: Is crop growth rate affected in the partial shade of solar panels? *Agricultural and Forest Meteorology*, 177, 117–132.

Milne, E., Banwart, S. A., Noellemeyer, E., Abson, D. J., Ballabio, C., Bampa, F., Bationo, A., Batjes, N. H., Bernoux, M., Bhattacharyya, T., Black, H., Buschiazzo, D. E., Cai, Z., Cerri, C. E., Cheng, K., Compagnone, C., Conant, R., Coutinho, H. L. C., de Brogniez, D., ... Zheng, J. (2015). Soil carbon, multiple benefits. *Environmental Development*, 13, 33–38.

Raudsepp-Hearne, C., Peterson, G. D., & Bennett, E. M. (2010). Ecosystem service bundles for analyzing tradeoffs in diverse landscapes. *Proceedings of the National Academy of Sciences*, 107(11), 5242–5247.

Sturchio, M. A., Macknick, J. E., Barron-Gafford, G. A., Chen, A., Alderfer, C., Condon, K., Hajek, O. L., Miller, B., Pauletto, B., Siggers, J. A., & Knapp, A. K. (2022). Grassland productivity responds unexpectedly to dynamic light and soil water environments induced by photovoltaic arrays. *Ecosphere*, 13(12), e4334.

Swinton, S. M., Lupi, F., Robertson, G. P., & Hamilton, S. K. (2007). Ecosystem services and agriculture: Cultivating agricultural ecosystems for diverse benefits. *Ecological Economics*, 64(2), 245–252.

Walston, L. J., Li, Y., Hartmann, H. M., Macknick, J., Hanson, A., Nootenboom, C., Lonsdorf, E., & Hellmann, J. (2022). Modeling the ecosystem services of native vegetation management practices at solar energy facilities in the Midwestern United States. *Ecosystem Services*, 56, 101456.

Wang, L., Jiao, W., MacBean, N., Rulli, M. C., Manzoni, S., Vico, G., & D'Odorico, P. (2022). Dryland productivity under a changing climate. *Nature Climate Change*, 12(11), 981–994.

CHAPTER 2: IMPACT OF SOLAR ENERGY INFRASTRUCTURE AND ECOVOLTAIC MANAGEMENT ON SEMI-ARID GRASSLAND CARBON CYCLING[1]

2.1 Summary

The expansion of solar photovoltaic (PV) infrastructure into semi-arid grasslands has the potential to alter carbon (C) cycling processes. We conducted a three-year field experiment in Colorado, USA to investigate the effects of PV panel microclimates and ecovoltaic management practices (interseeding native species and irrigation) on above and belowground net primary productivity (ANPP and BNPP), soil organic carbon (SOC) stocks, and soil CO_2 flux. Total SOC stocks from 0-30cm did not differ between baseline and 3 years after PV installation, but the microclimate directly under the PV panels (Under) had greater SOC and standing root biomass, and lower soil respiration rates than areas between rows (Open) or on the panel edges of the PV systems. Interannual precipitation variability modulated PV microclimate effects, with the Open microclimate having significantly higher BNPP during the wettest year and the Under microclimate having significantly lower BNPP during the driest year. The Under microclimate also promoted a deeper root distribution, potentially enhancing subsoil C inputs. Irrigation had limited effects on ANPP and BNPP, but increased soil CO_2 flux. Interseeding native plants did not significantly influence C cycling compared to maintaining existing pasture vegetation. Our findings highlight the complex interactions between PV infrastructure, microclimate, and precipitation in driving grassland C cycling in the years immediately following installation. Low-

[1] Toy, C., Heider-Kuhn, N., Schipanski, M. (2025). Impact of solar energy infrastructure and ecovoltaic management on semi-arid grassland carbon cycling. *Environmental Research Communications,* 7, 105005. https://doi.org10.1088/2515-7620/ae0b1d

impact PV installation methods that preserve vegetation and minimize disturbance appear crucial for maintaining soil C sequestration services. Ecologically-informed PV array design and management strategies may help optimize C cycling co-benefits in semi-arid grasslands and longer-term studies across diverse sites are needed to fully understand the environmental impacts of this emerging land use.

2.2 Introduction

Global energy demand is growing, driven largely by economic development, urbanization, electrification of heating and transportation, and the rise of new, energy intensive computing industries such as artificial intelligence and cryptocurrency mining (IEA 2024). In addition, the consequences of climate change have highlighted the need to transition from an energy system dominated by fossil fuels to an energy system with a greater proportion of renewable energy sources (IPCC 2022). Solar photovoltaic (PV) electricity generation has emerged as a leading technology in this transition due to system scalability, competitive costs, and low carbon (C) footprint (Dada and Popoola 2023). As nations around the world seek to diversify and decarbonize their energy systems, the deployment of solar PV infrastructure has accelerated worldwide (IRENA 2024). Large-scale solar installations have been preferentially sited in regions with high solar irradiance, including semi-arid grasslands, due to the low levelized cost of electricity (LCOE) in these regions (ESMAP 2020).

While these grasslands provide favorable conditions for solar PV due to their open landscapes and abundant sunlight, this expansion introduces new land-use dynamics that affect local ecosystems (Hernandez *et al* 2014; Walston *et al* 2016). Unlike siting solar PV on rooftops or degraded lands, siting solar PV on grasslands involves potential trade-offs between energy production and ecosystem services. Understanding how solar PV infrastructure interacts with the

ecosystem in these regions is essential for the successful integration of solar PV with grassland ecosystems and the communities that depend on the ecosystem services they provide.

Carbon cycling and sequestration are key ecosystem services provided by semi-arid grasslands. These services are relevant not only for climate regulation, but also as support for other valuable services such as nutrient cycling, erosion resistance, and water management (Milne *et al* 2015). Despite their relatively low productivity, semi-arid grasslands are vast, covering about 14% of the terrestrial surface and accounting for about 16% of global net primary production (NPP) (Wang *et al* 2022). These ecosystems store a substantial proportion of their C underground, particularly in soil organic carbon (SOC), making them vital for long-term C storage and climate regulation. Grasslands are also some of the most economically important ecosystems on earth because they support the majority of agricultural production either as range or pasture to graze livestock animals or through conversion to agricultural crop production.

One of the primary mechanisms by which solar PV influences grassland C cycling is via the creation of distinct microclimates beneath and around solar panels. Solar panels intercept radiation by design, creating bands of shade across the landscape. The panels are also impervious, meaning any precipitation that falls on a panel is redirected and concentrated as runoff onto the lower edge. This creates substantial heterogeneity in available moisture, radiation, and temperatures at small spatial scales, which has been observed to alter C cycling processes such as photosynthesis and net ecosystem exchange in grasslands that host solar PV infrastructure (Armstrong *et al* 2016). The exact dimensions of these microclimates can vary significantly based on factors such as tracking system (or lack thereof), row spacing, panel size, mounting height, and site latitude.

The main C input to grasslands is NPP. A number of studies have examined the influence of solar PV microclimates on aboveground productivity (Sturchio *et al* 2022; Adeh *et al* 2018), however little to no attention has been given to the belowground productivity of these systems. This is a significant gap as on average 67% of grassland biomass is produced belowground (Ma *et al* 2021). Unfortunately, aboveground productivity is often a poor predictor of belowground productivity in semi-arid systems because many species will preferentially allocate resources belowground under dry conditions (Eziz *et al* 2017), and increase rooting depth to access water deeper in the soil profile (Guswa 2010).

Soil CO_2 flux is the main source of C outputs in low disturbance grasslands. Like NPP, it is also highly sensitive to climatic variation, specifically soil temperature and moisture content which have a strong positive correlation with flux (Curiel Yuste *et al* 2007). Only one previous study has quantified the impact of solar PV microclimates on soil CO_2 flux (Lambert *et al* 2024). Shade from solar panels has been shown to reduce soil temperatures (Marrou *et al* 2013), which may lead to reduced CO_2 flux. Precipitation redistribution by panels has variable effects on soil moisture (Sturchio *et al* 2024a), potentially increasing flux where precipitation is concentrated or reducing flux where it is intercepted.

In addition to untangling the effects of solar PV infrastructure on grassland C cycling, we explored the impact of two ecovoltaic management practices, interseeding native species and irrigation, on C cycling within these systems. There is a large body of work to support ecosystem service benefits from revegetation and interseeding with native species in degraded grasslands (Tilman *et al* 2006; Rey Benayas *et al* 2009; Wratten *et al* 2012), however the benefits are less clear in healthy, established pastures, such as our study site, which are increasingly being used to host solar PV infrastructure. The productivity of semi-arid grasslands is generally more limited

by water availability than light (Sturchio and Knapp 2023) meaning that irrigation usually has a positive impact on productivity, however the microclimatic conditions of solar PV creates uncertainty around the effectiveness of irrigation practices in an ecovoltaic setting.

The objective of this study was to determine how solar PV microclimates and ecovoltaic management practices (interseeding native species and supplying irrigation) affect SOC stocks, NPP, and soil CO_2 flux (Figure 2.1). We expected that 1) the microclimate Under solar panels would have reduced NPP and soil CO_2 flux due to light and water interception, reducing SOC stocks, and the Edge microclimates where precipitation is redirected would have increased NPP and soil CO_2 flux, thereby increasing SOC stocks; 2) interseeding native species and their associated management regime would decrease ANPP but increase BNPP relative to established pasture; and 3) irrigation would reduce the influence of PV microclimates on C cycling processes and lead to a general increase in SOC stocks, NPP, and soil CO_2 flux.

2.3 Methods

2.3.1 Site Details

We established an experiment at Jack's Solar Garden in Colorado, USA (40°07'18.9"N 105°07'49.9"W). The study site is in a cold steppe Koppen climate at 1526.4 m elevation with a mean annual temperature of 9.7°C and 365 mm annual precipitation. The site has Nunn sandy clay loam soil (Fine, smectitic, mesic Aridic Argiustoll). Prior to the construction of the 1.3 MW solar PV array, the site was managed with flood-irrigated, perennial hay production for several decades. The dominant species on the site prior to construction were *Bromus inermis, Medicago sativa, Dactylis glomerata*, and *Trifolium pratense*. Construction of the solar PV array was completed in November 2020.

The 380W Boviet brand PV panels measuring 2 x 1m were mounted in series on a single-axis-tracking system. Rows of panels are oriented North-South, and track East-West. The tracking system reaches a maximum angle of 45° to the East or West in the morning and evening, respectively. There is ~5.2 m of interspace between the mounting posts used to support the PV panels. Panel mounting height at the torque tube is 1.8 m above the ground.

2.3.2 Experimental Design

We established a randomized complete block design (RCBD) experiment within the array in May 2021, consisting of four blocks and six treatments. Each treatment was a factorial combination of two independent variables: Vegetation Community and Irrigation (Figure 2.2). The vegetation treatments were: 1) Pasture, 2) Balanced Natives, and 3) Forb Dominant Natives. The Pasture treatment represented the pre-existing vegetation of the site that was left in place. The Balanced Natives and Forb Dominant Natives treatments were established following a shallow roto-tilling in May 2021, followed by broadcast seeding at a rate of 60 seeds per square foot, and then raking and landscape rolling to increase seed to soil contact. The balanced natives mixture consisted of 50% native forbs and 50% native grasses by seed count and the forb dominant natives mixture contained 80% native forbs and 20% native grasses by seed count. Seed mix composition and seeding rates are included in the supplemental materials (Table S1). The irrigation treatments were: 1) Irrigated and 2) Dryland. The Irrigated treatment received 10mm of supplemental irrigation per week from May through September, totaling 260mm annually, administered via drip tape. The drip tapes were arranged evenly across the plots to ensure consistent water distribution, creating a grid of drip emitters approximately every 60cm. In contrast, the Dryland treatment did not receive any supplemental irrigation, relying entirely on natural precipitation. Each plot was subdivided into four distinct microclimates created by the

solar PV infrastructure. These microclimates, which were our experimental units, were replicated across all treatments and blocks (Figure 2.3). Annual climate data was obtained from the Colorado Climate Center Longmont 2 ESE station (Colorado Climate Center, 2025; Figure 2.5).

2.3.3 Data Analysis

Data was analyzed using JMP Pro 18 (SAS Institute Inc., Cary, NC). Mixed model regression analysis was used to test which independent variables influenced the response variables. Block and plot were included as random factors to account for experimental design. All models are full factorial and their respective fixed effects can be found in Table 2.1. Soil CO_2 flux, ANPP, SWC, and Soil Temperature are split between two models each, one with data from 2021-2022 before the inclusion of an East Edge microclimate and one with data from 2023 after inclusion. For SOC stock analyses, baseline sampling was included as an additional microclimate level. ANOVA assumptions were tested using residual distributions, Q-Q plots, and Shapiro-Wilk tests. BNPP required log-transformation to meet assumptions, all other datasets met assumptions without transformation. Tukey post hoc tests ($\alpha = 0.05$) were used to determine significant differences between independent variables.

2.3.4 Aboveground Biomass

Aboveground biomass was harvested in 2021 and 2023. Biomass was harvested in June and September for Pasture vegetation to simulate typical forage cuttings. For the two Native vegetation treatments, biomass was harvested only once, in September at peak biomass to estimate aboveground primary productivity. Within each treatment plot we harvested $0.5m^2$ of vegetation at 7.5cm above the soil surface. These samples were then dried in an oven at 55°C until constant mass was achieved and weighed. Biomass samples were only collected at the end of the growing season in 2022, so that data was excluded from our analyses.

2.3.5 Soil CO_2 Flux, Water Content, and Temperature

We measured soil CO_2 flux once per week during the growing season (April – October), and once each month during the winter season (November – March). In May 2021 three PVC collars were installed within each plot, in the Open, West Edge, and Under microclimates, to an average offset height of 2cm. A fourth collar was installed in the East Edge microclimate of each plot in September 2022. All living vegetation was removed from within collars so that measurements were primarily from heterotrophic respiration sources. Collar height offsets were measured annually to account for any variation or settling over the study period. Gas flux was measured beginning in May 2021 and ending in November 2023 using a Licor Smart Chamber connected to an infrared gas analyzer (LI-870, LICOR, Lincoln, NE). All measurements were taken between 8:30am-12:30pm. At each measurement time point, the chamber was fitted over an installed PVC collar and the gas flux was measured for 2 minutes. Each gas flux sampling of the 102 collars took two consecutive days to complete with blocks 1 and 2 measured on day one and blocks 3 and 4 measured on day two. Soil volumetric water content and temperature were measured using the probe attached to the smart chamber (Stevens HydraProbe, Stevens Water, Portland, OR) to 10cm depth next to the collar at each gas flux measurement time point.

2.3.6 Fine Root Productivity

Annual fine root production was measured using root ingrowth cores. To construct the cores, soil was collected from the study site and separated into 0-15cm and 15-30cm depth intervals. The soil was sieved sequentially with 8mm and then 2mm sieves and roots were removed. Any remaining roots were manually removed with tweezers. We constructed mesh cores with a radius of 2.5cm, depth of 33cm, and mesh size of 2mm. These were filled in depth increments of 0-15cm and 15-30cm with their respective homogenized, root free soil. Soil was

packed to field bulk density. One core was installed at each sampling position within each plot in early April each year using an auger to excavate to 30cm, inserting the new ingrowth core, and back filling around the core with additional soil that was sieved to 2mm to ensure a uniform pack. The top 3cm of mesh was left above the soil and the cores were marked with flags to aid recovery. The ingrowth cores were removed after the onset of winter dormancy (Oct-Nov) each year. A soil knife was used to cut any roots growing into the core prior to removal. After removal, the cores were stored at 4°C until processed. The fine roots were recovered by cutting the cores into 0-15cm and 15-30cm depths and washing away the soil over a stack of sieves containing mesh sizes 2mm, 1mm, and 0.5mm. The roots were dried until constant mass at 55°C and weighed.

2.3.7 Standing Root Mass

We measured standing root biomass 3 years after experiment establishment in October 2023 by collecting one soil core per sampling position from 0-15cm and 15-30cm depths using an auger with a 7cm diameter. The roots were separated from the soil by washing them over a 1mm sieve. The roots were then dried at 55°C until constant mass and weighed.

2.3.8 Total C and N content

One soil sample was collected in each plot at 0-15cm and 15-30cm depths using an auger with a 7cm diameter in July 2021, to represent baseline values at experiment establishment. Sampling was repeated in October 2023 at each sampling position. Two cores were composited per sample. Samples were air dried, sieved to 8mm, and a representative subsample was sieved to 2mm. The subsamples were dried to constant mass at 55 degrees, roller ground for 24hrs, and analyzed for total C and N using standard combustion analysis (Velp CN 802 Analyzer, VELP Scientific Inc., Deer Park, NY).

2.3.9 Inorganic C content

Soil inorganic C content was measured using the pressure-calcimeter method of Sherrod *et al* 2002. Briefly, HCl was added to soils in a sealed container to evolve CO_2 gas. The volume of this gas was then measured by the pressure built up in the sealed container and converted to C content, which was then subtracted from total C values to calculate total organic C.

2.4 Results

2.4.1 Precipitation, Soil Water Content and Temperature

Cumulative annual precipitation was similar between 2021 and 2022 (40cm vs 39cm), however a greater proportion of the total was received from March through May in 2021, and then relatively little precipitation was received from September through December (Figure 2.5). Comparatively, in 2022 April was particularly dry, but the rest of the year had fairly uniform precipitation dynamics close to the long-term average. The 2023 season had substantially higher total precipitation (54cm, 34% higher than 2021 and 39% higher than 2022) and a large portion of that total was received in May and June. Soil water content (SWC) from May-September was influenced by PV microclimate, irrigation, and year, while vegetation treatment had no effect.

The Under microclimate had the lowest average SWC in all years ($p < 0.001$). Compared to Open areas, Under was 26% lower in 2021, 51% lower in 2022, and 45% lower in 2023 (Table S4). The West Edge microclimate had the highest average SWC in all years, significantly exceeding Open areas ($p < 0.001$) by 19% in 2021, 20% in 2022, and 9% in 2023. East Edge (measured only in 2023) had similar average SWC to Open and was 7% lower than West Edge ($p < 0.001$). The discrepancy between East and West Edge SWC is driven by diurnal precipitation timing. On average more precipitation occurs in the afternoon and evening when

solar panels are oriented to the West. Irrigation significantly increased average SWC in all years ($p < 0.001$), by 15% in 2021, 27% in 2022, and 18% in 2023 (Table S4).

The irrigation effect varied substantially between microclimates. Under showed the strongest response to irrigation in all years(31% increase in 2021, 87% in 2022, and 64% in 2023). Open showed moderate irrigation responses, (16% increase in 2021, 25% in 2022, and 11% in 2023). West Edge exhibited smaller relative irrigation effects, (no increase in 2021, 22% in 2022, and 12% in 2023), while East Edge SWC increased 10% in 2023. Soil temperature was not significantly influenced by PV microclimates, irrigation, or vegetation treatments (Table S4).

2.4.2 SOC Stocks

SOC stocks were significantly influenced by microclimate ($p=0.0175$), depth ($p<0.0001$), and vegetation treatment ($p=0.0141$), along with interactions between microclimate and depth ($p=0.0006$) and between microclimate and vegetation treatment ($p=0.0443$). Irrigation had no significant effect on SOC stocks. Overall, SOC stocks from 0-30cm neither increased nor decreased in the 3 years following PV system installation.

The Under microclimate had higher SOC stocks than the other solar microclimates in 2023, however none were significantly different from baseline values (Figure 2.6). In the more responsive shallow soil (0-15cm) the Under microclimate had 25% greater SOC stocks in 2023 relative to baseline stocks measured in 2021 (Figure 2.6). Under was also 22% and 19% above SOC of the West Edge and East Edge, respectively. Deeper in the soil profile (15-30cm) the Open microclimate SOC decreased by 25% from baseline (Figure 2.6). In 2023, there were no differences in SOC stocks between the microclimates at 15-30cm.

Baseline SOC stocks unexpectedly differed between vegetation treatments, with Pasture vegetation having 27% lower baseline SOC stocks than Forb Dominant Natives (Table S2). This was surprising as treatments were established only six weeks before baseline sampling. By 2023 SOC stocks of Balanced Native vegetation were about 8% higher than Forb Dominant Native and Pasture vegetation, which were nearly equal to each other (Table S2). However, no vegetation treatment changed SOC stocks significantly from baseline values. The significant interaction between vegetation and microclimate was driven by the unexpected differences in baseline SOC stocks between vegetation treatments, though this effect dissipated by 2023.

2.4.3 Standing Root Mass

Standing root mass was influenced by microclimate ($p=0.0047$), Depth ($p<0.0001$), Microclimate*Depth ($p=0.0139$), and Microclimate*Vegetation Treatment ($p=0.0167$). Irrigation and Vegetation did not have significant main effects.

Variation in root mass across microclimates was mainly driven by differences in the upper 0-15 cm layer, which contained 70-80% of the total root mass found in surface soils across all microclimates with the remaining 20-30% at the 15-30cm depth (Figure 2.7). At 0-15cm, the Under and Open microclimates had the highest standing root mass. Under root mass was 59% and 43% greater than West and East Edges, respectively. In contrast, no significant differences in root mass were observed between microclimates at 15-30 cm (Figure 2.7).

Despite the absence of differences in the deeper soil, the microclimate effect was pronounced enough to detect higher standing root mass in the Open and Under microclimates compared to the West Edge, across the full 0-30 cm soil profile (Figure 2.7). Pasture root mass had the highest root biomass of all Vegetation by Microclimate combinations on the East Edge and the lowest of all combinations on the Under and West Edges (Table S2).

2.4.4 Aboveground Net Primary Productivity

Microclimate and Vegetation Treatment had significant effects ($p<0.0001$) on ANPP. In 2021, Irrigation was significant ($p=0.0059$) and in 2023 Microclimate*Irrigation treatment was significant ($p=0.0095$).

ANPP of Pasture vegetation was 100% higher than the two Native vegetation treatments in 2021 and 65% higher in 2023 (Table S2). ANPP of the Under microclimate was 27% lower than the other PV microclimates in 2021 and 30% lower in 2023. Despite differences in light and water inputs, ANPP of Open, East Edge, and West Edge microclimates was not different in either year. In 2021, irrigation increased ANPP by 31% (Figure 2.8). In 2023 irrigation did not consistently increase ANPP, but instead the effect of irrigation on ANPP was contingent on an interaction with microclimate.

While there were no ANPP differences between microclimates when evaluated using multiple comparisons with irrigation in 2023, the significant interaction between microclimate and irrigation reflected the trend of a surprising, slight negative effect of irrigation on ANPP in Open, East Edge, and West Edge microclimates versus a strong positive effect in the Under microclimate (Figure 2.8).

2.4.5 BNPP

BNPP, which we estimated using annual fine root production, was influenced by Microclimate ($p<0.0001$), Depth ($p<0.0001$), Year ($p<0.0001$), Microclimate*Depth ($p=0.0010$), Microclimate*Year ($p<0.0001$), and Depth*Year ($p=0.0032$).

The Open microclimate consistently had the greatest BNPP across the 2021 – 2023 growing seasons, exceeding West Edge by 59% and Under by 79% (Figure 2.9). BNPP of the West Edge only exceeded Under by 13% (Figure 2.9) despite having the greatest difference in

SWC of all microclimates (Table S4). The shallow 0-15 cm soil had higher BNPP than the deeper 15-30 cm layer, however the effect of depth was influenced by microclimate. The Under microclimate showed increased allocation to deeper roots, with ~50% of its root production allocated to each depth, in contrast to West Edge and Open, which both grew ~70% of their roots at 0-15cm depth and ~30% at 15-30cm (Figure 2.9).

BNPP varied significantly across years, with an average BNPP 57% higher in 2023 than in 2021 and 85% higher than in 2022. Additionally, the interaction between microclimate and year was highly significant ($p<0.0001$), showing that microclimates responded differently to the effects of Year. The Under microclimate in particular demonstrated a greater BNPP reduction in 2022 than the other microclimates. Conversely, West Edge did not vary significantly across years suggesting that the characteristics of the West Edge microclimate may have moderated the variability caused by Year (Figure 2.10). The average depth of root inputs varied across years. In 2021 there was a 70/30 distribution between shallow and deep roots, whereas in 2022 and 2023 there was a 60/40 distribution (Table S2). Irrigation had no effect on BNPP in any year. Native vegetation treatments had more highly variable BNPP across microclimates, with 72% higher BNPP in the Open microclimate than in the West Edge and 85% more than Under, whereas Pasture vegetation did not differ across microclimates (Figure 2.10). BNPP of the under microclimate was the most variable across years, especially in 2022 which was the dryest year of our study. In 2022 BNPP of Under was 60% lower than West Edge and 70% lower than Open (Figure 2.10).

2.4.6 Soil CO_2 Flux

Soil CO_2 flux in 2021 and 2022 was influenced Date ($p<0.0001$), PV microclimates ($p<0.0001$), irrigation ($p=0.0039$), and several interactions between these factors, including interactions with vegetation treatment, which was not significant on its own ($p=0.6782$).

Microclimate only significantly affected soil CO_2 flux from May through August, when fluxes were highest each year. As temperatures began to decrease in September, causing overall flux rates to fall, the effect of microclimate became non-significant and then remained non-significant until the following May. The more sheltered a given microclimate was, the more soil CO_2 flux was reduced in that microclimate. From the months of May-August when microclimates impacted soil CO_2 flux Open had the highest soil CO_2 flux, followed by West Edge which was reduced by 5% in 2021 and 13% in 2022, and then Under which was reduced by 31% in 2021 and 28% in 2022 (Figure 2.11).

Our model showed a significant interaction between Date and Irrigation, however this was misleading because irrigation was only applied from May through September. Irrigation increased soil CO_2 flux, but only in the Under microclimate, which was the dryest of the microclimates. From May-September irrigation increased soil CO_2 flux Under panels by 25% in 2021 and 39% in 2022.

While still lower than Open and West Edge, the Under microclimate did not reduce soil CO_2 flux as greatly in plots managed as Forb Heavy Natives from May-August in 2021 and 2022 (21% lower than Open and 14% lower than West Edge) compared to Pasture (33% lower than Open and 27% lower than West Edge) and Balanced Natives (35% lower than Open and 29% lower than West Edge).

In the first two months after collar installation (May and June 2021), CO_2 flux was 11% higher in plots managed as Pasture vegetation compared to the two Native vegetation treatments.

Plots that received Native treatments were tilled prior to the installation of soil collars in order to facilitate interseeding, whereas Pasture vegetation plots were not tilled and only the soil collar was defoliated. Thus, elevated fluxes in the interseeded treatments were likely due to this soil disturbance.

Most of the effects observed in 2021 and 2022 continued to be observed in 2023, however there were some key differences. Irrigation no longer led to significantly higher soil CO_2 flux and the effect of PV microclimates was different than the previous two years. In 2023, West Edge had the lowest flux on average instead of Under. East Edge was also included in the third year and was comparable to the Open microclimate, with which it shared the highest flux.

Both standing root biomass ($R=0.249$, $p=0.0151$) and BNPP ($R=0.132$, $p=0.0425$) were significantly correlated with soil annual average CO_2 flux. Soil temperature ($R=0.654$, $p<0.0001$) and water content ($R=0.392$, $p<0.0001$) were more highly correlated with soil CO_2 flux than the biomass variables, suggesting that the local micro- and seasonal climatic effects were the most important drivers of soil CO_2 flux dynamics.

2.5 Discussion

Our study provides valuable insights into how utility-scale solar PV infrastructure affects C cycling in semi-arid grassland ecosystems. We found that the distinct microclimates created by solar panels, along with ecovoltaic management practices like interseeding native plant species and irrigation, had significant impacts on above and belowground productivity, SOC stocks, and soil CO_2 flux.

2.5.1 Under Microclimate: Reduced Light and Moisture

Shading from solar infrastructure can substantially moderate temperature stress and vapor pressure deficit, potentially creating more favorable conditions for plant growth compared to

unshaded environments for horticultural crops (Barron-Gafford *et al* 2019) and grassland species (Adeh *et al* 2019). Despite potential benefits of shading under PV systems observed in other climates and with different management, the Under microclimate has both the most intensive shading in addition to effectively no direct precipitation inputs. No studies that we are aware of have tried to disentangle these two factors that likely both contributed to the lowest ANPP and BNPP in the Under climate.

Despite having the lowest average BNPP, the Under microclimate had the highest standing root biomass three years after PV installation. In contrast to the Open and West Edge microclimates, where 70-80% of root biomass was concentrated in the top 15 cm of soil, the Under microclimate allocated approximately 50% of its root production to each depth increment (0-15 cm and 15-30 cm). In semi-arid grasslands, soil moisture is often the primary limiting factor for plant growth and productivity (Knapp *et al* 2008). The shelter of solar panels can reduce evapotranspiration and create a more stable moisture regime that is likely more influenced by lateral flow from the adjacent Edge microclimates leading to a deeper soil moisture distribution (Sturchio *et al* 2024b). Plants growing in these conditions may allocate more resources to root growth at depth to access this reliable water source and improve their overall water status (Nippert and Holdo 2015). This strategy could be particularly advantageous during periods of drought or in the later stages of the growing season when surface soils are depleted of moisture. Furthermore, cooler temperatures and lower evaporative demand may reduce the metabolic costs associated with maintaining deep roots (Schenk and Jackson 2002). This could allow plants to sustain a more extensive deep root system than would be possible in less sheltered areas, where higher temperatures and evapotranspiration rates may necessitate a

greater investment in shallow, opportunistic roots to capture transient moisture pulses (Schwinning and Sala 2004).

In 2022, the driest year of the study, the Under microclimate had the lowest BNPP among all microclimates. Shading and interception of precipitation by solar panels may exacerbate water limitation in the Under microclimate during dry years. While the cooler temperatures and reduced evaporative demand beneath the panels can help conserve soil moisture (Adeh *et al* 2018), this effect may be insufficient to offset the overall reduction in water inputs during extended periods of drought. Under these conditions, plants growing in the Under microclimate may experience greater water stress than those in the Open or Edge microclimates, which receive more direct precipitation. Water stress can lead to reduced photosynthetic activity, biomass allocation to roots, and overall productivity (Xu *et al* 2013).

The Under microclimate also had the lowest soil CO_2 flux. Surface soil SOC stocks increased modestly from baseline by 2023. Together, these results suggest that the increase in SOC stock and standing belowground biomass was due to reduced decomposition rates driven by reduced moisture and light intercepted by PV infrastructure. The drier and more stable conditions beneath PV panels reduced SOC turnover rates, thereby maintaining SOC stocks despite decreases in productivity. This finding contrasts with Carvalho *et al* (2025) which found reduced SOC under panels, however the sites they observed were fixed angle, which means the reduction of light inputs was more severe than in single-axis tracking arrays such as our study site. This suggests that the dynamic shading of tracking arrays is less likely to produce extreme microclimate conditions that would negatively impact soil C sequestration.

A deeper distribution of roots may also have implications for long-term soil C storage. Deep roots can transport photosynthetically-derived C compounds into the subsoil, where they

are more likely to be stabilized and protected from decomposition than in the surface soil layers (Kell 2012). Increasing the depth of soil C inputs has been proposed as a potential mechanism for enhancing soil C sequestration in grassland ecosystems (Lorenz and Lal 2005; Kell 2011). By promoting deeper root systems, PV microclimates could facilitate the transfer and storage of plant-derived C deeper in the soil profile.

2.5.2 Edge Microclimates: Enhanced Water with Moderate Light

The Edge microclimates, where redistribution of precipitation from solar panels led to increased soil water compared to the Open microclimate, showed unique patterns in productivity and carbon cycling. For example, West Edge, the wettest microclimate, had the lowest standing root mass of all the microclimates in 2023, suggesting an overall increase in decomposition and/or reduced root inputs in this wetter environment.

The lower BNPP in the Edge microclimates may be attributed to the combined effects of high water availability and light limitation. Under conditions of high water availability, plants may not need to invest as many resources in root growth and development to acquire the water needed for photosynthesis. Instead, plants in the Edge microclimates may allocate more C to aboveground structures to maximize light capture and compensate for the reduced solar radiation due to panel shading (Poorter *et al* 2012). This trade-off between water acquisition and light capture may result in lower root biomass production in the Edge microclimates compared to the Open microclimate, where plants need to maintain more extensive root systems to exploit soil resources in the absence of panel-induced water subsidies.

The significant Microclimate*Irrigation interaction in our 2023 ANPP model suggests a change in resource limitation patterns. Irrigation did not benefit the well-watered Open and Edge microclimates but remained beneficial in the water limited Under microclimate. In years with

more favorable natural precipitation patterns, additional irrigation may provide minimal benefits or even reduce productivity in well-watered microenvironments through mechanisms such as increasing decomposition rates, nutrient leaching or promotion of fungal pathogens.

2.5.3 Open Microclimate: Maximum Light with Ambient Moisture

The Open microclimate, which receives the least shelter from solar panels, showed distinct interannual patterns of productivity and carbon cycling. While the Open microclimate tended to have higher BNPP than the other microclimates, this effect was most pronounced in 2023, the wettest year. The high BNPP observed in the Open microclimate during wet years, despite Edge microclimates having higher soil water content, may be attributed to a shift from water limitation to light limitation.

In the Open microclimate, the absence of solar panel shading allows for greater photosynthetic activity and C assimilation, which can stimulate root growth and nutrient uptake (Pierson *et al* 1990). The increased solar radiation in the Open microclimate may also promote faster nutrient mineralization and cycling, as higher temperatures and moisture fluctuations can stimulate microbial activity and decomposition rates (Liu *et al* 2017), and the Open microclimate consistently had the highest soil CO_2 flux. This enhanced decomposition rate coupled with the lack of precipitation concentration occurring along the panel edges, may have contributed to the reduced SOC stocks at depth in the Open microclimate relative to baseline measurements.

2.5.4 PV Microclimate Implications for Carbon Cycling and Management

The introduction of solar infrastructure did not lead to a significant overall change in SOC stocks in the top 30cm within three years after construction. Our results suggest that solar energy infrastructure does not intrinsically pose a risk to C sequestration ecosystem services in the initial years after installation and may even have modest benefits. However, it is important to

note that this is likely contingent on solar developers and engineering, procurement and construction (EPC) firms minimizing ecological impact during the construction phase.

The differential responses of BNPP to precipitation extremes created by microclimates may suggest that land managers of semi-arid ecovoltaic systems should apply a targeted seeding approach of specific plant functional types within PV microclimates. In semi-arid grasslands, species with contrasting rooting strategies often coexist, with shallow-rooted grasses and deep-rooted forbs or shrubs partitioning soil moisture resources across different depth zones (Nippert and Knapp 2007). The altered moisture and radiation conditions in the Under microclimate may favor the persistence of deep-rooted, stress-tolerant species that can access stable water reserves in the subsoil (Comas *et al* 2013). These species may be less responsive to fluctuations in surface soil moisture and exhibit a more conservative growth strategy focused on long-term survival (Perez Ramos *et al* 2013). In contrast, the Open microclimate may support a higher proportion of shallow-rooted, opportunistic species that can rapidly increase root production during periods of high resource availability (Poorter *et al* 2012).

These patterns highlight the complex interplay between solar panel microclimates, precipitation variability, and grassland root dynamics. The contrasting responses of these microclimates to dry and wet years underscore the need to consider both the magnitude and temporal distribution of precipitation when assessing the ecological impacts of solar infrastructure. While the shelter provided by panels may buffer plants against moisture stress during moderately dry periods, our results suggest that this effect may be diminished or even reversed during extreme drought The benefits of PV microclimates for root growth may be contingent on a minimum threshold of water availability.

2.5.5 Irrigation and interseeding had minimal benefits for C cycling ecosystem services

We hypothesized that interseeding native species and their associated management regime, which entailed a reduction of mowing to once per year at the end of the growing season to allow all plants to bloom and set seed instead of twice per year to maximize forage quality and regrowth, would decrease ANPP but increase BNPP. ANPP was reduced significantly, which was driven by the change in management more so than any change to community composition, however BNPP did not increase as we expected. There is significant evidence of more robust root system development among many native species that are adapted to more arid environments compared to introduced pasture species in the Western US (Weaver 1958; Craine *et al* 2013; Wilsey and Polley 2006), however we had very poor establishment of native grasses in our treatments. All of the native species that were able to successfully establish were forbs. Native forbs can still have substantial root systems, however lack of BNPP response to our vegetation treatments is likely due to the overall similarity of community composition due to unsuccessful native grass establishment. A review by Carvalho *et al* (2024) also found that most studies that examined the effect of plant diversity on grassland soil C in the UK and Ireland found no change in soil C. The authors postulate that the presence (or absence) of key functional groups (legumes, C4 species) may account for the null responses they observed, which is congruent with our observations. A secondary factor in the lack of BNPP response may be that the native vegetation treatments were still in the establishment phase after only three years.

Despite the lack of BNPP response to our native vegetation treatments, SOC stocks of Balanced Native vegetation were 8% higher than stocks of Pasture and Forb Dominant Natives, although stocks of these plots were not higher than their baseline values. Due to the relatively small difference between vegetation treatments in 2023 and the lack of difference from baseline values, our results suggest that over the short term, there are no clear advantages to disturbing

established pastures to plant native vegetation purely for soil C benefits. However, the benefits of interseeding native vegetation on SOC stocks may increase over time or due to the provisioning of other ecosystem services.

We also hypothesized that irrigation would increase SOC stocks, NPP, and soil CO_2 flux. Irrigation did not increase SOC stocks or BNPP, however it did increase ANPP and soil CO_2 flux. In 2021, irrigation uniformly increased ANPP by 31% across all microclimates, however in 2023 it only increased ANPP Under. The increase of ANPP is a valuable service for grazers or hay operations, but the significant cost of irrigation would need to be weighed against the value of potential yield gains. If infrastructure and water are easily available at a given PV site, irrigation would likely increase site appeal for graziers, however if significant investment would be required the ecosystem service benefits would likely not outweigh the costs of implementation. Infrastructure to provide drinking water access for animals on site would likely be cheaper than irrigation infrastructure while still making a solar PV site much more attractive to potential graziers.

Our final hypothesis related to irrigation was that it would reduce the influence of PV microclimates on C cycling processes, which we observed to be true. Specifically, the Under microclimate which was the driest and most heavily shaded, showed the strongest ANPP and soil CO_2 flux response to irrigation. These results suggest that under more arid conditions irrigation is more effective, however due to SOC stock accruals being driven by a reduction in SOC turnover under the shelter of solar panels, this dynamic may actually mitigate some of the benefits of PV microclimates for C sequestration, casting further doubt on the utility of irrigation outside of highly arid conditions.

2.6 Conclusions

Ultimately, our findings demonstrate that the heterogeneous microclimates induced by solar PV arrays can significantly alter the spatial patterns and controls on grassland C cycling processes. While mounting evidence suggests that the shelter provided by solar panels can locally modify ANPP, our results indicate that soil C sequestration benefits are likely highly dependent on BNPP, rooting depth, SOC turnover rates, and the interaction of these factors with PV microclimates.

Our findings, along with recent research by Kannenberg *et al* (2023), suggest that solar infrastructure can be deployed in grassland ecosystems with minimal impacts on carbon cycling when properly designed. Using data from a separate experiment at the same site as our study, Kannenberg *et al* found that even with a 38% reduction in light availability, photosynthesis decreased by only 7.7% due to plants ability to adapt their photosynthetic traits to the dynamic shading environment. Our study similarly demonstrates the resilience of grassland carbon cycling under solar panels.

From a policy and management perspective, our results support the adoption of low-impact installation methods for solar energy infrastructure on agricultural lands. However, we found minimal evidence to suggest that interseeding with native species or supplying irrigation had meaningful benefits for C cycling ecosystem services. While there are other ecosystem service benefits associated with interseeding native plants, our study indicates that perennial vegetation with high soil coverage, whether native or introduced, perform similarly in terms of C cycling.

As solar energy development expands in semi-arid regions worldwide, it is imperative that we develop robust, contextual knowledge of how PV infrastructure affects ecosystem services. Our study provides data to inform land-use decisions and policy frameworks aimed at

managing ecological impacts. Understanding the nuances of how solar PV alters microclimatic conditions, vegetation dynamics, and SOC storage can help guide the design and management of future installations. Ultimately, we hope the findings of this study will contribute to a more holistic approach to energy planning, ensuring that efforts to combat climate change through clean energy do not come at the expense of critical ecosystem services. While this study analyzed SOC dynamics immediately following PV installation, longer-term monitoring across a diversity of sites, panel configurations, and climate conditions will be essential to fully elucidate the C cycle implications of this rapidly expanding land use.

2.7 Tables

Table 2.1: Factors (rows) included in each full factorial mixed model for the corresponding response variables (columns).

	SOC Stock	Standing Root Mass	ANPP	BNPP	Soil CO_2 Flux	SWC	Soil Temperature
Vegetation Treatment (Pasture, Balanced Natives, Forb Dominant Natives)	X	X	X	X	X	X	X
Irrigation Treatment (Irrigated, Dryland)	X	X	X	X	X	X	X
Microclimate (Open, West Edge, East Edge, Under)	X	X	X	X	X	X	X
Soil Depth (0-15cm, 15-30cm)	X	X		X			
Date	N/A	N/A		X	X	X	X

2.8 Figures

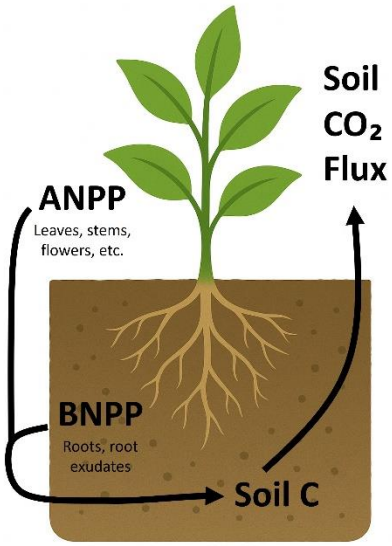

Figure 2.1. Diagram of C pools and fluxes measured in our experiment.

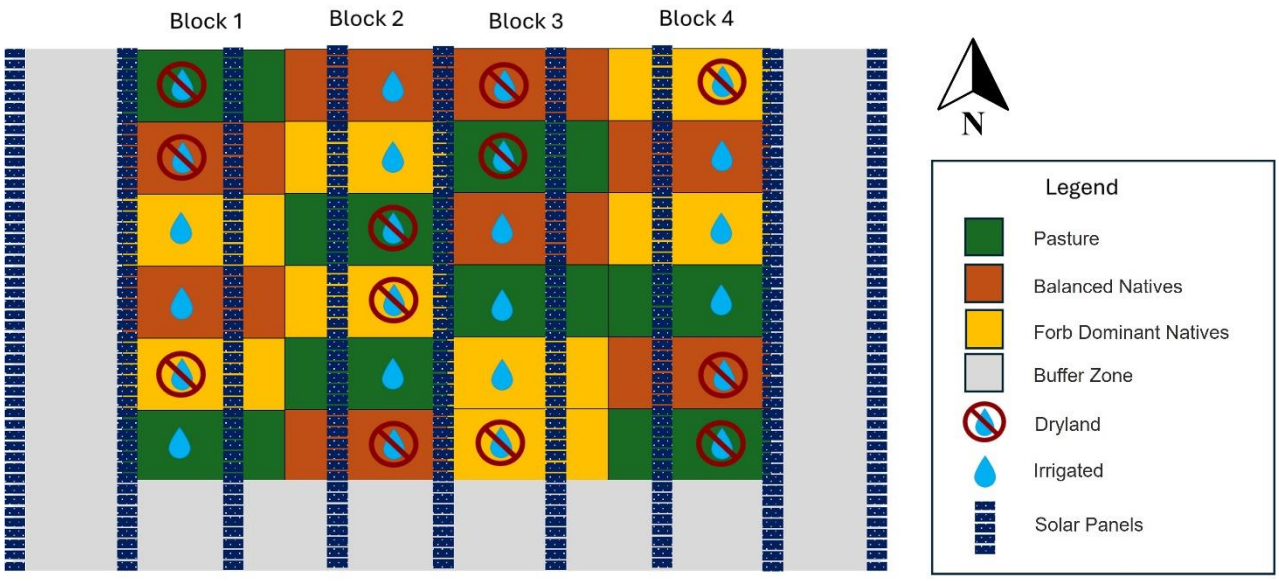

Figure 2.2. Diagram of our experimental design. There was not a buffer strip to the North of our experimental plots due to site constraints. Irrigation mainlines ran N-S between blocks 1 and 2 and blocks 3 and 4. Lateral drip tape branched off of the mainlines to deliver irrigation to the experimental plots.

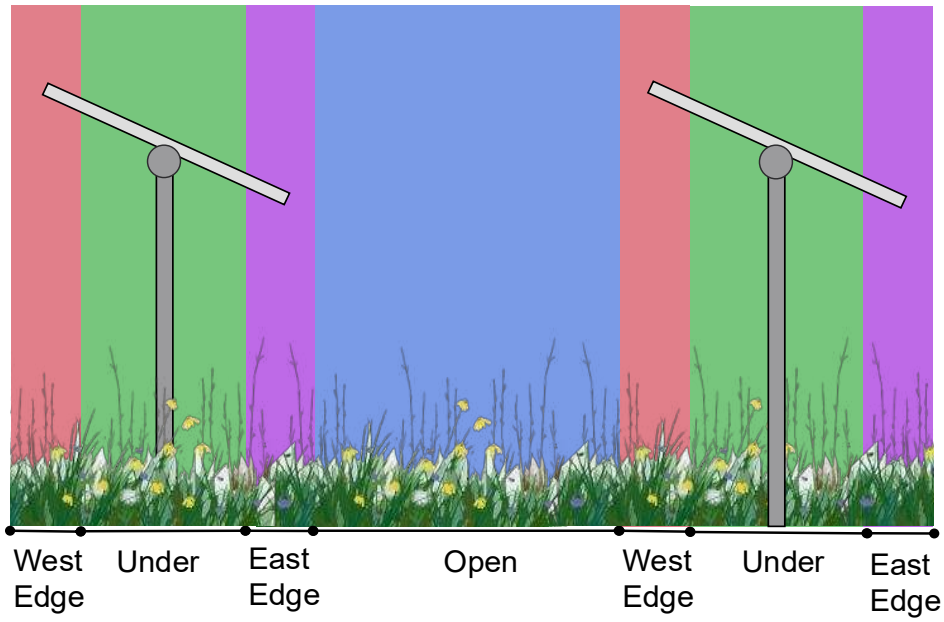

Figure 2.3. An illustration of the four distinct microclimates created by a single-axis tracking solar array.
Open – 50% of total area. ~7 hours of mid-day sunlight. 26% average growing season soil moisture.
West Edge – 11.5% of total area. ~4 hours of afternoon sunlight. 30% average growing season soil moisture.
East Edge - 11.5% of total area. ~4 hours of morning sunlight. 28% average growing season soil moisture.
Under - 27% of total area. Less than 2 hours of daily sunlight. 22% average growing season soil moisture.
Microclimate characterization data were collected by partners in 2022 and reported in Sturchio et al (2024a).

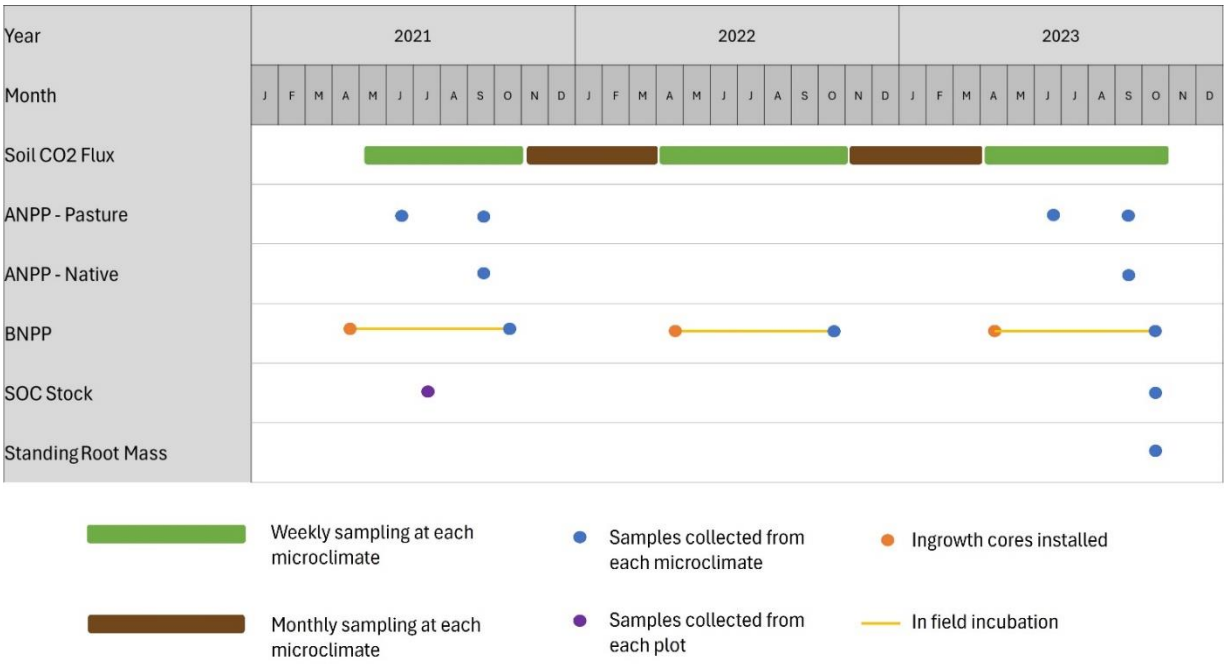

Figure 2.4. Timeline of data collection activities showing the temporal distribution of measurements across the three-year study period. Soil CO_2 flux measurements were conducted weekly during growing seasons (April-October) and monthly during winter (November-March). Aboveground biomass was harvested twice annually for pasture treatments (June and September) and once annually for native vegetation treatments (September). Fine root productivity was assessed using annual ingrowth cores installed each April and harvested after dormancy onset (October-November). Soil carbon and nitrogen content was measured at study beginning (Baseline, July 2021) and study conclusion (October 2023). Standing root mass was assessed once at study conclusion in October 2023.

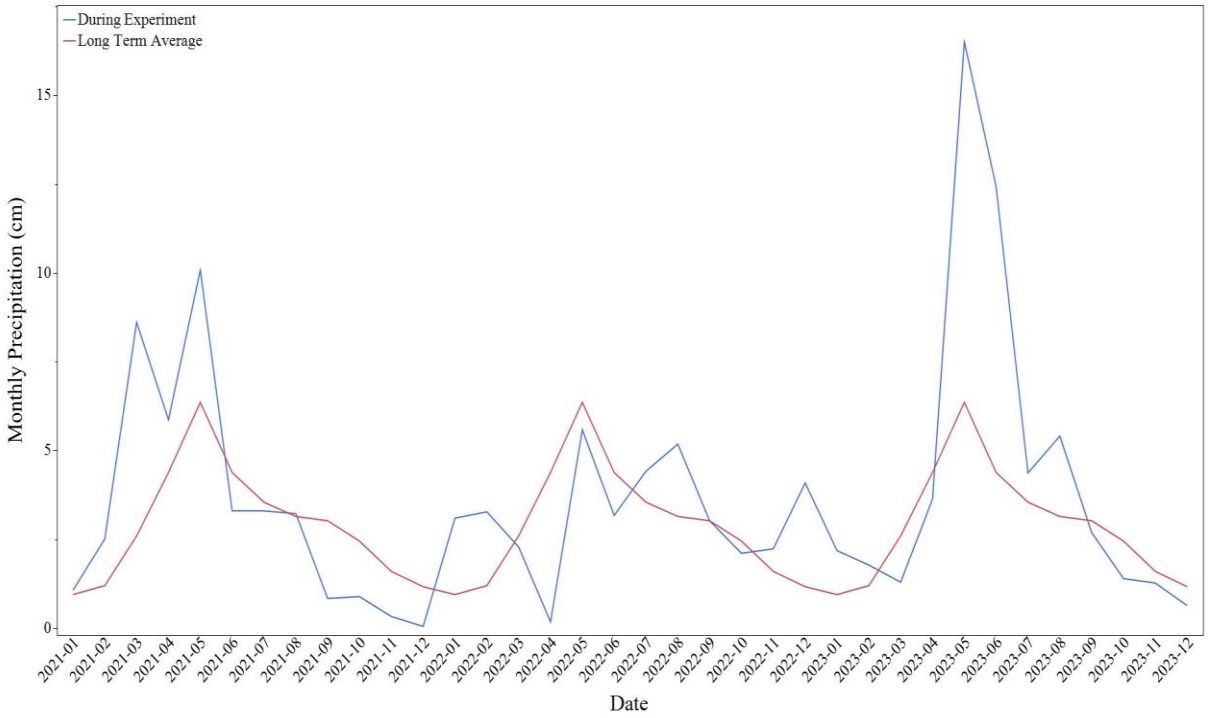

Figure 2.5. The blue line represents monthly precipitation totals at our study site from 2021-2023. The red line represents long-term average (1893 – 2023) monthly precipitation.

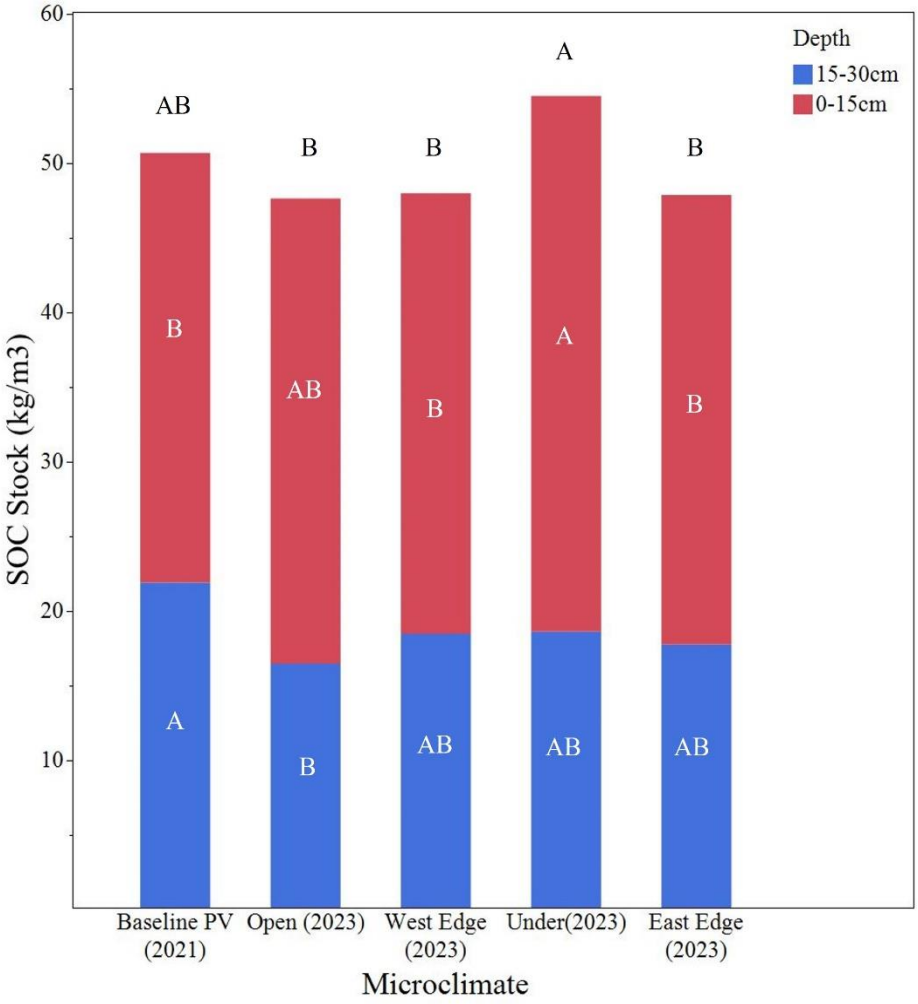

Figure 2.6. Mean SOC stocks by Microclimate and sampling Depth. The black multiple comparisons letters located above the bars compare microclimates averaging across depths. The white multiple comparisons letters located inside the bars compare microclimates within a single depth.

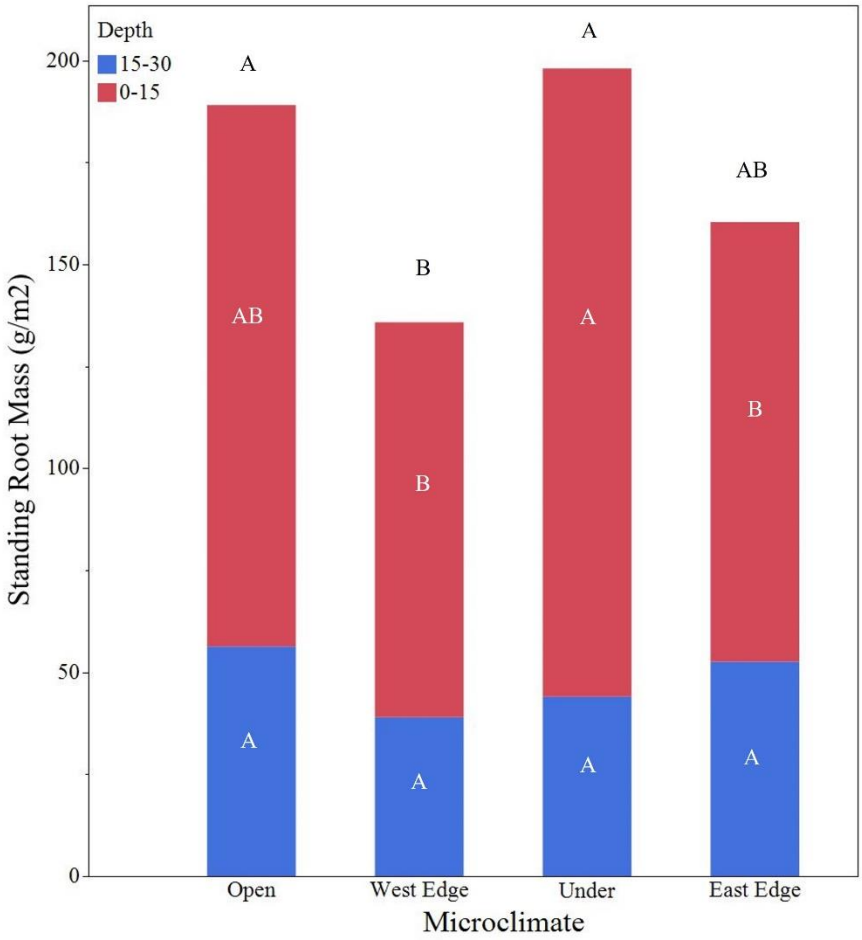

Figure 2.7. Mean standing root mass by Microclimate and sampling Depth. The black multiple comparisons letters located above the bars compare Microclimates only. The white multiple comparisons letters located inside the bars include both Microclimate and Depth factors.

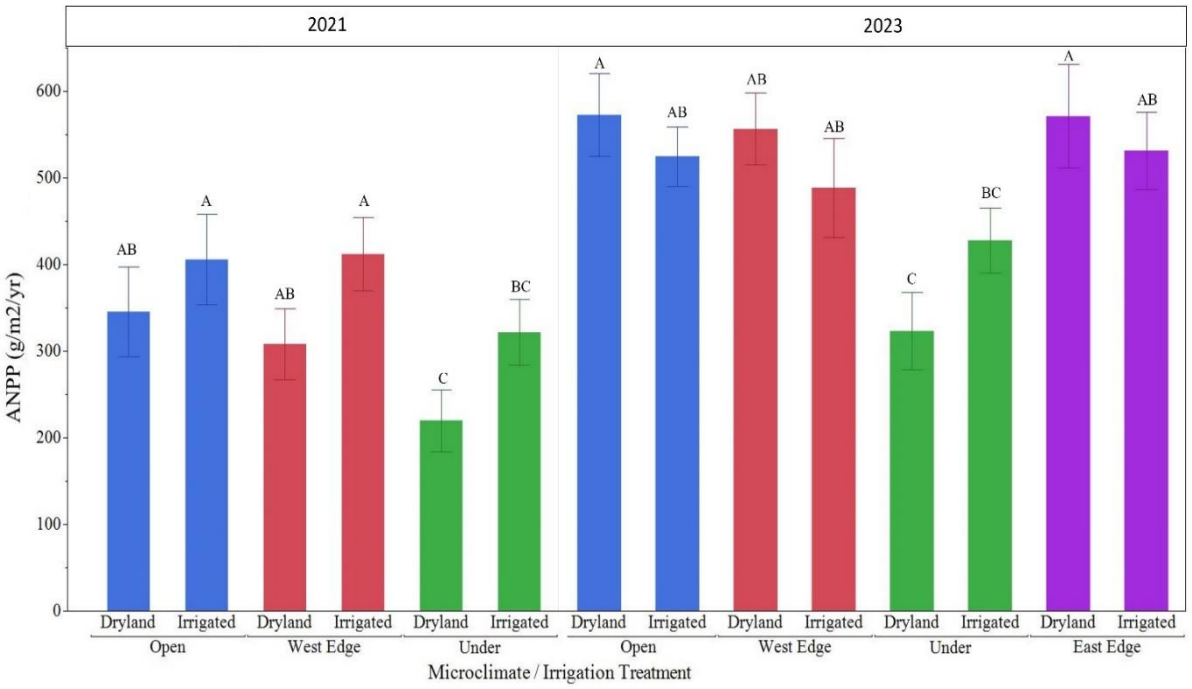

Figure 2.8. ANPP by Microclimate and Irrigation treatment. Note that separate models were created for 2021 and 2023 due to the addition of the East Edge microclimate in 2022. Thus, multiple comparison letters are only within each year, not across.

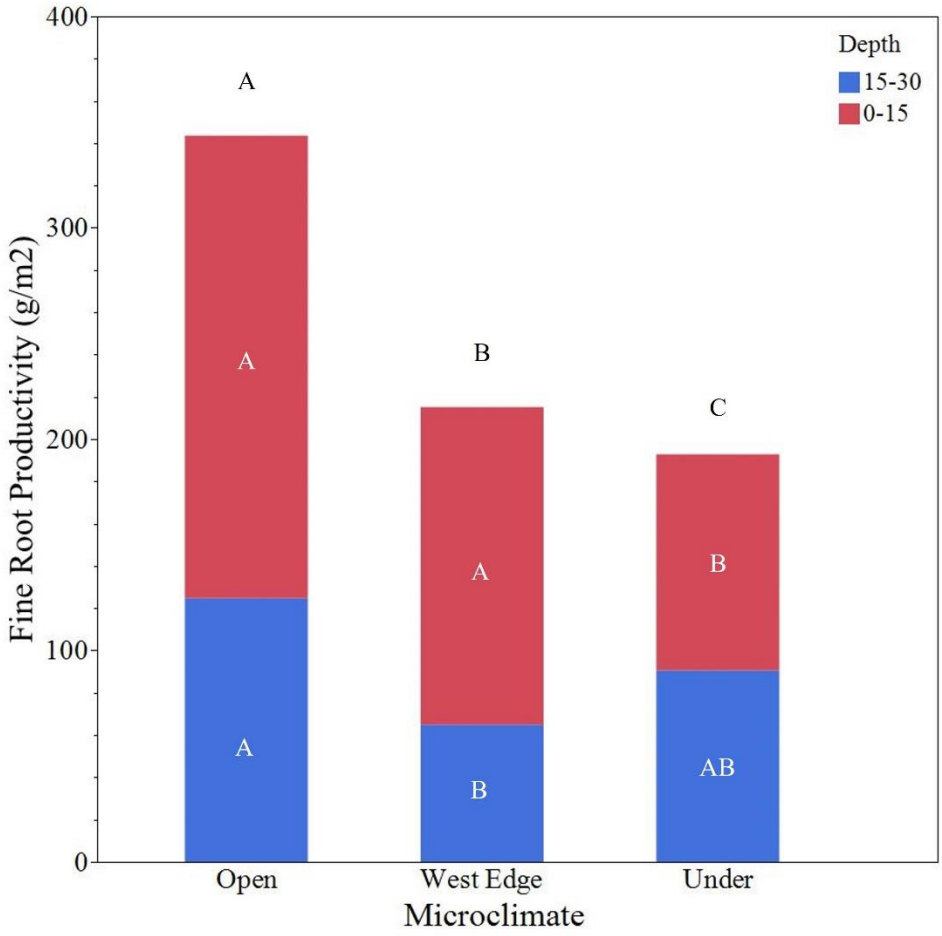

Figure 2.9. Annual fine root production by Microclimate and Depth. The black multiple comparisons letters located above the bars compare Microclimates only. The white multiple comparisons letters located inside the bars include both Microclimate and Depth factors.

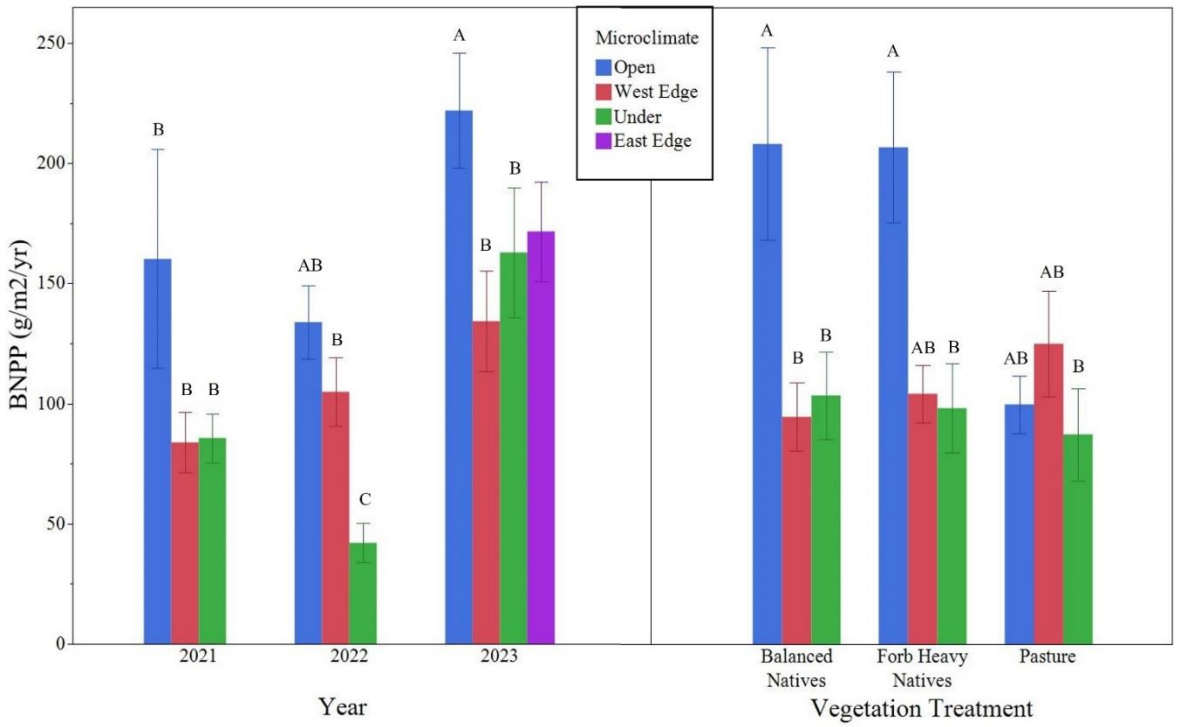

Figure 2.10. Annual fine root productivity by Microclimate and Year (left) and Microclimate and Vegetation Treatment (right). Note that East Edge was not included in the model and is shown only for reference.

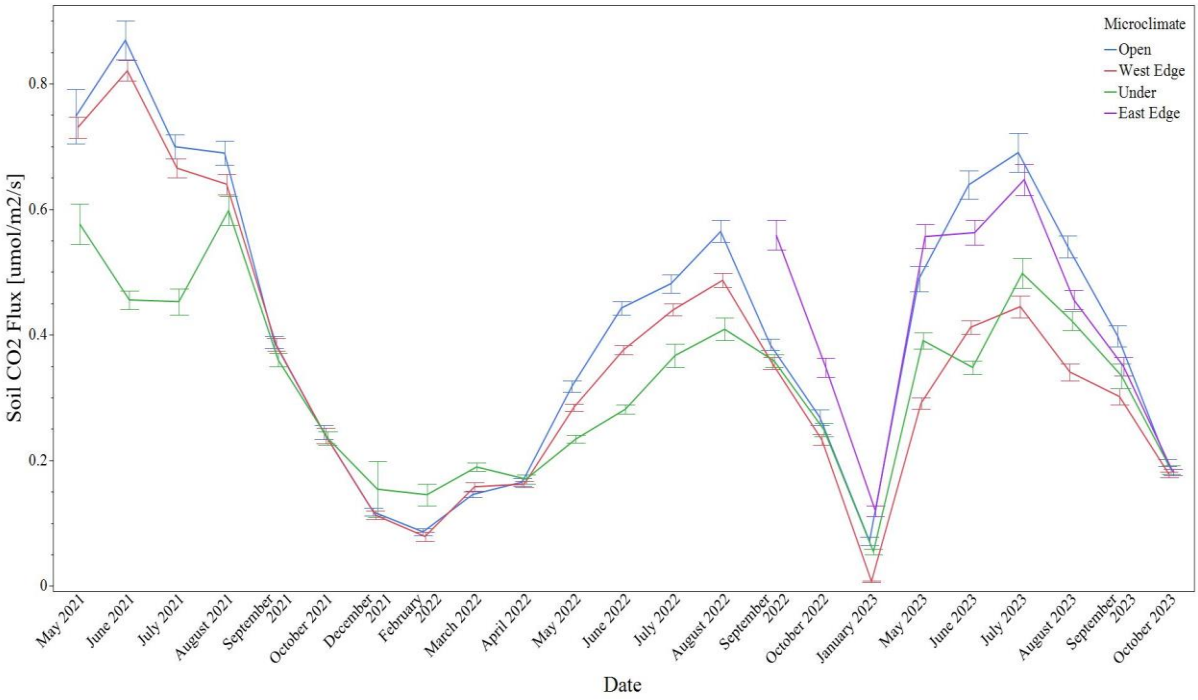

Figure 2.11. Average monthly Soil CO_2 flux by PV microclimate. Error bars represent one standard error

LITERATURE CITED

Adeh, E. H., Selker, J. S., & Higgins, C. W. (2018). Remarkable agrivoltaic influence on soil moisture, micrometeorology and water-use efficiency. *PLOS ONE*, *13*(11), e0203256. https://doi.org/10.1371/JOURNAL.PONE.0203256

Armstrong, A., Ostle, N. J., & Whitaker, J. (2016). Solar park microclimate and vegetation management effects on grassland carbon cycling. *Environmental Research Letters*, *11*(7), 074016. https://doi.org/10.1088/1748-9326/11/7/074016

Barron-Gafford, G. A., Pavao-Zuckerman, M. A., Minor, R. L., Sutter, L. F., Barnett-Moreno, I., Blackett, D. T., Thompson, M., Dimond, K., Gerlak, A. K., Nabhan, G. P., & Macknick, J. E. (2019). Agrivoltaics provide mutual benefits across the food–energy–water nexus in drylands. *Nature Sustainability 2019 2:9*, *2*(9), 848–855. https://doi.org/10.1038/s41893-019-0364-5

Carvalho, F., Healing, S., & Armstrong, A. (2024). Enhancing soil carbon in solar farms through active land management: a systematic review of the available evidence. *Environmental Research: Ecology*, *3*(4), 042001. https://doi.org/10.1088/2752-664X/AD8CE4

Carvalho, F., Montag, H., Bentley, L., Šarlej, R., Broyd, R. C., Blaydes, H., Cattin, M., Burke, M., Wallwork, A., Ramanayaka, S., White, P. C. L., Sharp, S. P., Clarkson, T., & Armstrong, A. (2025). Plant and soil responses to ground-mounted solar panels in temperate agricultural systems. *Environmental Research Letters*, *20*(2), 024003. https://doi.org/10.1088/1748-9326/ADA45B

Colorado Climate Center, 2025. Access Colorado Data. https://ccc.atmos.colostate.edu/data_access_new.html (accessed Jan 26 2025).

Comas, L. H., Becker, S. R., Cruz, V. M. v., Byrne, P. F., & Dierig, D. A. (2013). Root traits contributing to plant productivity under drought. *Frontiers in Plant Science*, *4*(NOV), 62325. https://doi.org/10.3389/fpls.2013.00442

Craine, J. M., Ocheltree, T. W., Nippert, J. B., Towne, E. G., Skibbe, A. M., Kembel, S. W., & Fargione, J. E. (2012). Global diversity of drought tolerance and grassland climate-change resilience. *Nature Climate Change 2012 3:1*, *3*(1), 63–67. https://doi.org/10.1038/nclimate1634

Curiel Yuste, J., Baldocchi, D. D., Gershenson, A., Goldstein, A., Misson, L., & Wong, S. (2007). Microbial soil respiration and its dependency on carbon inputs, soil temperature and moisture. *Global Change Biology*, *13*(9), 2018–2035. https://doi.org/10.1111/J.1365-2486.2007.01415.X

Dada, M., & Popoola, P. (2023). Recent advances in solar photovoltaic materials and systems for energy storage applications: a review. *Beni-Suef University Journal of Basic and Applied Sciences*, *12*(1), 1–15. https://doi.org/10.1186/s43088-023-00405-5

ESMAP. (2020). Global Photovoltaic Power Potential by Country. In *Global Photovoltaic Power Potential by Country*. https://doi.org/10.1596/34102

Eziz, A., Yan, Z., Tian, D., Han, W., Tang, Z., & Fang, J. (2017). Drought effect on plant biomass allocation: A meta-analysis. *Ecology and Evolution*, *7*(24), 11002–11010. https://doi.org/10.1002/ECE3.3630

Freschet, G. T., Roumet, C., Comas, L. H., Weemstra, M., Bengough, A. G., Rewald, B., Bardgett, R. D., de Deyn, G. B., Johnson, D., Klimešová, J., Lukac, M., McCormack, M. L., Meier, I. C., Pagès, L., Poorter, H., Prieto, I., Wurzburger, N., Zadworny, M., Bagniewska-Zadworna, A., … Stokes, A. (2021). Root traits as drivers of plant and ecosystem functioning: current understanding, pitfalls and future research needs. *New Phytologist*, *232*(3), 1123–1158. https://doi.org/10.1111/NPH.17072

Guswa, A. J. (2010). Effect of plant uptake strategy on the water−optimal root depth. *Water Resources Research*, *46*(9), 9601. https://doi.org/10.1029/2010WR009122

Hernandez, R. R., Easter, S. B., Murphy-Mariscal, M. L., Maestre, F. T., Tavassoli, M., Allen, E. B., Barrows, C. W., Belnap, J., Ochoa-Hueso, R., Ravi, S., & Allen, M. F. (2014). Environmental impacts of utility-scale solar energy. *Renewable and Sustainable Energy Reviews*, *29*, 766–779. https://doi.org/10.1016/j.rser.2013.08.041

Intergovernmental Panel on Climate Change (IPCC). (2023). Emissions Trends and Drivers. In *Climate Change 2022 - Mitigation of Climate Change* (pp. 215–294). Cambridge University Press. https://doi.org/10.1017/9781009157926.004

International Energy Agency (IEA). (2024). *Electricity 2024 - Analysis and forecast to 2026*. www.iea.org

International Renewable Energy Agency (IRENA). (2024). *Renewable Energy Statistics 2024*. www.irena.org

Kannenberg, S. A., Sturchio, M. A., Venturas, M. D., & Knapp, A. K. (2023). Grassland carbon-water cycling is minimally impacted by a photovoltaic array. *Communications Earth & Environment 2023 4:1*, *4*(1), 1–8. https://doi.org/10.1038/s43247-023-00904-4

Kell, D. B. (2011). Breeding crop plants with deep roots: their role in sustainable carbon, nutrient and water sequestration. *Annals of Botany*, *108*(3), 407–418. https://doi.org/10.1093/AOB/MCR175

Kell, D. B. (2012). Large-scale sequestration of atmospheric carbon via plant roots in natural and agricultural ecosystems: why and how. *Philosophical Transactions of the Royal Society B: Biological Sciences*, *367*(1595), 1589–1597. https://doi.org/10.1098/RSTB.2011.0244

Knapp, A. K., Beier, C., Briske, D. D., Classen, A. T., Yiqi, L., Reichstein, M., Smith, M. D., Smith, S. D., Bell, J. E., Fay, P. A., Heisler, J. L., Leavitt, S. W., Sherry, R., Smith, B., & Weng, E. (2008). Consequences of More Extreme Precipitation Regimes for Terrestrial Ecosystems. *BioScience*, *58*(9), 811–821. https://doi.org/10.1641/B580908

Lambert, Q., Bischoff, A., & Gros, R. (2024). *Effects of habitat restoration and solar panels on soil properties and functions in solar parks*. https://doi.org/10.1016/j.apsoil.2024.105614

Lorenz, K., & Lal, R. (2005). The Depth Distribution of Soil Organic Carbon in Relation to Land Use and Management and the Potential of Carbon Sequestration in Subsoil Horizons. *Advances in Agronomy*, *88*, 35. https://doi.org/10.1016/S0065-2113(05)88002-2

Ma, H., Mo, L., Crowther, T. W., Maynard, D. S., van den Hoogen, J., Stocker, B. D., Terrer, C., & Zohner, C. M. (2021). The global distribution and environmental drivers of aboveground versus belowground plant biomass. *Nature Ecology & Evolution 2021 5:8*, *5*(8), 1110–1122. https://doi.org/10.1038/s41559-021-01485-1

Marrou, H., Guilioni, L., Dufour, L., Dupraz, C., & Wery, J. (2013). Microclimate under agrivoltaic systems: Is crop growth rate affected in the partial shade of solar panels? *Agricultural and Forest Meteorology*, *177*, 117–132. https://doi.org/10.1016/j.agrformet.2013.04.012

Milne, E., Banwart, S. A., Noellemeyer, E., Abson, D. J., Ballabio, C., Bampa, F., Bationo, A., Batjes, N. H., Bernoux, M., Bhattacharyya, T., Black, H., Buschiazzo, D. E., Cai, Z., Cerri, C. E., Cheng, K., Compagnone, C., Conant, R., Coutinho, H. L. C., de Brogniez, D., … Zheng, J. (2015). Soil carbon, multiple benefits. *Environmental Development*, *13*, 33–38. https://doi.org/10.1016/J.ENVDEV.2014.11.005

Nippert, J. B., & Holdo, R. M. (2015). Challenging the maximum rooting depth paradigm in grasslands and savannas. *Functional Ecology*, *29*(6), 739–745. https://doi.org/10.1111/1365-2435.12390

Nippert, J. B., Knapp, A. K., Nippert, J. B., & Knapp, A. K. (2007). Soil water partitioning contributes to species coexistence in tallgrass prairie. *Oikos*, *116*(6), 1017–1029. https://doi.org/10.1111/J.0030-1299.2007.15630.X

Pérez-Ramos, I. M., Volaire, F., Fattet, M., Blanchard, A., & Roumet, C. (2013). Tradeoffs between functional strategies for resource-use and drought-survival in Mediterranean rangeland species. *Environmental and Experimental Botany*, *87*, 126–136. https://doi.org/10.1016/j.envexpbot.2012.09.004

Pierson, E. A., Mack, R. N., & Black, R. A. (1990). The effect of shading on photosynthesis, growth, and regrowth following defoliation for Bromus tectorum. *Oecologia*, *84*(4), 534–543.

Poorter, H., Niklas, K. J., Reich, P. B., Oleksyn, J., Poot, P., & Mommer, L. (2012). Biomass allocation to leaves, stems and roots: Meta-analyses of interspecific variation and environmental control. *New Phytologist*, *193*(1), 30–50. https://doi.org/10.1111/J.1469-8137.2011.03952.X

Rey Benayas, J. M., Newton, A. C., Diaz, A., & Bullock, J. M. (2009). Enhancement of biodiversity and ecosystem services by ecological restoration: A meta-analysis. *Science*, *325*(5944), 1121–1124. https://doi.org/10.1126/science.1172460

Schenk, H. J., & Jackson, R. B. (2002). Rooting Depths, Lateral Root Spreads and Below-Ground/Above-Ground Allometries of Plants in Water-Limited Ecosystems. *Source: Journal of Ecology*, *90*(3), 480–494. http://www.jstor.org/stable/3072232

Schwinning, S., & Sala, O. E. (2004). Hierarchy of responses to resource pulses in arid and semi-arid ecosystems. *Oecologia*, *141*(2), 211–220. https://doi.org/10.1007/s00442-004-1520-8

Sherrod, L. A., Dunn, G., Peterson, G. A., & Kolberg, R. L. (2002). Inorganic Carbon Analysis by Modified Pressure-Calcimeter Method. *Soil Science Society of America Journal*, *66*(1), 299–305. https://doi.org/10.2136/SSSAJ2002.2990

Sturchio, M. A., Kannenberg, S. A., & Knapp, A. K. (2024a). Agrivoltaic arrays can maintain semi-arid grassland productivity and extend the seasonality of forage quality. *Applied Energy*, 356,122418. https://doi.org/10.1016/j.apenergy.2023.122418

Sturchio, M. A., Kannenberg, S. A., Pinkowitz, T. A., & Knapp, A. K. (2024b). Solar arrays create novel environments that uniquely alter plant responses. *Plants, People, Planet*, *6*(6), 1522–1533. https://doi.org/10.1002/PPP3.10554

Sturchio, M. A., & Knapp, A. K. (2023). Ecovoltaic principles for a more sustainable, ecologically informed solar energy future. *Nature Ecology & Evolution 2023 7:11*, *7*(11), 1746–1749. https://doi.org/10.1038/s41559-023-02174-x

Sturchio, M. A., Macknick, J. E., Barron-Gafford, G. A., Chen, A., Alderfer, C., Condon, K., Hajek, O. L., Miller, B., Pauletto, B., Siggers, J. A., Slette, I. J., & Knapp, A. K. (2022). Grassland productivity responds unexpectedly to dynamic light and soil water environments induced by photovoltaic arrays. *Ecosphere*, *13*(12). https://doi.org/10.1002/ECS2.4334

Tilman, D., Reich, P. B., & Knops, J. M. H. (2006). Biodiversity and ecosystem stability in a decade-long grassland experiment. *Nature 2006 441:7093*, *441*(7093), 629–632. https://doi.org/10.1038/nature04742

Walston, L. J., Rollins, K. E., LaGory, K. E., Smith, K. P., & Meyers, S. A. (2016). A preliminary assessment of avian mortality at utility-scale solar energy facilities in the United States. *Renewable Energy*, *92*, 405–414. https://doi.org/10.1016/J.RENENE.2016.02.041

Wang, L., Jiao, W., MacBean, N., Rulli, M. C., Manzoni, S., Vico, G., & D'Odorico, P. (2022). Dryland productivity under a changing climate. *Nature Climate Change 2022 12:11*, *12*(11), 981–994. https://doi.org/10.1038/s41558-022-01499-y

Weaver, J. E. (1958). Summary and Interpretation of Underground Development in Natural Grassland Communities. *Ecological Monographs*, *28*(1), 55–78. https://doi.org/10.2307/1942275

Wilsey, B. J., & Wayne Polley, H. (2006). Aboveground productivity and root-shoot allocation differ between native and introduced grass species. *Oecologia*, *150*(2), 300–309. http://dx.doi.org/10.1007/s00442-006-0515-z

Wratten, S. D., Gillespie, M., Decourtye, A., Mader, E., & Desneux, N. (2012). Pollinator habitat enhancement: Benefits to other ecosystem services. *Ecosystems and Environment*, *159*, 112–122. https://doi.org/10.1016/j.agee.2012.06.020

Xu, Z., Zhou, G., & Shimizu, H. (2010). Plant responses to drought and rewatering. *Plant Signaling and Behavior*, *5*(6), 649–654. https://doi.org/10.4161/psb.5.6.11398

CHAPTER 3: BEYOND ENERGY PRODUCTION: QUANTIFYING TRADE-OFFS AND SYNERGIES AMONG ECOSYSTEM SERVICES IN A WORKING AGRIVOLTAIC LANDSCAPE

3.1 Summary

Agrivoltaic systems must balance renewable energy production with agricultural and ecological functions, yet comprehensive assessments of multiple ecosystem services remain rare. We evaluated how vegetation management and irrigation interacted with solar panel-induced microclimates to affect pollinator resources, forage production, carbon sequestration, and erosion control in a semi-arid grassland over three years.

Solar infrastructure created distinct microclimate zones with divergent ecosystem service provisioning. Open areas between panels supported 2.7× more floral resources and 45% higher biomass production than beneath panels, providing superior pollinator habitat and forage production. However, under-panel areas demonstrated 25% greater surface soil carbon stocks (0-15 cm) despite lower plant productivity, likely through reduced decomposition. Edge zones showed intermediate values for most services. Native vegetation plantings remained dominated by existing non-native rhizomatous pasture grasses regardless of seed mix, with native species achieving only 0.1-5.8% cover. Multifunctionality analysis revealed clear trade-offs among ecosystem services, with no single management strategy optimizing all services simultaneously. Traditional pasture maximized forage quality and productivity (80-84% greater than native treatments) but provided minimal floral resources, while forb-heavy native plantings supported 2.2× more flowers and higher biodiversity. Irrigation increased aboveground productivity by 11% and forage quality by 16% but failed to enhance soil carbon stocks and reduced floral

resources by 55%. Vegetation cover remained near-complete (>98%) across all treatments, indicating minimal erosion risk.

Solar arrays created a mosaic landscape where different microclimate zones optimized different services—pollinator resources in open areas, carbon sequestration beneath panels, and intermediate forage production at edges. This spatial complementarity suggests agrivoltaic systems can maintain aggregate ecosystem service provision through appropriate design and microclimate-specific management strategies. Active vegetation management and irrigation interventions at the full array scale showed limited efficacy within our three-year timeframe, suggesting passive management leveraging existing spatial heterogeneity may be more cost-effective than intensive interventions.

3.2 Introduction

The accelerating deployment of renewable energy infrastructure on agricultural lands presents both opportunities and challenges for managing multiple ecosystem services in working landscapes. Agrivoltaic systems, the co-location of solar photovoltaic panels with agricultural production, have emerged as a promising approach to address competing demands for land while potentially enhancing both energy and food security (Walston et al., 2022). However, the introduction of solar infrastructure fundamentally alters the spatial distribution of resources within agricultural ecosystems, creating novel environmental gradients that affect multiple ecological processes. Understanding how these infrastructure-induced gradients affect the provision of ecosystem services is critical for optimizing agrivoltaic design and management strategies.

Solar panels create predictable microclimate gradients through their modification of light availability, temperature regimes, and moisture patterns. Research consistently demonstrates that

photovoltaic installations can reduce photosynthetically active radiation by up to 89% directly beneath panels while creating intermediate conditions at panel edges (Li et al., 2025). These light gradients interact with altered precipitation patterns—where panels concentrate rainfall at drip edges—and modified wind exposure to generate a mosaic of microhabitats ranging from heavily shaded, moisture-variable zones to exposed areas between panel rows (Wu et al., 2022; Lambert et al., 2021). The ecological implications of these gradients extend beyond simple light reduction by restructuring plant communities, altering competitive dynamics, and modifying ecosystem functions across the installation. Recent work has shown that these altered conditions can affect carbon cycling, with reduced decomposition rates beneath panels potentially enhancing soil carbon sequestration in semi-arid systems (Toy et al., 2025).

The ecosystem services provided by agricultural lands encompass much more than food and energy production. Agricultural landscapes support critical pollination services valued at over $1.5 billion annually in the United States alone (Reilly et al., 2020), provide habitat for biodiversity conservation, regulate water and nutrient cycles, sequester carbon in soils and vegetation, and offer cultural value to nearby communities (Swinton et al., 2007; Robertson et al., 2014). The integration of solar infrastructure into these multifunctional landscapes raises fundamental questions about trade-offs and synergies among different ecosystem services. Can agrivoltaic systems simultaneously support renewable energy production, maintain agricultural productivity, enhance pollinator habitat, and provide other ecological benefits? Or do the novel environmental conditions created by solar panels necessitate prioritizing certain services at the expense of others?

Recent evidence suggests that the relationship between solar infrastructure and ecosystem service provision is neither uniformly positive nor negative, but rather depends on complex

interactions among panel design, environmental conditions, vegetation management, and the specific services under consideration. Studies in arid environments have documented enhanced crop yields under partial shading during drought conditions (Barron-Gafford et al., 2019), while research at solar installations has demonstrated potential for creating valuable pollinator habitat that could benefit surrounding agricultural lands (Walston et al., 2021). However, these benefits are not universal; the same infrastructure that enhances water availability in arid regions might reduce productivity in energy-limited environments, and vegetation communities that maximize pollinator resources may not optimize forage quality for livestock production.

The challenge of managing multiple ecosystem services in agrivoltaic systems is particularly acute in semi-arid rangelands, where solar development increasingly competes with livestock grazing for land use. These ecosystems naturally experience high spatial and temporal variability in resource availability, making them potentially resilient to novel disturbances but also sensitive to changes in key limiting factors (Wilmer et al., 2021). Understanding how the microclimate gradients created by solar panels interact with existing environmental heterogeneity to influence vegetation dynamics, forage production, and habitat quality is essential for developing management strategies that balance energy production with agricultural and ecological goals.

3.2.1 Knowledge Gaps and Theoretical Framework

Despite growing interest in agrivoltaic systems, significant gaps remain in our understanding of how these systems affect the provision of multiple ecosystem services. Most existing research has focused on single services, typically either crop/forage production or energy generation, without considering the full suite of ecosystem services or their interactions (Hernandez et al., 2019). This narrow focus limits our ability to identify trade-offs and synergies that emerge when managing for multiple objectives simultaneously.

The ecosystem services literature provides a robust framework for analyzing such trade-offs through concepts like ecosystem service bundles—sets of services that repeatedly occur together across landscapes (Raudsepp-Hearne et al., 2010). Agricultural systems often exhibit characteristic bundles where provisioning services (food, fiber) trade off against regulating services (water quality, carbon storage) and cultural services (recreation, aesthetics) (Finney et al., 2017). However, the application of bundle analysis to agrivoltaic systems remains unexplored, despite the clear potential for solar infrastructure to alter traditional service relationships. Understanding whether agrivoltaic systems create novel service bundles or simply reorganize existing ones has important implications for landscape planning and policy development.

Furthermore, most agrivoltaic research has treated solar installations as homogeneous units, reporting average values across entire arrays without considering the spatial heterogeneity created by panel infrastructure. This aggregated approach masks important variation in ecosystem service provision and may lead to incorrect conclusions about system performance. For example, claims about pollinator habitat value based on total flower production ignore the spatial distribution of resources and how this affects pollinator foraging behavior and habitat quality. Similarly, assessments of carbon sequestration potential that average across microclimate zones may miss important spatial patterns in soil carbon dynamics.

The temporal dimension of ecosystem service provision in agrivoltaic systems also remains poorly understood. While some studies have documented short-term responses to solar installation, few have tracked how services evolve as vegetation communities establish and adapt to altered conditions. The role of management interventions—such as irrigation, species

selection, or grazing regimes—in mediating ecosystem service provision requires systematic evaluation across multiple services rather than optimization for single objectives.

3.2.2 Study Objectives

This study addresses these knowledge gaps by comprehensively evaluating how the microclimate gradients created by solar panels affect multiple ecosystem services in a semi-arid grassland system. We apply the ecosystem service bundle framework to understand trade-offs and synergies among services across the spatial heterogeneity created by solar infrastructure. Specifically, we examine: (1) how solar panel-induced microclimates alter the provision of floral resources for pollinators across space and time; (2) the effects of these gradients on vegetation productivity and its implications for both forage production and erosion control; (3) changes in forage quantity and quality that affect livestock production potential; and (4) impacts on soil carbon sequestration as a climate regulating service.

By quantifying these services across the full gradient from open areas to panel edges to directly beneath panels, we aim to identify both trade-offs and potential synergies in ecosystem service provision. Furthermore, by testing how different vegetation communities (traditional pasture versus native plant assemblages) and management practices (irrigation versus dryland conditions) mediate these relationships, we seek to develop evidence-based recommendations for optimizing agrivoltaic systems to deliver multiple benefits to society. Our approach recognizes that understanding the spatial and temporal dynamics of ecosystem service provision is essential for designing and managing agrivoltaic systems as multifunctional landscapes that can meet renewable energy goals while maintaining agricultural production and ecological integrity.

3.3 Methods

3.3.1 Site Details

We established an experiment at Jack's Solar Garden, near the city of Longmont in Colorado, USA (40°07'18.9"N 105°07'49.9"W). The study site is in a cold steppe Koppen climate with a mean annual temperature of 9.7°C and 365 mm annual precipitation. The site has Nunn sandy clay loam soil (Fine, smectitic, mesic Aridic Argiustoll). Prior to the construction of the 1.3 MW solar PV array, the site was managed as flood-irrigated, perennial hay production for several decades. The dominant species on the site prior to construction were *Bromus inermis, Medicago sativa, Dactylis glomerata*, and *Trifolium pratense*. Construction of the solar PV array was completed in November 2020.

The 380W Boviet brand PV panels measuring 2 x 1 m were mounted in series on a single-axis-tracking system. Rows of panels are oriented North-South, and track East-West. The tracking system reaches a maximum angle of 45° to the East or West in the morning and evening, respectively. There is ~5.2 m of interspace between the mounting posts used to support the PV panels. Panel mounting height at the torque tube is 1.8 m above the ground.

3.3.2 Experimental Design

We established a randomized complete block design (RCBD) experiment within the array in May 2021, consisting of four blocks and six treatments. Each treatment was a factorial combination of two independent variables: Vegetation Community and Irrigation (Figure 3.1). The vegetation treatments were: 1) pasture, 2) balanced natives, and 3) forb dominant natives. The pasture treatment represented the pre-existing vegetation of the site that was left in place. The balanced natives and forb dominant natives treatments were established following a shallow roto-tilling in May 2021, followed by broadcast seeding at a rate of 60 seeds per square foot, and then raking and landscape rolling to increase seed to soil contact. The balanced natives mixture consisted of 50% native forbs and 50% native grasses by seed count and the forb dominant

natives mixture contained 80% native forbs and 20% native grasses by seed count. Seed mix composition and seeding rates are included in the supplemental materials (Table S1). The irrigation treatments were: 1) irrigated and 2) dryland. The irrigated treatment received 10 mm of supplemental irrigation per week from May through September, totaling 260 mm annually, administered via drip tape. The drip tapes were arranged evenly across the plots to ensure consistent water distribution, creating a grid of drip emitters approximately every 60 cm. In contrast, the dryland treatment did not receive any supplemental irrigation, relying entirely on natural precipitation.

Each plot was subdivided into four distinct microclimates created by the solar PV infrastructure. These microclimates, which were our experimental units, were replicated across all treatments and blocks (Figure 3.2). Annual climate data was obtained from the Colorado Climate Center Longmont 2 ESE station (Colorado Climate Center, 2025).

Microclimate-level measurements were aggregated to plot-scale values using area-weighted averages based on the proportional spatial extent of each microclimate position within solar array plots. Weights were determined from array dimensions and panel configuration: Open areas between panel rows represented 50% of plot area, Under-panel positions 27%, and East Edge and West Edge positions each 11.5%. For each plot, the area-weighted mean was calculated as the sum of microclimate-specific values multiplied by their respective weights, divided by the sum of weights for available positions. This approach accounts for the unequal spatial distribution of microclimate conditions within plots and provides plot-level estimates comparable to traditional agronomic measurements while preserving the spatial heterogeneity information available at the microclimate scale.

3.3.3 Data Collection

We quantified six ecosystem services across the agrivoltaic array using multiple indicators. Services were selected to represent key agricultural, ecological, and climate regulation functions: pollinator resources (total flower abundance and floral diversity), erosion control (soil cover), plant community biodiversity (Shannon diversity index, species richness, and functional group composition), forage quality (acid detergent fiber, crude protein content, dry matter digestibility), forage productivity (annual aboveground biomass), and soil carbon storage (SOC stock).

3.3.4 Plant Community Cover and Composition

Plants were identified to species and percent cover was visually estimated by two observers in a 1 m x 7.5 m quadrat in each experimental unit. Plant community surveys were conducted in August 2022, May 2023, July 2023, and September 2023.

3.3.5 Floral Resource Surveys

All flowering plants were identified to species and their flowers were counted once per week from May to October in a 1m x 7.5m area in each experimental unit. Flowers were defined according to the methods of Helle (2021) in order to account for differences in inflorescence morphology.

3.3.6 Aboveground Biomass

Aboveground biomass was harvested in 2021 and 2023. Biomass was harvested in June and September for pasture vegetation to simulate the historical management of the study site. For the two Native vegetation treatments, biomass was harvested only once in September at peak biomass to estimate forage productivity. Within each treatment plot we harvested 0.5 m^2 of vegetation at 7.5 cm above the soil surface. These samples were then dried in an oven at 55°C until constant mass was achieved and then weighed.

3.3.7 Forage Quality

A SpectraStar 2600 XT NIR analyzer (Unity Scientific, KPM Analytics, Westborough MA) was used to assess aboveground biomass for nutritional quality as a livestock feed source. Briefly, each dry aboveground biomass sample was first ground to 2 mm using a Wiley mill and then subsequently ground to 0.5 mm using a cyclone grinder. After grinding, one small subsample was analyzed using the NIRS set to the "Grass Forage" standard. Data obtained included Crude Protein (CP), Acid detergent fiber (ADF), Starch, andIn vitro true dry matter digestibility at 30 hours (DMD).

3.3.8 Soil Organic Carbon (SOC)

One soil sample was collected in each plot at 0-15 cm and 15-30 cm depths using an auger with a 7 cm diameter in October 2023 at each observational unit. Two cores were composited per sample. Samples were air dried, sieved to 8 mm, and a representative subsample was sieved to 2 mm. The subsamples were dried to constant mass at 55°C, roller ground for 24 hrs, and analyzed for total C and N using standard combustion analysis (Velp CN 802 Analyzer, VELP Scientific Inc., Deer Park, NY). Soil inorganic C content was measured using the pressure-calcimeter method of Sherrod et al. (2002). Briefly, HCl was added to soils in a sealed container to evolve CO_2 gas. The volume of this gas was then measured by the pressure built up in the sealed container and converted to C content, which was then subtracted from total C values to calculate total organic C.

3.3.9 Statistical Analysis

All statistical analyses were conducted in R version 4.3.0 using mixed-effects models to account for the randomized complete block design. Response variables were assessed for normality using Shapiro-Wilk tests and Q-Q plots, with homoscedasticity evaluated through

residual diagnostics using the DHARMa package. Two general model structures were used across analyses. Plot-scale models included Vegetation Treatment, Irrigation Treatment, and their interaction as fixed effects with Block as a random effect. Microclimate-scale models added Microclimate Position as a fixed effect along with its interactions with Vegetation and Irrigation and a random effect for Block. Specific modifications to these structures are detailed below.

Multiple model types were employed depending on data structure: Gaussian linear mixed models (LMMs) for normally distributed continuous data, Poisson generalized linear mixed models (GLMMs) for count data, zero-inflated negative binomial models (glmmTMB package) for count data with >30% zeros, and Tobit regression for right-skewed data. Transformations were applied when assumptions were violated: square-root for positively skewed count data and functional group cover with <30% zeros, and reciprocal for strongly right-skewed proportions. All models were fitted using REML = FALSE with Kenward-Roger degrees of freedom approximation. Pairwise comparisons for significant main effects used estimated marginal means with Tukey adjustment (emmeans package), and effect sizes were calculated using Cohen's d.

For community cover and composition, temporal covariates (days since experiment start) were added to both model structures. Total vegetation cover, which showed extreme ceiling effects (74% of observations at 100%), was analyzed using Tobit regression. Shannon diversity was calculated at the microclimate level then area-weighted to plot level for plot-scale analysis. Floral resource models added temporal covariates (polynomial day-of-year, year) to the general structures. Zero-inflation in abundance models was predicted by vegetation treatment and microclimate position. Forage quality models added Harvest Date as a fixed effect along with its interactions with other factors, and included Year as an additional random effect. The Vegetation Treatment × Harvest Date interaction was excluded as only pasture plots were harvested in

summer. Soil organic carbon was measured at two depth increments (0-15 cm and 15-30 cm) and converted from kg/m³ to Mg/ha. Both model structures added Depth as a fixed effect. The microclimate-scale model was simplified to include only Microclimate × Depth, Vegetation Treatment × Depth, Irrigation Treatment × Depth, and selected two-way interactions. Year was excluded as all treatment data were collected in 2023. Baseline comparisons used an augmented dataset approach where 2021 baseline data were added to 2023 treatment data as a pseudo-level of the treatment factor, with custom contrasts testing each 2023 treatment level against baseline separately for each depth increment and for total soil carbon (0-30 cm). Statistical significance was assessed at $\alpha = 0.05$, with baseline comparison significance levels denoted as * $p<0.05$, ** $p<0.01$, *** $p<0.001$.

3.3.10 Ecosystem Service Multifunctionality Analysis

We selected individual indicators of the six ecosystem services to assess multifunctionality and identify trade-offs among services using multiple indicators. The services selected and their indicators were: pollinator resources (total flower abundance), erosion control (soil cover), plant community biodiversity (Shannon diversity index), forage quality (crude protein content), forage productivity (annual aboveground biomass), and soil carbon sequestration (SOC stock). Total flower abundance was chosen over floral diversity metrics as it directly quantifies the resource pool available to pollinators, with higher abundance supporting larger and more diverse pollinator populations regardless of plant species composition. Total vegetation cover was selected as the primary indicator of erosion control because it represents the physical barrier protecting soil from raindrop impact and water runoff, which are the dominant erosion mechanisms in this system. Shannon diversity index was preferred over species richness alone because it incorporates both the number of species and their relative

abundances, providing a more comprehensive assessment of community structure and functional diversity. Crude protein content was chosen as the forage quality indicator because protein is typically the primary limiting nutrient for livestock production in rangeland systems and is a key determinant of animal growth and reproduction, whereas other quality metrics like fiber and digestibility are secondary considerations. Annual aboveground biomass directly measures the quantity of forage available for livestock and is the standard metric for productivity in grazing systems. Soil organic carbon stock across the 0-30 cm profile was selected over depth-specific measurements because it represents the net carbon sequestration potential of the system and captures both surface accumulation and subsurface dynamics observed in this study.

For each service, we calculated mean values by vegetation treatment (Balanced Natives, Forb Heavy Natives, Pasture), irrigation treatment (Dryland, Irrigated), and microclimate position (open, under, east edge, west edge). Annual biomass production was adjusted to account for harvest frequency differences, with pasture values doubled to reflect biannual harvest versus single annual harvest for native treatments. SOC stocks were averaged across both sampling depths (0-15 and 15-30 cm) to capture the full root zone dynamics.

To enable cross-service comparison, we standardized all values to a 0-1 scale using min-max normalization across all treatment combinations. This approach preserved the relative differences among treatments while allowing services measured in different units to be visualized simultaneously. We generated radar plots using the fmsb package to visualize multifunctionality patterns, with vertices representing individual ecosystem services and distance from center indicating relative performance (0 = minimum observed, 1 = maximum observed).

3.4 Results

3.4.1 Community Cover and Composition

Overall, vegetation cover was near 100% across all treatments and microclimate positions, with the only exception being a 4% reduction in areas directly under solar panels ($p < 0.001$; Figure 3.3D).

Plant community diversity patterns diverged between spatial scales. At the microclimate level, under-panel areas had 29% lower Shannon diversity than open areas and 27% lower than edge positions ($p < 0.001$; Figure 3.3A). At the plot scale, vegetation treatment significantly affected diversity ($p < 0.001$; Figure 3.3B), with balanced native plots having 31% lower diversity than forb heavy natives ($p = 0.005$) and 40% lower than pasture ($p < 0.001$). The microclimate × vegetation × irrigation interaction ($p < 0.001$; Figure 3.3D) indicated irrigation increased diversity in pasture plots by 34% but only in open and edge positions, with minimal effect under panels or in native treatments. Temporal increases in diversity ($p < 0.001$ at microclimate scale, $p = 0.004$ at plot scale) were strongest in edge positions, which gained 27% over the study period compared to 20% in under-panel areas.

Species richness exhibited the strongest microclimate effect. Under-panel areas supported 27% fewer species than open areas and 25% fewer than edge positions ($p < 0.001$; Figure 3.4A). The microclimate × vegetation interaction ($p = 0.001$; Figure 3.3D) revealed microclimate effects were strongest in native treatments: forb-heavy natives showed a 37% reduction under panels versus open areas, while pasture maintained consistent richness across microclimates (13% variation). The microclimate × irrigation interaction ($p = 0.036$; Figure 3.4D) indicated irrigation reduced richness by 18% in open areas but increased it by 9% under panels.

Plot-level models revealed clearer treatment hierarchies. Forb-heavy natives supported 75% more species than pasture and 30% more than balanced natives (all $p < 0.001$; Figure 3.4B). Irrigation reduced richness by 14% overall ($p = 0.005$; Figure 3.4C), but the vegetation ×

irrigation interaction ($p = 0.023$; Figure 3.4D) showed this reduction occurred primarily in native treatments (22% decrease) with minimal effect in pasture (7% decrease). All treatments showed temporal increases ($p < 0.001$), with forb-heavy natives gaining 2.1 species versus 0.8 species in pasture plots.

Vegetation and irrigation treatments influenced the relative abundance of plant functional groups at the plot level. Non-native rhizomatous grasses outcompeted other plant groups where soil was disturbed and native species planted, averaging 86% cover across native treatments under both dryland and irrigated conditions (VegTreatment: $p < 0.001$; Figure 3.5). In contrast, non-native clump grasses were 2.7-fold more abundant in irrigated pasture (56% cover) compared to dryland pasture (21% cover), while rhizomatous grass cover was reduced by 47% with irrigation in pasture treatments (VegTreatment × IrrigTreatment: $p < 0.001$; Figure 3.5). Native forb establishment was limited, reaching only 5.7% cover in forb-heavy native dryland plots. Weedy forb cover remained low throughout (< 5%), but increased over time ($p < 0.001$) and was 65% lower under irrigation ($p < 0.001$; Figure 3.3).

3.4.2 Floral Resources

The actively flowering plant community was dominated by a mix of native prairie species and agricultural taxa. The five most abundant species by total flower production were *Medicago sativa* (7,606 floral units, 149 observations), *Thelesperma filifolium* (4,450 floral units, 329 observations), *Ratibida columnifera* (3,465 floral units, 351 observations), *Convolvulus arvensis* (3,242 floral units, 217 observations), and *Gaillardia aristata* (2,891 floral units, 273 observations). The community exhibited a core group of seven frequently occurring species (>10% frequency), twelve occasional species (1-10% frequency), and four rare species (<1% frequency). Temporal patterns showed establishment dynamics with minimal flowering in 2021

(mean = 1.8 flowers/unit area), increasing to 4.5 flowers in 2022 and 7.2 flowers in 2023 ($p < 0.001$).

Microclimate position strongly influenced flower production ($p < 0.001$; Figure 3.6A), with open areas between panels supporting 2.7-fold more flowers than under-panel positions ($p < 0.001$) and 1.8-fold more than west edge positions ($p < 0.001$). East edge positions showed intermediate abundance, not differing significantly from open areas but supporting 2-fold more flowers than under-panel areas ($p = 0.024$).

The microclimate × vegetation interaction ($p < 0.001$; Figure 3.6D) revealed treatment-specific spatial patterns: under-panel flower suppression was partially mitigated in forb-heavy native ($p = 0.002$) and pasture treatments ($p = 0.022$), which showed only 60% reduction versus 85% reduction in balanced native plots. The microclimate × irrigation interaction ($p < 0.001$; Figure 3.6D) indicated irrigation increased under-panel flowering 3-fold while having minimal effect in open areas (10% increase).

At the plot level, vegetation treatment significantly affected floral production ($p < 0.001$; Figure 6B), with forb-heavy natives producing 60% more flowers than balanced natives ($p = 0.008$) and 2.2-fold more than pasture ($p < 0.001$). Counter to expectations, dryland conditions supported 83% higher flower abundance than irrigated plots at the plot scale, though this irrigation effect was not significant ($p = 0.130$; Figure 3.6C). The vegetation × irrigation interaction was non-significant at the plot scale.

Flowering species richness patterns paralleled floral abundance but with distinct treatment responses. At the microclimate level, open areas supported 3.5-fold more flowering species than under-panel positions and 1.9-fold more than west edges (both $p < 0.001$; Figure 3.7A), while east edges showed intermediate richness not differing from open areas. The

microclimate × vegetation interaction ($p < 0.001$; Figure 3.7D) revealed forb-heavy natives maintained 40% higher richness than other treatments specifically in open and edge positions, with all treatments converging to similarly low richness (0.4-0.6 species) under panels.

Plot-level richness showed clearer treatment separation ($p < 0.001$; Figure 3.7B), with forb-heavy natives supporting 49% more flowering species than balanced natives and 3.3-fold more than pasture (both $p < 0.001$). The vegetation × irrigation interaction ($p = 0.031$; Figure 3.7D) indicated irrigation reduced richness by 23% in balanced native plots but increased it by 15% in pasture, with no effect in forb-heavy natives. Irrigation showed no significant main effect at the plot scale ($p > 0.05$; Figure 3.7C). Temporal increases ($p < 0.001$) were consistent across treatments, with 0.5-0.7 species gained per year after establishment.

3.4.3 Forage Production

Annual biomass production showed strong vegetation treatment effects ($p < 0.001$). Pasture produced 84% more biomass than balanced natives and 80% more than forb-heavy natives at the plot scale (Figure 3.8B). The two native treatments did not differ significantly from each other. Microclimate position strongly influenced biomass production ($p < 0.001$), with under-panel positions producing 31% less biomass than open areas, 33% less than east edge positions, and 28% less than west edge positions. Open, east edge, and west edge positions did not differ significantly from each other (Figure 3.8A). Irrigation showed a marginal main effect at the plot scale ($p = 0.060$), with irrigated plots producing 11% more biomass than dryland conditions, though this difference was not statistically significant in post-hoc comparisons (Figure 3.8C).

The microclimate × irrigation interaction was significant ($p = 0.002$), with under microclimates showing greater response to irrigation than other microclimate positions.

Irrigation increased biomass under panels by 43%, while other positions showed negligible responses averaging only 0.8% (range: -6% to +5%) (Figure 3.8D). This differential response suggests that water becomes critically limiting in the light-stressed under-panel environment, where irrigation can substantially compensate for reduced photosynthetic capacity. In contrast, microclimates that do not experience precipitation interception showed no meaningful response to supplemental water.

3.4.4 Forage Quality

Vegetation treatment significantly affected forage quality at both spatial scales, with pasture outperforming native treatments for most metrics. At the plot scale, pasture contained 36% higher crude protein than balanced natives ($p < 0.001$) and 24% higher than forb-heavy natives ($p < 0.001$; Figure 3.9B). The two native treatments did not differ significantly in crude protein content ($p = 0.357$). Acid detergent fiber showed the inverse pattern, with pasture exhibiting 8.9% lower ADF than balanced natives (41.28% vs 45.31%; $p < 0.001$) and 8.2% lower than forb-heavy natives (41.28% vs 44.94%; $p < 0.001$), indicating superior digestibility. Dry matter digestibility at 30 hours (DMD) was 6.7% higher in pasture than balanced natives (75.28% vs 70.53%; $p = 0.036$) and 7.3% higher than forb-heavy natives (75.28% vs 70.13%; $p = 0.021$). The two native treatments did not differ for ADF or DMD (both $p > 0.41$).

Native treatments demonstrated superior starch accumulation at the plot scale ($p < 0.001$), with balanced natives containing 49% more starch than pasture (3.86% vs 2.59%; $p < 0.001$) and forb-heavy natives containing 46% more than pasture (3.78% vs 2.59%; $p < 0.001$). Balanced natives and forb-heavy natives showed equivalent starch content ($p = 0.893$).

Solar panel microclimate significantly influenced crude protein ($p = 0.005$) but not ADF, starch, or DMD (all $p > 0.06$). Crude protein was highest under panels, exceeding east edge

positions by 21% ($p = 0.018$) and west edge positions by 15% ($p = 0.047$; Figure 3.9C). Open area protein content was intermediate and did not differ significantly from under-panel positions ($p = 0.365$) or edges ($p = 0.290$). This under-panel protein enhancement occurred alongside biomass suppression in the same locations.

Irrigation effects varied by response variable and scale. At the plot scale, irrigation increased crude protein by 19% ($p < 0.001$). However, this main effect was modified by a vegetation treatment interaction at the microclimate scale ($p = 0.015$; Figure 3.9D), where irrigation increased protein by 39% in forb-heavy natives but only 14% in balanced natives and 7% in pasture. At the plot scale, irrigation did not effect ADF ($p = 0.397$). Dryland conditions promoted starch accumulation, with 13% higher starch under dryland versus irrigated treatments at the plot scale ($p = 0.001$). Digestibility showed 5.0% higher DMD under irrigation at the plot scale ($p = 0.019$), though a microclimate-scale vegetation × irrigation interaction ($p = 0.032$) indicated this effect varied by treatment, with minimal irrigation effects in native treatments but reductions in pasture.

Harvest timing strongly influenced forage quality. Summer harvests showed 11% lower ADF than fall harvests (40.93% vs 45.67%; $p < 0.001$), indicating improved fiber quality during active growth. Digestibility was 19% higher in summer harvests (DMD: 78.73% vs 66.15%; $p < 0.001$), while fall harvests accumulated 36% more starch (3.73% vs 2.74%; $p < 0.001$). Crude protein showed no seasonal variation ($p = 0.466$).

3.4.5 Soil Organic Carbon

Soil depth was the dominant factor controlling SOC distribution ($p < 0.001$), with surface soils containing substantially more SOC than deeper layers (Figure 3.10A-C). At the microclimate scale position significantly influenced SOC stocks ($p < 0.001$), and this effect

varied by depth (Microclimate × Depth: $p = 0.003$). Vegetation treatment and irrigation treatment were not significant ($p = 0.069$ and $p = 0.505$, respectively).

All microclimate positions and treatments exhibited significant vertical redistribution of soil carbon from 2021 baseline to 2023, with surface layer accumulation partially or fully offset by subsurface depletion (Figure 3.10A). In the 0-15 cm layer, under-panel positions showed the strongest accumulation at 25% above baseline ($p < 0.001$), while open areas increased by 8% ($p < 0.001$), east edges by 5% ($p = 0.038$), and west edges showed no significant change ($p = 0.247$). Conversely, all positions lost 15-25% of carbon from the 15-30 cm layer (all $p \leq 0.004$), with open areas showing the largest proportional loss at 25% ($p < 0.001$).

Across the full 0-30 cm profile, under-panel positions were the only microclimate showing net carbon accumulation at 8% above baseline ($p < 0.001$), while all other positions showed 5-6% net depletion (all $p \leq 0.003$; Figure 3.10A).

Vegetation treatments showed similar vertical redistribution patterns at the plot scale (Figure 3.10B). Surface layers increased 14-17% under balanced natives and pasture (both $p < 0.001$), while forb-heavy natives showed no significant surface change ($p = 0.056$). All vegetation treatments lost 18-24% of carbon from deeper layers (all $p < 0.001$). Across the 0-30 cm profile, only forb-heavy natives showed significant net change, declining 6% from baseline ($p < 0.001$), while balanced natives and pasture showed no significant net change ($p = 0.135$ and $p = 0.093$, respectively).

Irrigation treatments exhibited universal vertical redistribution (Figure 3.10C). Both dryland and irrigated treatments accumulated approximately 12% more carbon in surface soils (both $p < 0.001$) while losing 18-23% from deeper layers (both $p < 0.001$). Across the full

profile, irrigated treatments showed 3% net loss from baseline ($p = 0.007$), while dryland showed no significant net change ($p = 0.293$).

The agrivoltaic installation induced system-wide vertical redistribution of soil carbon rather than net accumulation or loss across most positions and treatments. Under-panel positions uniquely showed both the strongest surface enrichment and the smallest subsurface depletion, resulting in net carbon gain across the soil profile.

3.4.6 Ecosystem Multifunctionality

Our multifunctionality analysis revealed distinct ecosystem service patterns across the agrivoltaic landscape, with no single treatment maximizing all ecosystem services simultaneously (Figure 3.11).

Vegetation treatments showed clear functional trade-offs (Figure 3.11A). Pasture maximized provisioning services, achieving the highest forage quality and productivity, both greater than native treatments. Conversely, Forb Heavy Natives optimized supporting services, producing more floral resources than Pasture while maintaining intermediate biodiversity levels. Balanced Natives was broadly similar to Forb Heavy Natives, but with lower biodiversity and floral resources.

Irrigation effects varied by service type (Figure 3.11B). Irrigated treatments maintained marginally higher vegetation cover compared to dryland conditions, increased forage quality, and plant diversity. However, dryland conditions unexpectedly supported greater floral resources, suggesting that moderate water stress may benefit native forb establishment.

Microclimate positions within the array created the strongest functional zonation (Figure 3.11C). Open areas between panels functioned as pollinator resource hotspots, supporting more flowers than under-panel areas. Under-panel positions demonstrated the highest soil carbon

stocks, greater than open areas, alongside higher forage quality, despite large reductions in productivity and floral resources. East edge positions maximized forage productivity, suggesting these transitional zones provide unique ecological value. West edge positions showed intermediate values for most services.

3.5 Discussion

5.5.1 Spatial Heterogeneity as a Driver of Ecosystem Service Provision

Our comprehensive assessment of ecosystem services in an agrivoltaic landscape reveals that solar infrastructure reorganizes, rather than uniformly enhances or degrades, ecosystem service provision across space. The microclimate effects—with open areas supporting 2.67× more floral resources but under-panel areas maintaining 25% greater soil carbon stocks—demonstrate that agrivoltaic systems create distinct functional zones where different services are optimized. This spatial complementarity within solar installations aligns with ecosystem service bundle theory, which recognizes that services often show non-random associations across landscapes (Raudsepp-Hearne et al., 2010).

The trade-offs we observed between provisioning services (forage production and quality), regulating services (carbon sequestration, erosion control), and supporting services (pollinator habitat, biodiversity) exemplify the challenge of managing for multifunctionality in working landscapes (Bennett et al., 2009). Our finding that no single microclimate or management strategy optimized all services simultaneously reflects fundamental ecological constraints documented across diverse agroecosystems (Finney et al., 2017). However, unlike commercial agricultural systems where trade-offs often require landscape-level segregation of functions, the fine-scale spatial heterogeneity created by solar arrays enables service complementarity within a single field. Our results suggest that embracing the spatial

heterogeneity created by solar infrastructure and managing different zones for different primary services may maximize landscape-level multifunctionality.

The persistence of these spatial patterns across three years and multiple management interventions suggests that microclimate effects influence ecosystem service provision regardless of vegetation or irrigation treatments. Under-panel areas consistently showed reduced productivity metrics (15% lower biomass) but enhanced soil carbon storage through reduced decomposition—a pattern that persisted across all vegetation types. This finding extends recent work by Sturchio et al. (2024) at the same site, who documented altered carbon cycling dynamics beneath panels, and suggests that the carbon sequestration potential of agrivoltaic systems may be underappreciated in current climate mitigation strategies.

3.5.2 Vegetation Dynamics: Legacy Effects Overwhelm Design Intentions

The dominance of pre-existing non-native rhizomatous grasses (75% cover) across all vegetation treatments, including those subjected to intensive tillage and native seeding, demonstrates the powerful role of legacy effects in constraining community assembly. This result aligns with extensive restoration ecology literature showing that established perennial grasses, particularly rhizomatous species, resist displacement even under substantial environmental change (Bakker & Wilson, 2004; Grman et al., 2013). Critically, the similar vegetation composition between control plots (outside the array) and treatment plots (within the array) indicates that competitive exclusion by established vegetation, rather than solar-induced stress, was the primary barrier to native establishment.

The differential success of plant functional groups—with native forbs achieving modest establishment (up to 5.8% cover) while native grasses completely failed (one individual observed)—suggests that functional trait filtering operates differently under agrivoltaic

conditions. This pattern may reflect the intersection of light limitation beneath panels with competitive pressure from established grasses, creating a narrow regeneration niche that only certain forb species can exploit. The strong negative correlation between rhizomatous and clump grass cover ($r = -0.985$) further illustrates how competitive hierarchies established before solar installation continue to structure communities despite altered environmental conditions.

These findings have important implications for the growing interest in establishing pollinator habitat at solar installations. Our results suggest that successful native plant establishment may require more aggressive site preparation than typically employed, potentially including herbicide application or solarization to reduce the competitive advantage of established vegetation. Alternatively, working with existing vegetation while selectively introducing compatible native forbs may represent a more realistic strategy for enhancing ecological value while maintaining agricultural functionality.

3.5.3 Reconsidering Pollinator Habitat Value in Solar Landscapes

While recent studies have promoted solar installations as valuable pollinator habitat (Walston et al., 2021), our spatially-explicit analysis reveals important nuances that complicate this narrative. The 63% reduction in floral resources beneath panels and 35-39% reduction at edges means that approximately 50% of the array area provided suboptimal pollinator resources. This spatial heterogeneity could create an ecological trap if pollinators are attracted to arrays by abundant edge flowering but then experience resource limitation when foraging in interior zones.

The phenological compression we observed beneath panels—with synchronized flowering peaks around day 189—contrasts with studies from mesic regions that documented extended flowering periods under shade (Adeh et al., 2018). This discrepancy likely reflects our semi-arid climate, where water limitation beneath panels (due to panel interception of

precipitation) overrides potential benefits of temperature moderation. The concentration of flowering in open areas between panels suggests these zones function as pollinator resource hotspots that may subsidize foraging in adjacent resource-poor areas, similar to dynamics observed in fragmented agricultural landscapes (Scheper et al., 2013).

The dominance of non-native species in the floral community, particularly *Medicago sativa*, raises questions about conservation value. While these species support generalist pollinators and may provide ecosystem services like crop pollination, they fail to provision specialist pollinators requiring native host plants. Future research should examine whether the patchy resource distribution created by solar arrays affects pollinator community composition, foraging efficiency, and ultimately, pollination services to adjacent agricultural lands.

3.5.4 Implications for Livestock Integration and Forage Management

The superior performance of established pasture over native treatments across all forage quality metrics (27% higher digestibility, 45% greater biomass, 43% higher crude protein) highlights fundamental tensions between ecological restoration goals and agricultural production in agrivoltaic systems. This finding adds nuance to optimistic reports of successful livestock grazing in solar arrays (Marrou et al., 2013; Andrew et al., 2021), suggesting that forage quality and quantity trade-offs must be explicitly considered in system design.

The spatial reorganization of forage quality—with crude protein enhanced by 21% beneath panels despite 36% biomass reduction—presents both challenges and opportunities for grazing management. This pattern mirrors silvopastoral systems where shade-induced changes in plant physiology improve forage quality (Jose, 2009), potentially offsetting quantity reductions through improved digestibility and protein content. The microclimate × irrigation interaction we observed, where water supplementation provided maximum benefit in dry under-panel zones

while showing negligible effects in open areas, suggests that targeted irrigation strategies could optimize the spatial distribution of forage resources.

From a practical grazing perspective, the heterogeneous forage landscape created by solar arrays is unlikely to require adaptive management strategies so long as aggregate forage production and quality is sufficiently high. The high mobility of grazing animals in combination with the small spatial scale of microclimate driven forage differences means that animal behavior will likely compensate for the effects of heterogeneity.

3.5.5 Management Implications: Embracing Heterogeneity

Our finding that no single management intervention enhanced all ecosystem services simultaneously within our three-year timeframe challenged the assumption that active management can overcome structural constraints imposed by solar infrastructure. The limited efficacy of irrigation (32% productivity increase but no soil carbon benefit) and native seeding efforts suggest that passive management leveraging existing vegetation and natural processes may be more cost-effective than intensive interventions.

The spatial segregation of ecosystem services across microclimate zones points toward a zoning approach to agrivoltaic management: (1) open areas optimized for pollinator resources or maximum forage production, (2) under-panel zones managed for carbon sequestration with shade-tolerant species, and (3) edge zones maintained as multifunctional buffers supporting intermediate levels of multiple services. This spatially explicit strategy aligns with precision agriculture principles but requires abandoning uniform management prescriptions in favor of zone-specific approaches.

Economic considerations further support this differentiated management strategy. The high cost of interventions like irrigation and reseeding, combined with their limited effectiveness

in this study, suggests that economic optimization should focus on stacking revenue streams (energy production, grazing leases, carbon credits, habitat payments) rather than maximizing any single service. However, policy frameworks must evolve to recognize and compensate for the full range of ecosystem services provided by well-designed agrivoltaic systems.

3.6. Conclusion: Toward Multifunctional Energy Landscapes

Our results demonstrate that agrivoltaic systems represent a novel form of multifunctional landscape where renewable energy infrastructure creates predictable patterns of ecosystem service provision. Rather than viewing the spatial heterogeneity created by solar panels as a management challenge to overcome, our findings suggest this heterogeneity represents an opportunity to strategically allocate different zones for different primary ecosystem services while maintaining landscape-level multifunctionality.

This perspective shifts the conversation from whether agrivoltaic systems can maintain agricultural productivity—clearly, they reorganize rather than eliminate it—to how they can be designed and managed to optimize the portfolio of ecosystem services society demands from working landscapes. The consistent spatial patterns we documented across treatments suggest that panel design parameters (height, spacing, tracking systems) may be more important than vegetation management for determining ecosystem service outcomes so long as certain minimum thresholds of vegetation community health are met. Future research should examine how alternative array configurations affect the spatial distribution and magnitude of ecosystem services, potentially identifying designs that minimize trade-offs while maximizing synergies.

As pressure intensifies to deploy renewable energy infrastructure while maintaining agricultural production and ecological integrity, our results provide evidence that agrivoltaic systems can contribute to multifunctional landscape management. However, realizing this

potential requires moving beyond simplistic assessments focused on single services or average values to embrace the spatial complexity these systems create. Policy frameworks, economic incentive structures, and management strategies must evolve to recognize that the value of agrivoltaic systems lies not in their ability to maximize any single ecosystem service, but in their capacity to provide diverse services across a heterogeneous landscape mosaic.

3.7 Tables

Table 3.1. P values of all models for treatment effects (microclimate, vegetation, and irrigation, plus all interactions.

Response Variable	Microclimate	Vegetation	Irrigation	Micro×Veg	Micro×Irrig	Veg×Irrig	Micro×Veg×Irrig
Total Cover	<0.001***	0.161	0.003**	0.194	<0.001***	0.944	—
Shannon Diversity	<0.001***	<0.001***	0.426	0.076.	0.003**	0.149	<0.001***
Species Richness	<0.001***	0.013*	0.389	0.001**	0.036*	0.235	0.017*
Flower Abundance	<0.001***	0.878	0.868	0.011*	0.001**	0.461	—
Flowering Species Richness	<0.001***	<0.001***	0.627	<0.001***	<0.001***	0.739	—
Biomass	<0.001***	0.057.	0.782	0.056.	0.005**	0.807	0.329
Crude Protein	0.005**	<0.001***	<0.001***	0.612	0.950	0.015*	0.906
ADF	0.065.	<0.001***	0.014*	0.654	0.107	0.448	0.778
Starch	0.571	<0.001***	0.003**	0.840	0.080.	0.585	0.203
Digestibility	0.184	<0.001***	0.001**	0.688	0.457	0.032*	0.367
Soil Organic Carbon	<0.001***	0.008**	0.372	0.130	0.476	0.073.	0.180

3.8 Figures

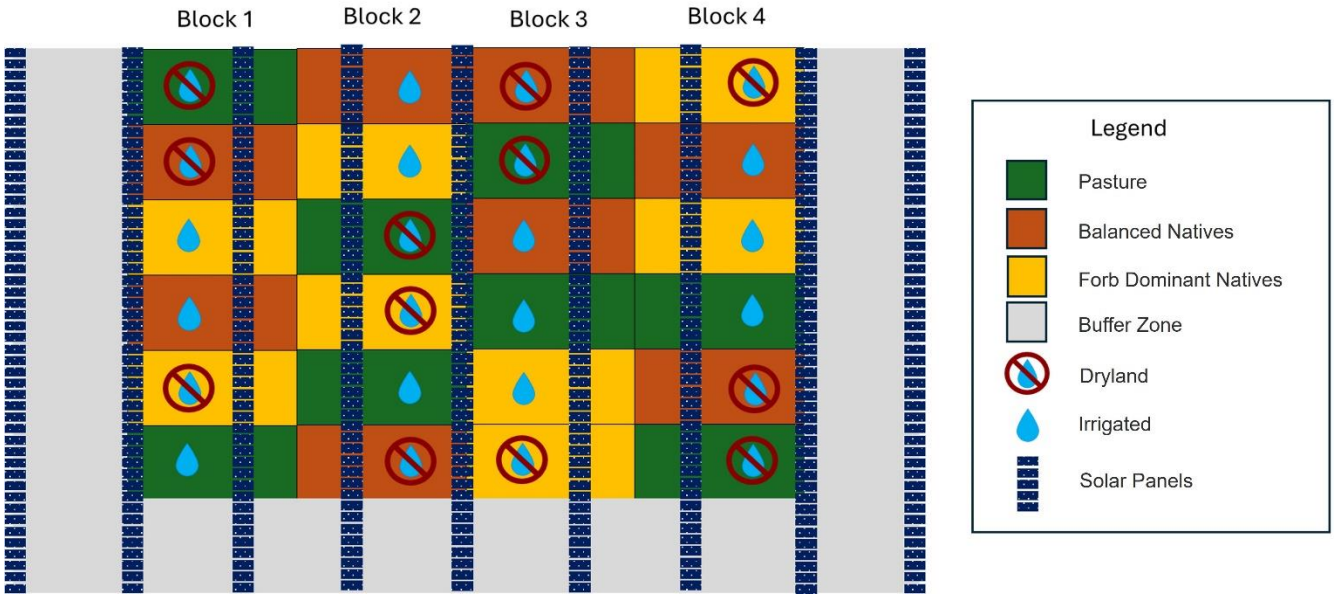

Figure 3.112. Diagram of our experimental design. There was not a buffer strip to the North of our experimental plots due to site constraints. Irrigation mainlines ran N-S between blocks 1 and 2 and blocks 3 and 4. Lateral drip tape branched off of the mainlines to deliver irrigation to the experimental plots. Adapted from Toy et al. 2025

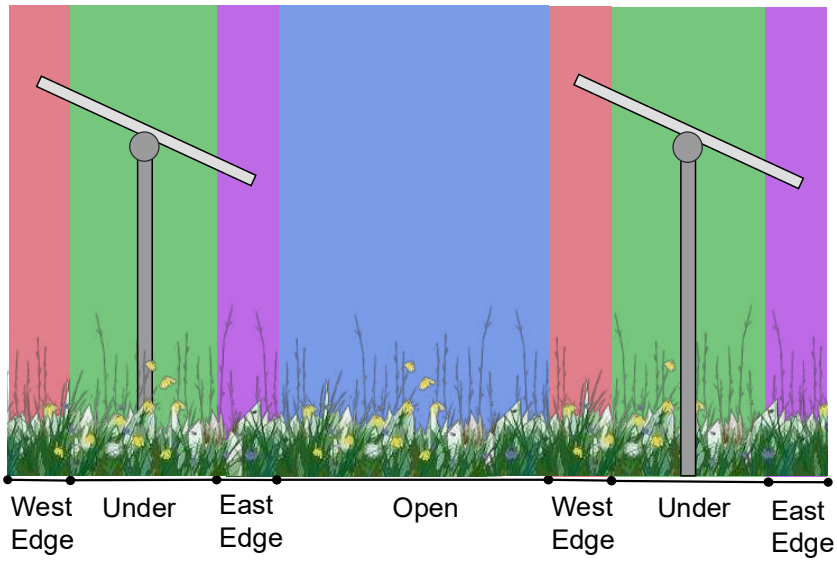

Figure 3.2.13 An illustration of the four distinct microclimates created by a single-axis tracking solar array.
Open – 50% of total area. ~7 hours of mid-day sunlight. 26% average growing season soil moisture.
West Edge – 11.5% of total area. ~4 hours of afternoon sunlight. 30% average growing season soil moisture.
East Edge - 11.5% of total area. ~4 hours of morning sunlight. 28% average growing season soil moisture.
Under - 27% of total area. Less than 2 hours of daily sunlight. 22% average growing season soil moisture.
Microclimate characterization data were collected by partners in 2022 and reported in Sturchio et al, 2024.

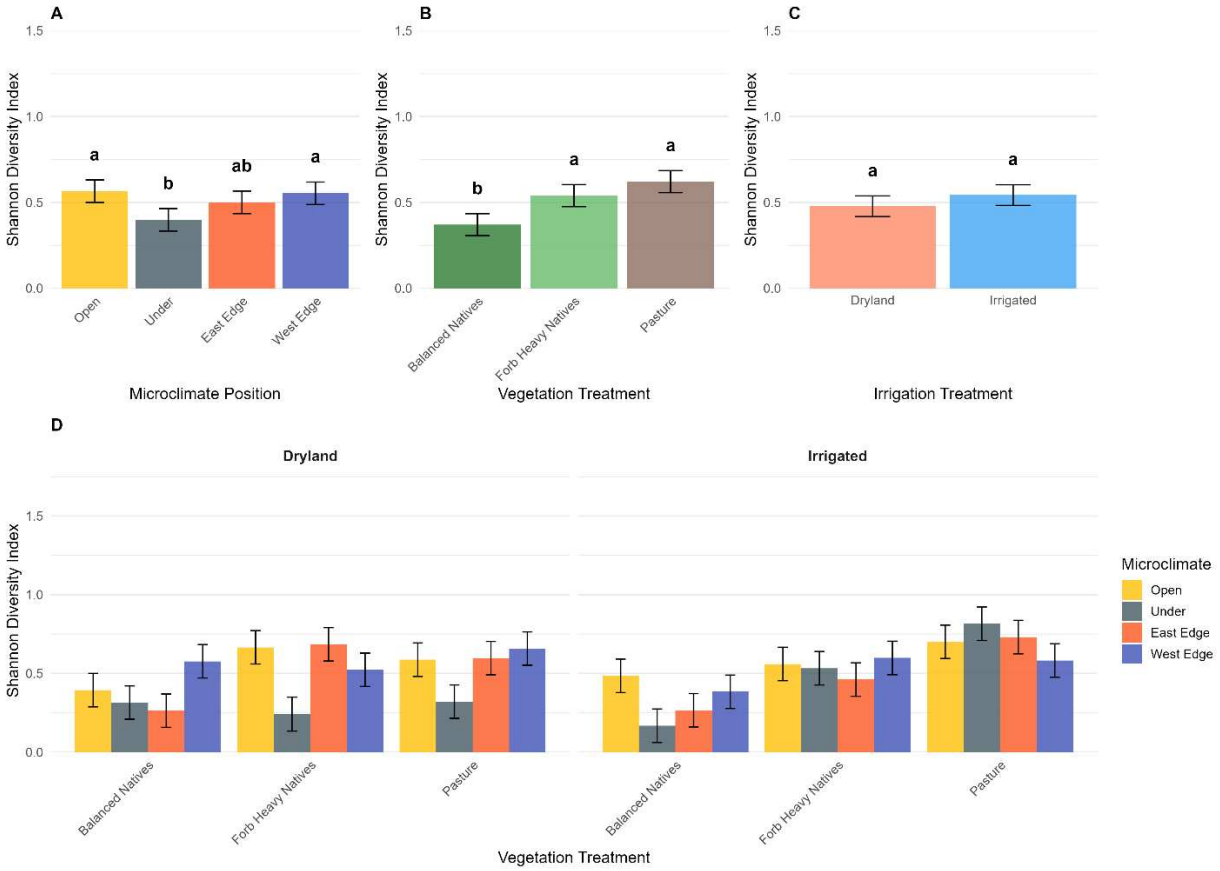

Figure 3.3. Shannon diversity responses to microclimate position, vegetation treatment, and irrigation. Panel A shows microclimate-scale diversity patterns within solar array positions. Panel B displays plot-scale area-weighted diversity across vegetation treatments. Panel C shows plot-scale area-weighted diversity by irrigation treatment. Panel D illustrates the three-way interaction among vegetation treatment, microclimate position, and irrigation at the microclimate scale, revealing treatment-specific spatial patterns. Bars represent estimated marginal means ± SE from linear mixed models. Letters indicate significant differences based on Tukey HSD post-hoc tests ($\alpha = 0.05$).

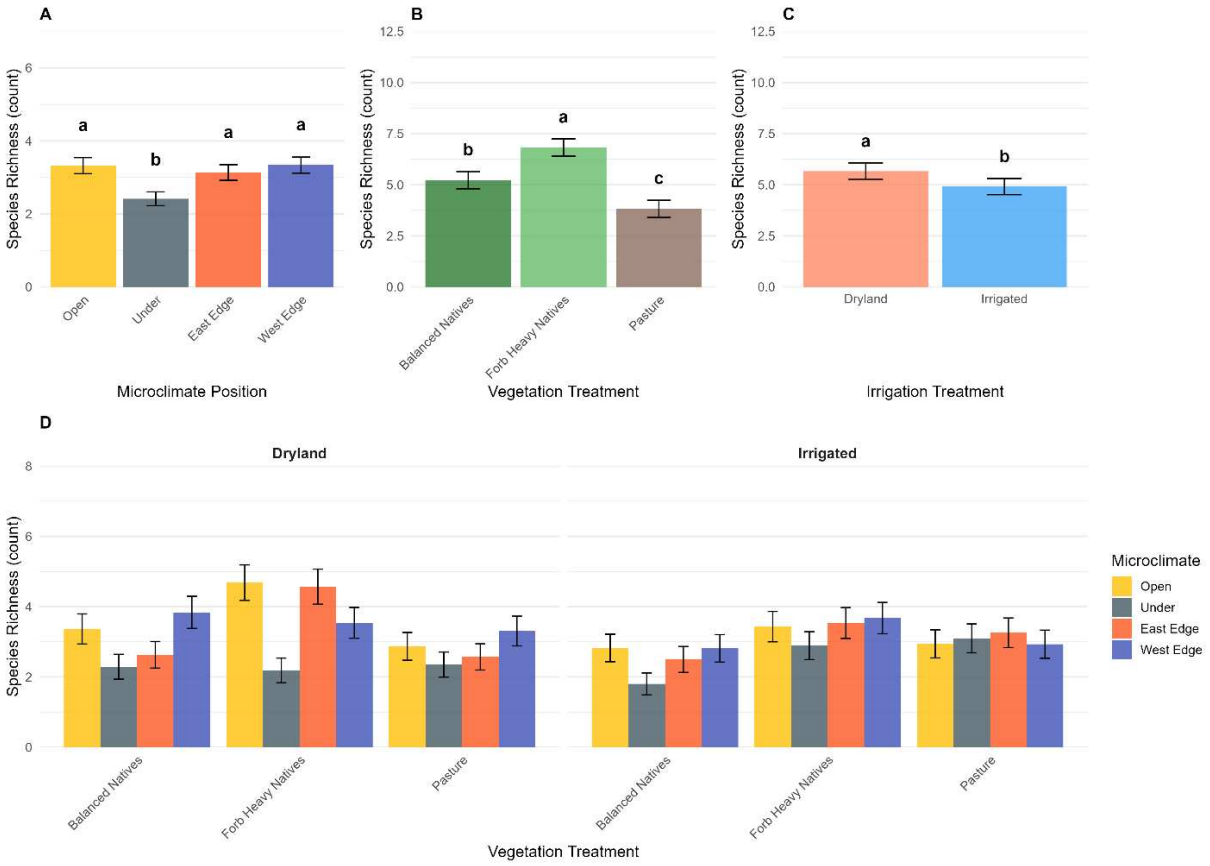

Figure 3.4. Species richness responses to microclimate position, vegetation treatment, and irrigation. Panel A shows microclimate-scale richness patterns (unique species per sampling unit) across solar array positions. Panel B displays plot-scale richness (total unique species per plot) across vegetation treatments. Panel C shows plot-scale richness by irrigation treatment. Panel D illustrates the three-way interaction among vegetation treatment, microclimate position, and irrigation at the microclimate scale. Bars represent estimated marginal means ± SE from linear mixed models. Letters indicate significant differences based on Tukey HSD post-hoc tests (α = 0.05). Note different y-axis scales between microclimate-level (A, D) and plot-level (B, C) panels reflecting scale-dependent richness patterns.

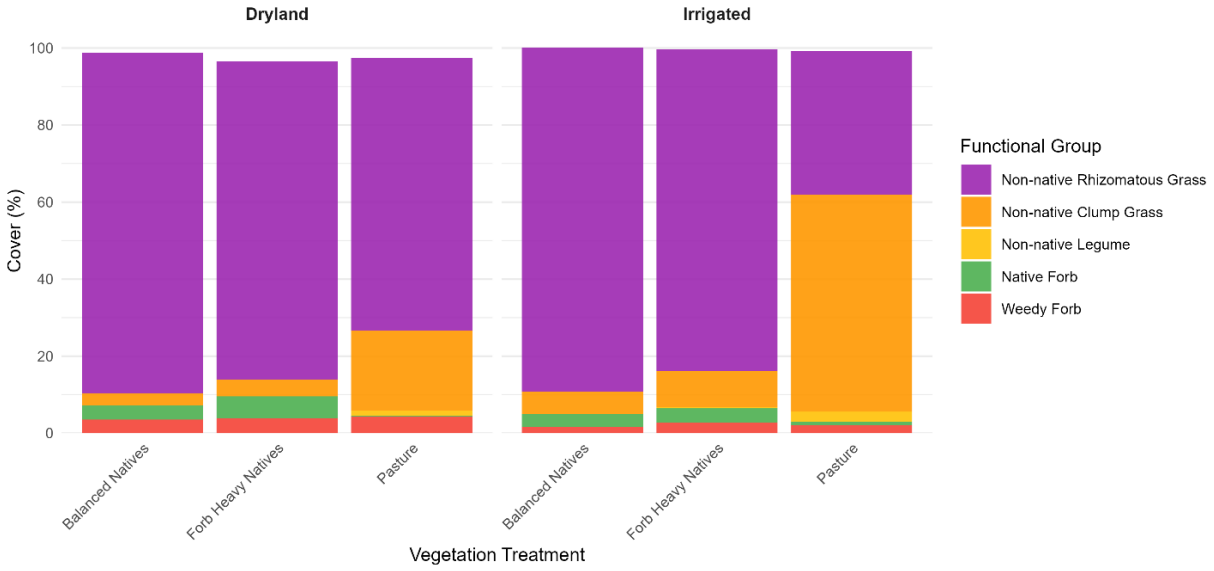

Figure 3.5. Functional group composition across vegetation and irrigation treatments. Stacked bars showing the contribution of each functional group to total vegetation cover by vegetation treatment under dryland and irrigated conditions. Bars represent mean cover (%) across all plots within each treatment combination.

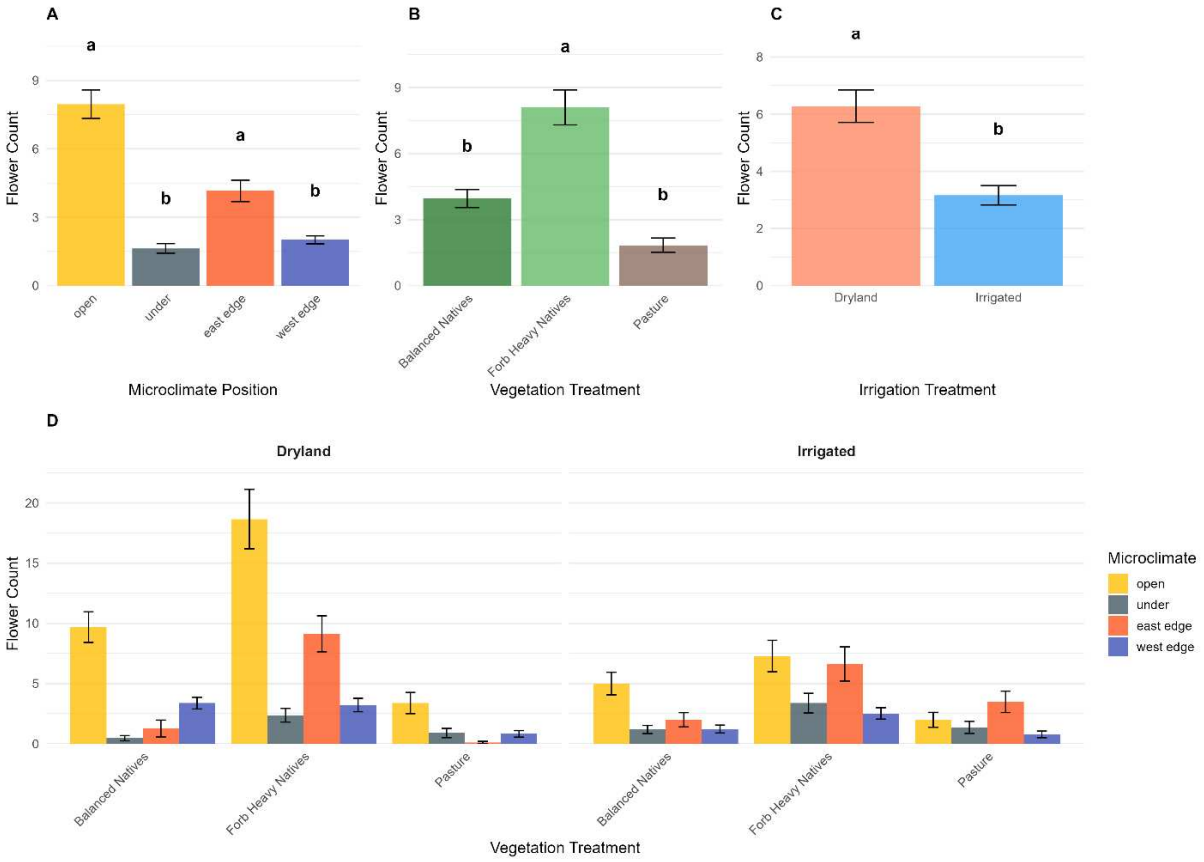

Figure 3.6. Floral abundance responses to microclimate position, vegetation treatment, and irrigation. Panel A shows microclimate-scale flower production patterns across solar array positions. Panel B displays plot-scale area-weighted flower production across vegetation treatments. Panel C shows plot-scale area-weighted flower production by irrigation treatment. Panel D illustrates the three-way interaction among vegetation treatment, microclimate position, and irrigation at the microclimate scale. Bars represent mean flower counts ± SE. Letters indicate significant differences based on Tukey HSD post-hoc tests ($\alpha = 0.05$) from zero-inflated negative binomial models. Note: 77% of microclimate observations and 54% of plot observations had zero flowers.

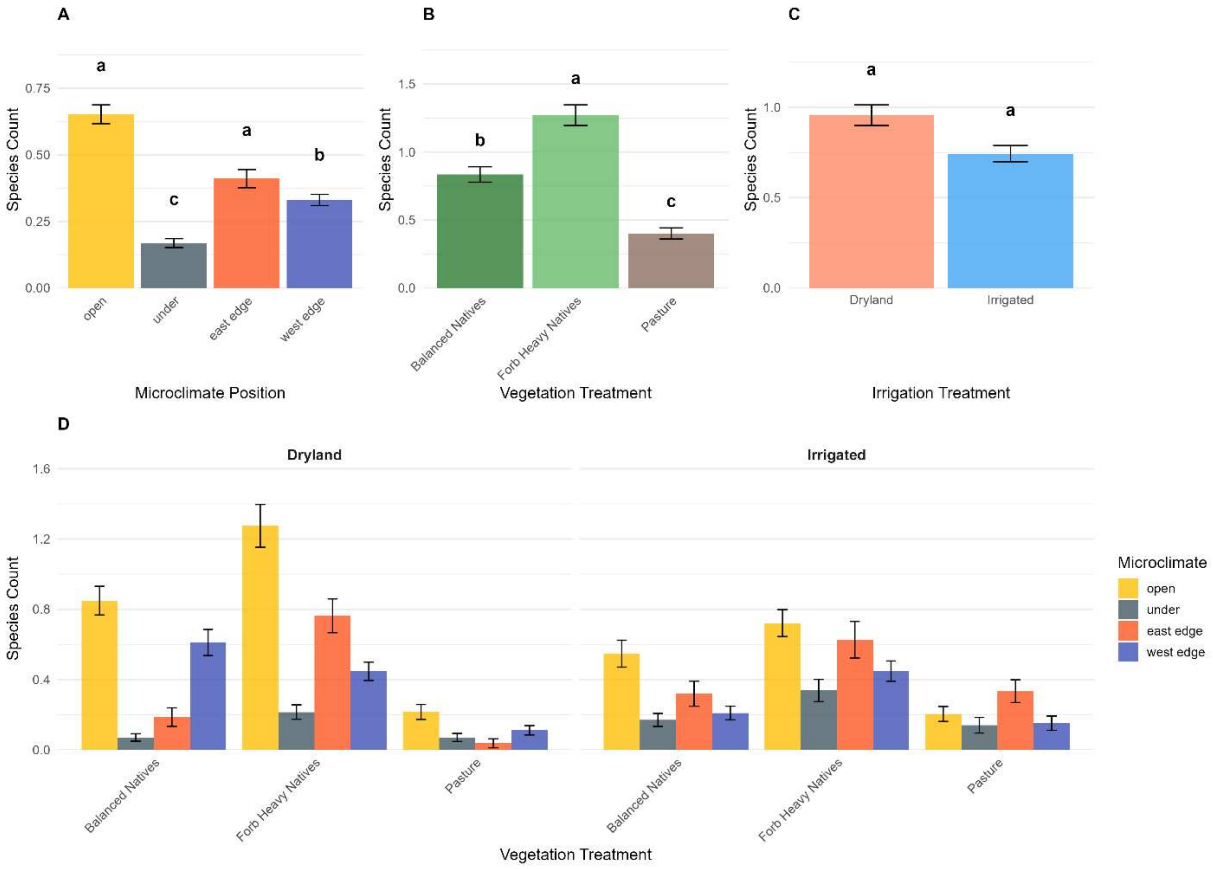

Figure 3.7. Flowering species richness responses to microclimate position, vegetation treatment, and irrigation. Panel A shows microclimate-scale richness patterns (unique flowering species per sampling unit) across solar array positions. Panel B displays plot-scale richness (maximum unique flowering species per plot) across vegetation treatments. Panel C shows plot-scale richness by irrigation treatment. Panel D illustrates the three-way interaction among vegetation treatment, microclimate position, and irrigation at the microclimate scale. Bars represent mean species counts ± SE. Letters indicate significant differences based on Tukey HSD post-hoc tests ($\alpha = 0.05$) from Poisson mixed models. Note different y-axis scales between microclimate-level (A, D) and plot-level (B, C) panels.

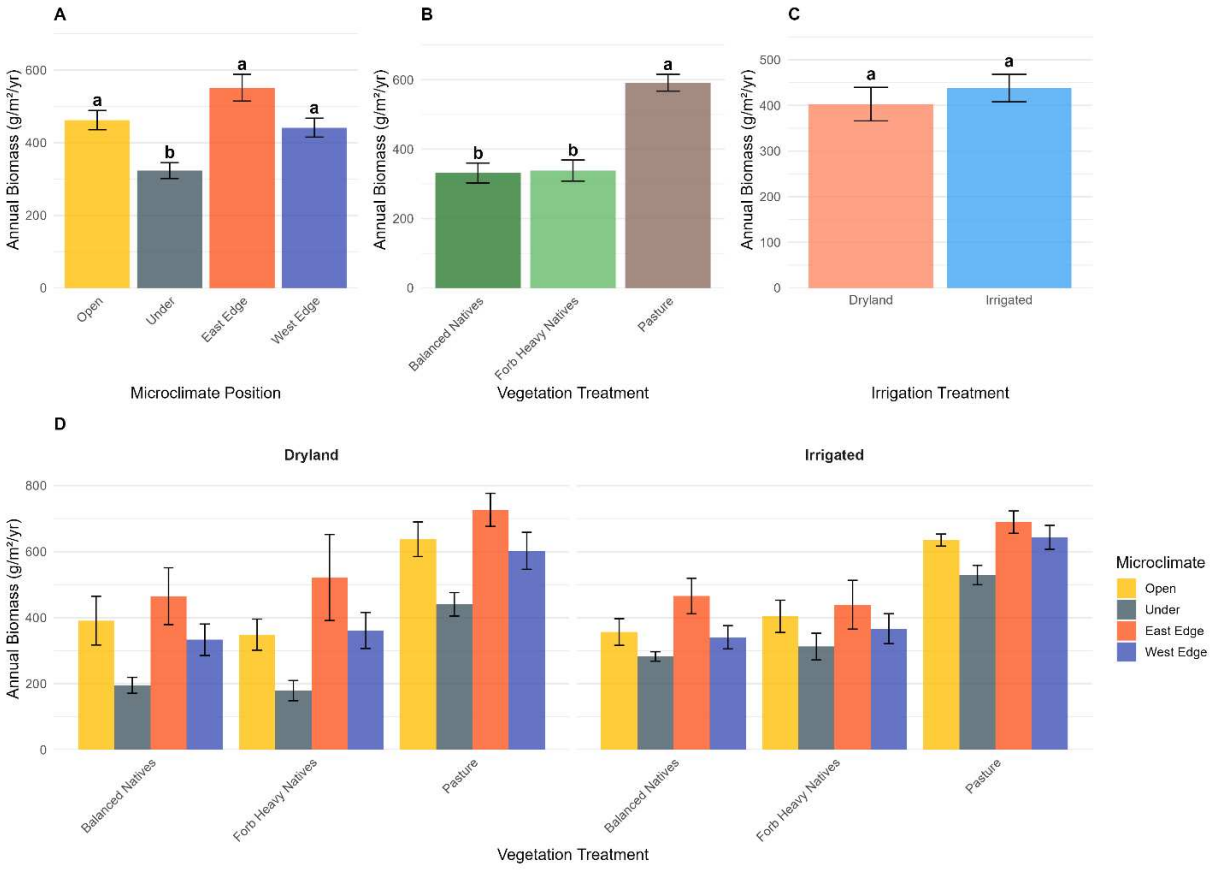

Figure 3.8. Annual forage biomass production responses to microclimate position, vegetation treatment, and irrigation. Panel A shows microclimate-scale biomass production across solar array positions. Panel B displays plot-scale area-weighted biomass across vegetation treatments. Panel C shows plot-scale area-weighted biomass by irrigation treatment. Panel D illustrates the three-way interaction among vegetation treatment, microclimate position, and irrigation at the microclimate scale. Bars represent mean annual biomass (g/m²/yr) ± SE from square-root transformed linear mixed models, back-transformed to original scale. Letters indicate significant differences based on Tukey HSD post-hoc tests ($\alpha = 0.05$). Annual biomass represents total aboveground production integrated across the growing season, with pasture values incorporating both summer and fall harvests.

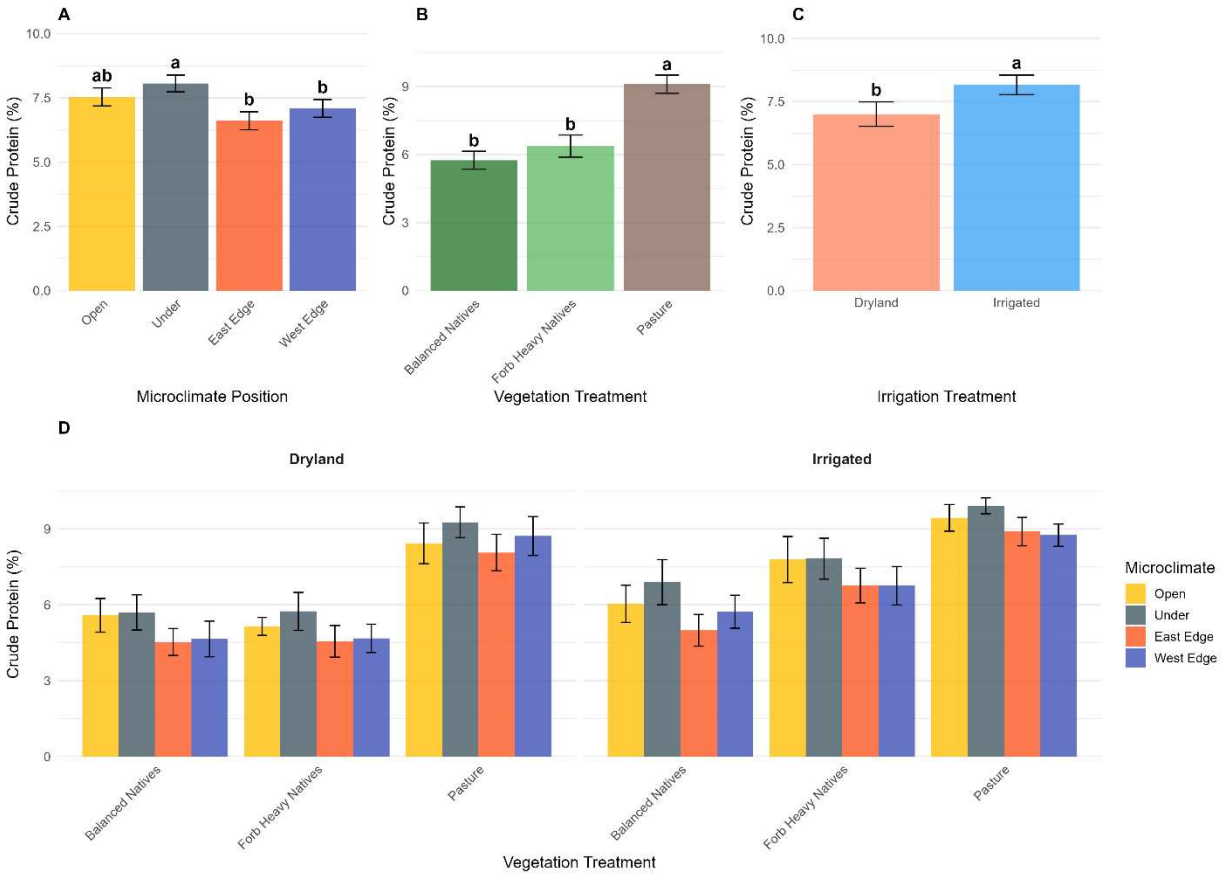

Figure 3.9. Crude protein responses to microclimate position, vegetation treatment, and irrigation. Panel A shows microclimate-scale crude protein content across solar array positions. Panel B displays plot-scale area-weighted crude protein across vegetation treatments. Panel C shows plot-scale area-weighted crude protein by irrigation treatment. Panel D illustrates the three-way interaction between vegetation treatment, microclimate, and irrigation at the microclimate scale. Bars represent mean crude protein content (%) ± SE. Letters indicate significant differences based on Tukey HSD post-hoc tests ($\alpha = 0.05$) from linear mixed models. Crude protein is a key indicator of forage nutritional quality, with higher values indicating greater livestock feed value.

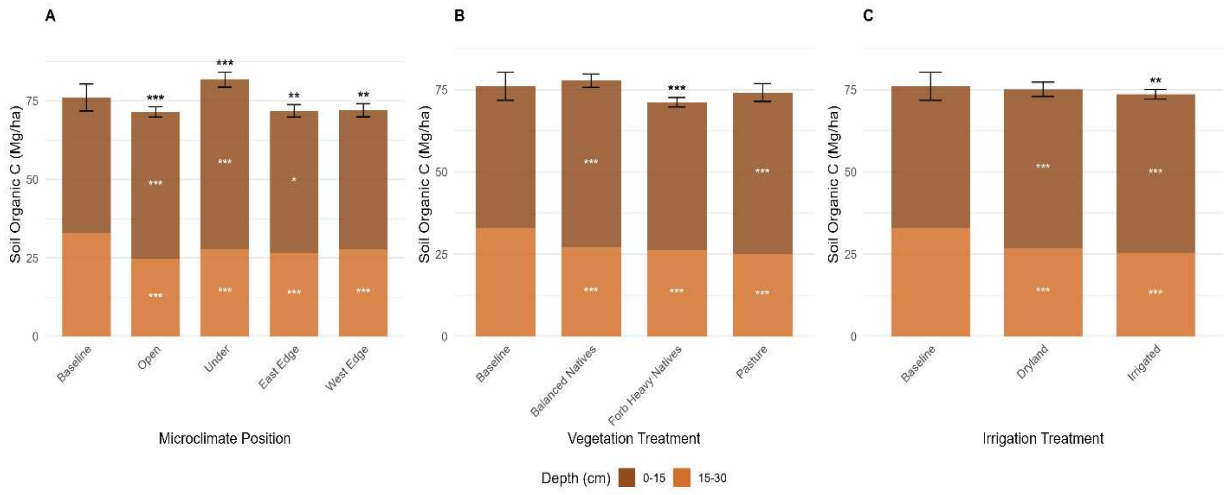

Figure 3.10. Soil organic carbon stocks by depth showing changes from baseline (2021) across microclimate positions and management treatments in 2023. Panel A shows microclimate-scale soil C distribution. Panels B and C display plot-scale area-weighted soil C across vegetation and irrigation treatments. Bars are stacked by depth increment (15-30 cm in darker brown at bottom, 0-15 cm in lighter brown at top). Baseline pre-treatment values shown on left of each panel. White asterisks within depth increments indicate significant change from baseline for that specific layer; black asterisks above bars indicate significant change in total soil C (0-30 cm). Asterisk notation: * $p<0.05$, ** $p<0.01$, *** $p<0.001$. Error bars represent ±SE of SOC across both depths. Plot-scale values (Panels B-C) are area-weighted averages across microclimate positions.

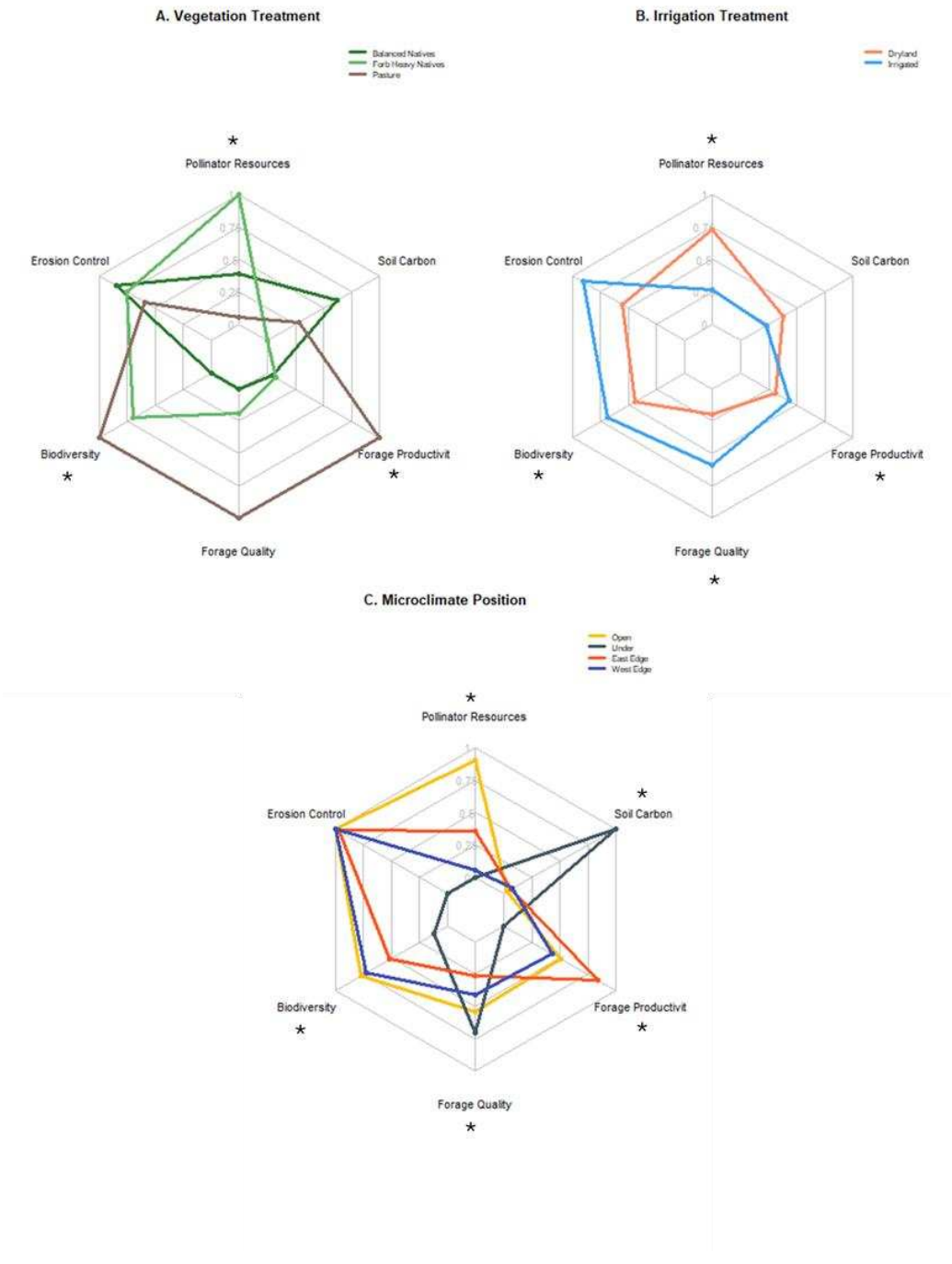

Figure 3.11. Multifunctionality of ecosystem services across: a) vegetation treatments, b) irrigation treatments, and c) microclimates in the agrivoltaic system. Values are standardized from 0 (center) to 1 (edge) based on the range of observed means across all treatments. Services measured include: Pollinator Resources (total flower abundance), Erosion Control (total cover %), Biodiversity (Shannon diversity index), Forage Quality (crude protein content), Forage Productivity (annual aboveground biomass), and Soil Carbon (SOC stock in Mg/ha from 0-30 cm depth). Significant model effects for each service are indicated by asterisks.

LITERATURE CITED

Adeh, E. H., Selker, J. S., & Higgins, C. W. (2018). Remarkable agrivoltaic influence on soil moisture, micrometeorology and water-use efficiency. *PLOS ONE*, *13*(11), e0203256. https://doi.org/10.1371/JOURNAL.PONE.0203256

Andrew, A. C., Higgins, C. W., Smallman, M. A., Graham, M., & Ates, S. (2021). Herbage yield, lamb growth and foraging behavior in agrivoltaic production system. *Frontiers in Sustainable Food Systems*, *5*, Article 659175. https://doi.org/10.3389/fsufs.2021.659175

Armstrong, A., Ostle, N. J., & Whitaker, J. (2016). Solar park microclimate and vegetation management effects on grassland carbon cycling. *Environmental Research Letters*, *11*(7), 074016. https://doi.org/10.1088/1748-9326/11/7/074016

Bakker, J. D., & Wilson, S. D. (2004). Using ecological restoration to constrain biological invasion. *Journal of Applied Ecology*, *41*(6), 1058-1064. https://doi.org/10.1111/j.0021-8901.2004.00962.x

Barron-Gafford, G. A., Pavao-Zuckerman, M. A., Minor, R. L., Sutter, L. F., Barnett-Moreno, I., Blackett, D. T., Thompson, M., Dimond, K., Gerlak, A. K., Nabhan, G. P., & Macknick, J. E. (2019). Agrivoltaics provide mutual benefits across the food–energy–water nexus in drylands. *Nature Sustainability*, *2*(9), 848–855. https://doi.org/10.1038/s41893-019-0364-5

Bennett, E. M., Peterson, G. D., & Gordon, L. J. (2009). Understanding relationships among multiple ecosystem services. *Ecology Letters*, *12*(12), 1394-1404. https://doi.org/10.1111/j.1461-0248.2009.01387.x

Colorado Climate Center. (2025). Access Colorado Data. https://ccc.atmos.colostate.edu/data_access_new.html (accessed Jan 26, 2025).

Finney, D. M., Murrell, E. G., White, C. M., Baraibar, B., Barbercheck, M. E., Bradley, B. A., Cornelisse, S., Hunter, M. C., Kaye, J. P., Mortensen, D. A., Mullen, C. A., & Schipanski, M. E. (2017). Ecosystem services and disservices are bundled in simple and diverse cover cropping systems. *Agricultural & Environmental Letters*, *2*(1), 170033. https://doi.org/10.2134/ael2017.09.0033

Grman, E., Bassett, T., & Brudvig, L. A. (2013). Confronting contingency in restoration: Management and site history determine outcomes of assembling prairies, but site characteristics and landscape context have little effect. *Journal of Applied Ecology*, *50*(5), 1234-1243. https://doi.org/10.1111/1365-2664.12135

Hernandez, R. R., Easter, S. B., Murphy-Mariscal, M. L., Maestre, F. T., Tavassoli, M., Allen, E. B., Barrows, C. W., Belnap, J., Ochoa-Hueso, R., Ravi, S., & Allen, M. F. (2014). Environmental impacts of utility-scale solar energy. *Renewable and Sustainable Energy Reviews*, *29*, 766–779. https://doi.org/10.1016/j.rser.2013.08.041

Hernandez, R. R., Armstrong, A., Burney, J., Ryan, G., Moore-O'Leary, K., Diédhiou, I., Grodsky, S. M., Saul-Gershenz, L., Davis, R., Macknick, J., Mulvaney, D., Heath, G. A., Easter, S. B., Hoffacker, M. K., Allen, M. F., & Kammen, D. M. (2019). Techno-ecological synergies of solar energy for global sustainability. *Nature Sustainability*, *2*(7), 560-568. https://doi.org/10.1038/s41893-019-0309-z

Jose, S. (2009). Agroforestry for ecosystem services and environmental benefits: An overview. *Agroforestry Systems*, *76*(1), 1-10. https://doi.org/10.1007/s10457-009-9229-7

Kannenberg, S. A., Sturchio, M. A., Venturas, M. D., & Knapp, A. K. (2023). Grassland carbon-water cycling is minimally impacted by a photovoltaic array. *Communications Earth & Environment*, *4*(1), 1–8. https://doi.org/10.1038/s43247-023-00904-4

Lambert, Q., Bischoff, A., & Gros, R. (2021). Effects of solar parks on soil quality, microclimate, CO2 effluxes, and vegetation under a Mediterranean climate. *Land Degradation & Development*, *32*(18), 5190-5202. https://doi.org/10.1002/ldr.4080

Li, Y., Armstrong, A., Simmons, C., Krasner, N. Z., & Hernandez, R. R. (2025). Ecological impacts of single-axis photovoltaic solar energy with periodic mowing on microclimate and vegetation. *Frontiers in Sustainability. 6.* https://doi.org/10.3389/frsus.2025.1497256

Marrou, H., Guilioni, L., Dufour, L., Dupraz, C., & Wery, J. (2013). Microclimate under agrivoltaic systems: Is crop growth rate affected in the partial shade of solar panels? *Agricultural and Forest Meteorology*, *177*, 117–132. https://doi.org/10.1016/j.agrformet.2013.04.012

Raudsepp-Hearne, C., Peterson, G. D., & Bennett, E. M. (2010). Ecosystem service bundles for analyzing tradeoffs in diverse landscapes. *Proceedings of the National Academy of Sciences*, *107*(11), 5242-5247. https://doi.org/10.1073/pnas.0907284107

Reilly, J. R., Artz, D. R., Biddinger, D., Bobiwash, K., Boyle, N. K., Brittain, C., Brokaw, J., Campbell, J. W., Daniels, J., Elle, E., Ellis, J. D., Fleischer, S. J., Gibbs, J., Gillespie, R. L., Gundersen, K. B., Gut, L., Hoffman, G., Joshi, N., Lundin, O., Mason, K., McGrady, C. M., Peterson, S. S., Pitts-Singer, T. L., Rao, S., Rothwell, N., Rowe, L., Ward, K. L., Williams, N. M., Wilson, J. K., Isaacs, R., & Winfree, R. (2020). Crop production in the USA is frequently limited by a lack of pollinators. *Proceedings of the Royal Society B: Biological Sciences*, *287*(1931), 20200922. https://doi.org/10.1098/rspb.2020.0922

Robertson, G. P., Gross, K. L., Hamilton, S. K., Landis, D. A., Schmidt, T. M., Snapp, S. S., & Swinton, S. M. (2014). Farming for ecosystem services: An ecological approach to production agriculture. *BioScience*, *64*(5), 404-415. https://doi.org/10.1093/biosci/biu037

Scheper, J., Holzschuh, A., Kuussaari, M., Potts, S. G., Rundlöf, M., Smith, H. G., & Kleijn, D. (2013). Environmental factors driving the effectiveness of European agri-environmental measures in mitigating pollinator loss – a meta-analysis. *Ecology Letters*, *16*(7), 912-920. https://doi.org/10.1111/ele.12128

Sherrod, L. A., Dunn, G., Peterson, G. A., & Kolberg, R. L. (2002). Inorganic Carbon Analysis by Modified Pressure-Calcimeter Method. *Soil Science Society of America Journal*, *66*(1), 299–305. https://doi.org/10.2136/SSSAJ2002.2990

Sturchio, M. A., Macknick, J. E., Barron-Gafford, G. A., Chen, A., Alderfer, C., Condon, K., Hajek, O. L., Miller, B., Pauletto, B., Siggers, J. A., Slette, I. J., & Knapp, A. K. (2022). Grassland productivity responds unexpectedly to dynamic light and soil water environments induced by photovoltaic arrays. *Ecosphere*, *13*(12), e4334. https://doi.org/10.1002/ECS2.4334

Sturchio, M. A., & Knapp, A. K. (2023). Ecovoltaic principles for a more sustainable, ecologically informed solar energy future. *Nature Ecology & Evolution*, *7*(11), 1746–1749. https://doi.org/10.1038/s41559-023-02174-x

Sturchio, M. A., Kannenberg, S. A., & Knapp, A. K. (2024a). Agrivoltaic arrays can maintain semi-arid grassland productivity and extend the seasonality of forage quality. *Applied Energy*, *356*, 122418. https://doi.org/10.1016/j.apenergy.2023.122418

Sturchio, M. A., Kannenberg, S. A., Pinkowitz, T. A., & Knapp, A. K. (2024b). Solar arrays create novel environments that uniquely alter plant responses. *Plants, People, Planet*, *6*(6), 1522–1533. https://doi.org/10.1002/PPP3.10554

Swinton, S. M., Lupi, F., Robertson, G. P., & Hamilton, S. K. (2007). Ecosystem services and agriculture: Cultivating agricultural ecosystems for diverse benefits. *Ecological Economics*, *64*(2), 245-252. https://doi.org/10.1016/j.ecolecon.2007.09.020

Toy, C., Heider-Kuhn, N., Schipanski, M. (2025). Impact of solar energy infrastructure and ecovoltaic management on semi-arid grassland carbon cycling. *Environmental Research Communications,* 7, 105005. https://doi.org10.1088/2515-7620/ae0b1d

Walston, L. J., Hartmann, H. M., Fox, L., Macknick, J., McCall, J., Janski, J., & Jenkins, L. (2021). If you build it, will they come? Insect community responses to habitat establishment at solar energy facilities in Minnesota, USA. *Environmental Research Letters*, *19*(1), 014053. https://doi.org/10.1088/1748-9326/ad10a8

Walston, L. J., Barley, T., Bhandari, I., Campbell, B., McCall, J., Hartmann, H. M., & Dolezal, A. G. (2022). Opportunities for agrivoltaic systems to achieve synergistic food-energy-environmental needs and address sustainability goals. *Frontiers in Sustainable Food Systems*, *6*, Article 932018. https://doi.org/10.3389/fsufs.2022.932018

Wilmer H, Augustine DJ, Derner JD, Milchunas DG. (2021) Assessing the rate and reversibility of large-herbivore effects on community composition in a semi-arid grassland ecosystem. *Journal of Vegetation Science,* 32:e12934. https://doi.org/10.1111/jvs.12934

Wu, C., Liu, H., Yu, Y., Zhao, W., Liu, J., Yu, H., & Yetemen, O. (2022). Ecohydrological effects of photovoltaic solar farms on soil microclimates and moisture regimes in arid Northwest China: A modeling study. *Science of the Total Environment*, *802*, Article 149946. https://doi.org/10.1016/j.scitotenv.2021.149946

CHAPTER 4: DECOUPLED PLANT AND ARTHROPOD COMMUNITY RESPONSES TO SOLAR ENERGY DEVELOPMENT

4.1 Summary

Understanding ecological impacts of solar energy infrastructure is critical as installations expand across agricultural lands. We assessed the effects of single-axis tracking solar arrays on multiple ecosystem functions using paired comparisons at nine sites in Northern Colorado's semi-arid grasslands. Plant communities, arthropods (flying and ground-dwelling), root biomass, and soil properties were measured across distinct microclimates created by solar panels (open, under, east edge, west edge) and compared to adjacent control fields that represented pre-installation management conditions. Overall, we found positive, negative and neutral effects of solar installations on ecosystem functions. Solar installations significantly enhanced plant species richness (up to 47% increase) and diversity, particularly where solar arrays replaced crop monocultures. However, arthropod communities showed consistent negative responses across functional groups, with total abundance reduced by 27-48% despite improved vegetation diversity. Pollinators and beetles showed the strongest reductions (50% and 74% respectively), raising concerns about ecosystem service provision to surrounding agricultural lands. Soil analyses revealed reduced organic carbon (5%) and nitrogen stocks (10%) in solar areas, alongside 7% higher soil bulk density, which likely increased due to construction impacts. Site history strongly influenced outcomes: cropland conversions showed dramatic increases in plant biodiversity while sites with established perennial vegetation showed little change. The decoupling of plant diversity from arthropod abundance suggests solar infrastructure itself deters arthropods through mechanisms beyond habitat quality—potentially including polarized light pollution, electromagnetic fields, or visual obstruction. Our results suggest standard vegetation

management alone cannot mitigate negative impacts on arthropods, indicating need for targeted interventions addressing infrastructure effects. Strategic siting on degraded lands, design modifications to reduce sensory interference, and active habitat management may help minimize ecological trade-offs while meeting renewable energy goals.

4.2 Introduction

The rapid expansion of solar photovoltaic (PV) infrastructure represents one of the most significant land use changes of the 21st century. Global solar capacity reached 1,177 GW in 2022 and continues to grow at approximately 73% annually (IRENA, 2023), with ground-mounted installations accounting for 46-52% of new capacity (IEA, 2024). In the United States, the Solar Futures Study projects that meeting decarbonization goals will require 5.7 million acres of land by 2035 and potentially 10-12 million acres by 2050 (DOE, 2021), with approximately 70-80% of this development expected to occur on agricultural lands in regions like the Midwest (Walston et al., 2022; USDA, 2023). This unprecedented transformation of working landscapes necessitates comprehensive understanding of the ecological consequences of solar energy development.

While the climate benefits of renewable energy transition are well-established, with solar PV achieving lifecycle emissions of 40-50 g CO_2-eq/kWh compared to 820 g CO_2-eq/kWh for coal (IPCC, 2014), the impacts on biodiversity and ecosystem functioning remain incompletely understood. Early foundational work by Hernandez et al. (2014) identified potential environmental impacts including habitat loss, soil erosion, and hydrological changes, while Lovich and Ennen (2011) noted that at the time only one peer-reviewed study existed on direct wildlife impacts from utility-scale solar. Although research has expanded substantially since

then, significant knowledge gaps persist, particularly regarding the responses of multiple taxa to the novel environmental conditions created by solar infrastructure.

Solar installations fundamentally alter local environmental conditions through multiple mechanisms. PV panels intercept and redistribute solar radiation, creating spatial heterogeneity in light availability that can range from less than 10% to over 90% of ambient conditions depending on panel configuration and position (Armstrong et al., 2016; Liu et al., 2019; Li et al., 2025). Panels also redistribute precipitation, concentrating rainfall at drip edges while intercepting moisture beneath panels (Elamri et al., 2018; Lambert et al., 2021). These modifications cascade through ecosystems, affecting soil temperature and moisture regimes (Marrou et al., 2013), plant community composition (Lambert et al., 2021), and habitat suitability for various fauna (Walston et al., 2023; Barré et al., 2024).

Recent research has documented both positive and negative biodiversity outcomes, with effects strongly dependent on context. Studies at solar facilities with restored native vegetation have shown dramatic increases in pollinator abundance, including a 3-fold increase in total arthropods and 20-fold increase in native bees over five years (Walston et al., 2023), while research on bat activity has documented substantial reductions at solar sites, with some species showing 7-fold decreases in activity (Tinsley et al., 2023). Bird responses vary by species and management practices, with mixed-habitat solar farms supporting three times the abundance of adjacent cropland but deterring ground-nesting species like skylarks (Badelt et al., 2025; Szabo et al., 2024). These contrasting outcomes highlight the importance of understanding mechanisms driving ecological responses rather than simply documenting patterns.

A critical limitation of existing research is the predominance of single-taxon studies and the lack of integrated assessments examining multiple trophic levels simultaneously. A recent

systematic map found that plants and arthropods are the most studied taxonomic groups in solar arrays, however few studies integrated across taxonomic groups (Bennun et al., 2023). Furthermore, most studies examine either presence/absence patterns or simple abundance metrics without investigating the functional consequences of community changes for ecosystem processes. This fragmented approach limits our ability to predict cascading effects through food webs or understand how changes at one trophic level influence others.

The role of solar infrastructure design in mediating ecological impacts remains poorly understood, particularly for single-axis tracking systems that now dominate utility-scale installations. Unlike fixed-tilt arrays that create static shade patterns, tracking systems produce dynamic light environments as panels rotate to follow the sun's path (Sturchio et al., 2022). Recent work at Jack's Solar Garden in Colorado demonstrated that despite 38% light reduction, grassland productivity decreased only 6-7% due to photosynthetic plasticity of C3 grasses (Kannenberg et al., 2023). However, this research focused primarily on plant physiological responses, leaving questions about how dynamic shading affects arthropod communities, soil processes, and multi-trophic interactions largely unexplored.

Semi-arid grasslands, which host an increasing proportion of solar development due to high irradiance and relatively flat topography, present unique challenges and opportunities for understanding solar-ecosystem interactions. These water-limited systems may respond differently to solar infrastructure than mesic environments, as light is typically not the primary limiting resource (Sturchio & Knapp, 2023). Previous work has shown that solar panels can mitigate the effects of aridity during drought periods (Adeh et al., 2018), but comprehensive assessments of how this affects multiple ecosystem components across spatial and temporal scales are lacking.

We addressed these knowledge gaps through an integrated assessment of ecological responses to single-axis tracking solar arrays across nine sites in Northern Colorado's semi-arid grasslands. By employing a paired study design with control sites managed using pre-installation conditions, we isolated the effects of solar infrastructure from other land use changes. Our multifunctional approach examined: (1) flying and ground-dwelling arthropod communities across functional groups, (2) plant community composition, diversity, and cover responses, (3) belowground biomass allocation patterns, and (4) soil organic carbon and nitrogen stocks. Importantly, we quantified these responses across the distinct microclimate zones created by tracking systems (open areas between panels, directly under panels, and eastern/western edges), allowing us to understand both the mechanisms driving change and the spatial heterogeneity of impacts.

4.3 Methods

4.3.1 Study Design and Site Information

We collected data from nine single axis tracking solar arrays in Northern Colorado (Figure 4.1) established between 5 – 8 years prior to data collection. Each solar array was paired with an adjacent field that was managed in the same manner as the paired solar array site was managed prior to installation to act as a proxy for baseline conditions. Three sites were previously managed as annual crop production, two of which were irrigated. Three sites were managed as improved pasture, two of which were previously irrigated. Two sites were disturbed vegetation communities and one was native rangeland (Table 4.1).

4.3.2 Data Collection

Arthropod and plant community data was collected at each field site at three time points within the 2024 growing season; Early (May-June), Mid (July-August), and Late (September).

Soil and root samples were only collected once, mid-season. All samples collected inside the solar arrays were collected from each of the four distinct microclimates created by single axis tracking solar arrays (Open, Under, East Edge, and West Edge). These microclimate specific measurements were collected at two representative locations within each solar array (8 sampling points total with the exception of flying arthropods). Control field samples collected at four representative locations within each paired control field.

4.3.3 Flying Arthropods

Two blue vane traps (Banfield Bio, Seattle, WA) were mounted on 1.5 m stakes and deployed for one week at a time in the Open microclimate between solar arrays and in the most physically distant two sampling locations in the paired control fields. Traps were filled with windshield washer fluid to preserve arthropod specimens and a drop of detergent to break surface tension. After removal from the field, samples were brought back to the lab and individuals were counted and identified to order level using a dissecting microscope. Specimens were preserved in 75% ethanol after identification.

4.3.4 Ground Dwelling Arthropods

Pitfall traps were deployed at each sampling location for one week at a time. Pitfalls were constructed using 150 ml specimen cups filled with windshield washer fluid for specimen preservation and a drop of detergent to break surface tension. Each pitfall was covered by a canopy constructed using wooden stakes and a Styrofoam plate to prevent flooding from precipitation. After removal from the field, samples were brought back to the lab and individuals were counted and identified to order level using a dissecting microscope. Specimens were preserved in 75% ethanol after identification.

4.3.5 Plant Community Cover and Composition

Cover was identified to species level (or litter/soil in the case of non-vegetative cover) every 30 cm along a 30 m30m transect at each sampling location.

4.3.6 Belowground Biomass

Due to varying mowing practices across the sites, we chose not to attempt to measure aboveground biomass production. Instead, we measured standing root mass as an indicator of the relative belowground productivity across sites. Bulk root mass was collected at 0-15 cm and 15-30 cm depth increments at each sampling position using one 7 cm diameter bucket auger sample. The roots were separated from the soil by washing them over a 2 mm sieve. The roots were then dried at 55°C until constant mass and weighed.

4.3.7 Soil Sampling

Bulk soil samples were collected at 0-15 cm and 15-30 cm depth increments at each sampling location using a 7 cm diameter bucket auger. Four cores were composited per location. Samples were air dried, sieved to 8 mm, and a representative subsample was sieved to 2 mm. The subsamples were dried to constant mass at 55 °C to prepare the soils for further analyses.

4.3.8 Soil C and N analysis

The 2 mm sieved and oven dried soil samples were ground and analyzed for total C and N using standard combustion analysis (Velp CN 802 Analyzer, VELP Scientific Inc., Deer Park, NY). Soil inorganic C content was measured using the pressure-calcimeter method of Sherrod et al (2002). Briefly, HCl was added to soils in a sealed container to evolve CO_2 gas. The volume of this gas was then measured by the pressure built up in the sealed container and converted to C content, which was then subtracted from total C values to calculate total organic C.

4.3.9 Soil Texture and Chemical Properties

Soil texture (hydrometer method), pH and extractable nutrient analyses were measured on air-dried, 2-mm sieved soils by Ward Labs (Lincoln, Nebraska, US).

4.3.10 Statistical Analysis

All statistical analyses were conducted in R (version 4.3.x) using linear mixed-effects models to account for the hierarchical structure of our paired study design. The general model structure for all response variables was:

Response ~ Microclimate × Fixed_Effect + (1|Site)

where Site was included as a random effect to account for site-level variation inherent in the paired design, and microclimate was treated as a fixed effect. Additional fixed effects (e.g., Season, Depth) varied by dataset.

Prior to analysis, all datasets were evaluated for distributional properties using histograms, quantile-quantile plots, and Shapiro-Wilk tests. Response variables exhibiting skewed distributions were transformed to meet model assumptions, with specific transformations detailed in each subsection. Model assumptions were verified using diagnostic plots and, where applicable, DHARMa residual simulations for mixed models.

Post-hoc comparisons were conducted using estimated marginal means with Tukey's HSD adjustment for multiple comparisons. Compact letter displays (CLDs) were generated to identify statistically significant differences among treatment combinations ($\alpha = 0.05$). Results for transformed variables are presented on back-transformed scales for ecological interpretation.

Primary R packages used across all analyses included lme4 and lmerTest for mixed-effects modeling, emmeans for post-hoc comparisons, vegan for community ecology analyses, and tidyverse for data manipulation. Additional dataset-specific packages are noted below.

4.4 Results

4.4.1 Plant Community Cover and Composition

We observed 324 transects with 100 species observation points each. Plant functional group analysis revealed substantial shifts in functional group composition between control and solar areas. Control areas were dominated by crops and litter, with minimal native species presence. Solar installations virtually eliminated crop cover while dramatically increasing grass coverage, particularly native grasses in Open areas (nearly 7-fold increase) and non-native grasses at edges (5- to 6-fold increases). Weedy forb proportions remained relatively stable across treatments, though solar areas showed slightly higher coverage than controls.

Paired analyses confirmed consistent increases in species richness across solar microclimates. Under panels showed the strongest positive effect across sites ($p < 0.001$), followed by West Edge ($p < 0.001$) and East Edge positions ($p = 0.002$). Open areas showed the smallest increase, approaching statistical significance ($p = 0.071$).

Seven of nine sites had significantly different community composition than their paired controls ($p < 0.05$). Site 3 showed the strongest treatment effect, explaining 73% of compositional variation, followed by Site 1 (65%), Site 7 (64%), and Site 9 (54%). Sites 2, 4, and 5 showed moderate but significant effects (47-53% of variation explained). Sites 6 and 8 showed no significant compositional differences ($p > 0.20$).

Plant functional group analysis revealed substantial heterogeneity in vegetation responses to solar installation across sites. Sites exhibited three primary response patterns based on previous land use (Figure 4.2):

Cropland Conversion Sites: Sites 1, 2, and 3 showed the most dramatic shifts from agricultural to semi-natural communities. Control areas at these sites had cover heavily dominated by crops, litter, and soil with minimal perennial vegetation coverage. Solar

installations completely eliminated crop cover and reduced soil and litter cover while establishing diverse grassland communities, with non-native grasses becoming the dominant functional group across solar microclimates. This conversion also increased weed cover, especially at Site 2.

Disturbed Sites: Site 4 and 5 control areas were dominated by weedy vegetation and litter coverage. Solar areas at Site 5 maintained very similar cover compositions to control areas, however they did show modest increases in desirable non-native forb cover. Open and Edge microclimates in solar areas at Site 4 showed a decrease in weed cover and an increase in bare soil.

Non-Native Grass Conversion Sites: Control areas at Sites 6, 7, and 8 were dominated by non-native grass species because these sites had been managed as improved pastures prior to solar installation. Solar areas at these sites demonstrated minimal effects on community composition in Open and Edge microclimates, but strong effects in Under microclimates. Bare soil and litter cover increased with a corresponding loss of non-native grass cover in Under microclimates at Sites 7 and 8, while weedy forb and litter cover increased with a corresponding loss of non-native grass cover at Site 6.

Solar installations significantly increased plant species richness across all microclimate positions compared to control areas ($p < 0.001$). Under panels showed the greatest increase (47% higher than controls, $p < 0.001$), followed by West Edge (40% higher, $p < 0.001$), East Edge (33% higher, $p < 0.001$), and Open areas (19% higher, $p = 0.009$) (Figure 4.3). Seasonal effects were significant, with Late season showing reduced richness compared to Early season ($p = 0.005$).

Shannon diversity followed similar patterns, with all solar positions showing significantly higher diversity than controls ($p < 0.001$ for Under, West Edge, and East Edge positions; $p = 0.001$ for Open areas). The Under panel position showed the highest diversity increase (37% above controls), while Open areas showed the smallest but still significant increase (21% above controls) (Figure 4.3).

Total vegetation cover varied significantly among microclimates ($p < 0.001$). West Edge positions showed the highest vegetation cover, approximately 28% greater than controls ($p < 0.001$), followed by East Edge with 17% greater coverage ($p < 0.001$). Under panel positions showed slightly lower coverage than controls, though this difference was not statistically significant ($p = 0.224$). Bare soil was significantly higher Under panels compared to controls (45% increase, $p = 0.012$). Litter cover was significantly reduced at both edge positions relative to controls, with West Edge showing the greatest reduction (54% decrease, $p < 0.001$) and East Edge showing a moderate reduction (27% decrease, $p < 0.001$) (Figure 4.2).

4.4.2 Flying Arthropod Diversity and Abundance

We collected a total of 4,829 flying arthropods from 16 taxonomic orders across all sampling time points. Total arthropod abundance was significantly lower in solar arrays compared to control sites ($p < 0.001$). Solar arrays exhibited 48% lower total arthropod abundance compared to control sites. This reduction remained consistent across the growing season, with no significant interaction between treatment and season.

All six functional groups showed reduced abundance in solar arrays, though the magnitude varied considerably (Figure 4.4). The interaction between solar treatment and functional group was not significant ($p = 0.42$), indicating that while effect sizes differed, the directional response was consistent across groups. Two functional groups showed statistically

significant reductions in solar arrays. Coleoptera exhibited the strongest response with 64.7% lower abundance ($p < 0.001$), while Pollinators (Hymenoptera and Lepidoptera combined) showed 49.6% lower abundance ($p = 0.001$). Herbivores showed a marginally significant 58.0% reduction ($p = 0.087$), while Predators (43.9% reduction), Diptera (14.2% reduction), and Other arthropods (no change) did not differ significantly between treatments (Figure 4.4).

Site accounted for substantial variability in functional group responses (variance = 0.37), indicating that local site characteristics influenced the magnitude of solar array effects on arthropod communities. Seasonal patterns were consistent across functional groups, with abundance declining from early to late season regardless of treatment.

Analysis at the taxonomic level largely confirmed the functional group patterns. The taxonomic model revealed no significant interaction between solar treatment and taxonomic order ($p = 0.75$), suggesting that while individual orders varied in their response magnitude, no taxonomic groups benefited from solar array presence. Among major orders not already captured in the functional group analysis, only minor departures from the overall pattern were observed, with all taxa showing neutral to negative responses to solar arrays.

4.4.3 Ground Dwelling Arthropod Diversity and Abundance

We collected 3,908 individuals in pit-fall traps from 18 taxonomic orders. Total ground-dwelling arthropod abundance was significantly lower in solar arrays compared to control sites ($p = 0.004$). Solar arrays exhibited 27% lower total arthropod abundance compared to control sites (Figure 4.5). This reduction remained consistent across the growing season, with no significant interaction between treatment and season.

The interaction between solar presence and functional group was significant ($p = 0.025$), indicating differential responses across ecological groups (Figure 4.5). Mixed Feeders (primarily

Coleoptera and Dermaptera) showed the strongest negative response with 71.2% lower abundance in solar arrays ($p < 0.001$). The "Other" category, comprising less common families, showed 44.1% lower abundance ($p = 0.025$). Ground Predators showed a marginally significant 49.9% reduction ($p = 0.064$). In contrast, Hymenoptera (primarily ants) showed a non-significant 11.3% increase in solar arrays, while Herbivores showed minimal change ($p = 0.117$). Decomposers ($p = 0.559$) and Aerial Visitors ($p = 0.412$) showed non-significant reductions.

Site-level variation in functional group responses was moderate (variance = 0.12), indicating relatively consistent patterns across sites. The conditional R^2 of 0.182 suggests that while treatment effects explain a modest portion of variance, site-level factors contribute additional variation in ground arthropod communities.

Analysis at the taxonomic order level largely confirmed the functional group patterns, with no significant interaction between solar treatment and taxonomic family ($p > 0.05$). The strong reduction in Mixed Feeders was driven primarily by Coleoptera, which comprised 24.3% of total abundance in the dataset. The relatively neutral response of Hymenoptera at the functional group level was consistent with family-level patterns, as these social insects (39.5% of total abundance) appeared to utilize both solar and control habitats effectively. The marginally significant reduction in Ground Predators reflected consistent negative responses across Araneae, Chilopoda, and Opiliones families, suggesting that solar arrays may reduce habitat quality for ground-dwelling predatory arthropods.

4.4.4 Root Mass

We collected 216 root mass samples. Root mass was substantially higher in the shallow soil layer (0-15 cm) compared to the deeper layer (15-30 cm), as expected. The overall depth effect ($p < 0.0001$) represented a 2.9-fold greater root mass in the shallow layer than in the

deeper layer. This pattern was consistent within each microclimate position, with all showing significantly higher root mass at 0-15 cm depth (Control: $p = 0.0003$; East Edge: $p = 0.004$; Open: $p = 0.005$; Under: $p = 0.0001$; West Edge: $p < 0.0001$) (Figure 4.6)

While the overall microclimate effect was statistically significant ($p=0.047$), post-hoc pairwise comparisons revealed no significant differences between individual microclimate pairs (Figure 4.6). The comparison between Control and Under panel positions approached significance ($p = 0.063$), suggesting a trend toward reduced root mass directly beneath solar panels.

4.4.5 Soil Bulk Density, Organic Carbon, and Nitrogen

We collected 216 soil samples across five microclimate positions at nine sites. Microclimate position significantly affected bulk density ($p < 0.01$), with all solar microclimate positions exhibiting elevated values compared to controls. Mean bulk density was 1.42 g cm^{-3} in control plots compared to 1.50-1.53 g cm^{-3} across solar positions. Post-hoc comparisons confirmed that control plots had significantly lower bulk density than all four solar microclimate positions.

The microclimate effect was significant in the soil organic carbon model ($p = 0.006$), however only Control and East Edge at 15-30 cm depth differed significantly in multiple comparisons analysis. Total nitrogen stocks similarly had a significant microclimate model effect ($p = 0.02$), however no differences were detected using multiple comparisons analysis.

To assess overall solar array impacts, we compared control plots to area-weighted solar values that account for the proportional representation of each microclimate (Open: 50%, Under: 27%, East Edge: 11.5%, West Edge: 11.5%). Solar plots exhibited significantly higher bulk density compared to control plots ($p < 0.001$). Mean bulk density in area-weighted solar plots

was 7% higher than controls (Figure 4.7). Neither depth ($p = 0.19$) nor the treatment × depth interaction ($p = 0.97$) significantly affected bulk density. Post-hoc comparisons confirmed that solar plots maintained consistently higher bulk density across both soil depths.

Soil organic carbon stocks were significantly lower in area-weighted solar plots compared to controls ($p = 0.004$). Solar sites had 5% lower SOC stocks than controls. Depth significantly affected SOC stocks ($p < 0.001$), with surface soils (0-15 cm) containing approximately 65% more carbon than subsurface soils (15-30 cm) across both solar and control sites (Figure 4.7). The solar × depth interaction was not significant ($p = 0.61$), indicating that solar installation effects on SOC were consistent across depths.

Total nitrogen stocks followed a similar pattern to SOC, with area-weighted solar plots showing significantly lower N stocks than controls ($p = 0.043$). Solar sites had 10% lower N stocks than controls. Depth significantly influenced N stocks ($p < 0.001$), with surface soils containing 35% more nitrogen than subsurface soils (Figure 4.7). The solar × depth interaction was not significant ($p = 0.28$).

4.5 Discussion

This research contributes to the growing body of literature on solar-ecosystem interactions in several key ways. First, we provide one of the few studies simultaneously examining multiple trophic levels, allowing assessment of potential cascading effects. Second, our focus on functional groups enables prediction of ecosystem process changes. Third, by examining belowground responses, we capture often-overlooked soil and root dynamics that may have long-term implications for carbon storage and ecosystem resilience. Fourth, our replicated design across nine sites provides insights into the consistency of solar effects across the landscape rather than only site-specific patterns.

Understanding these ecological dynamics is critical for informing management decisions as solar development accelerates. With Colorado alone projecting 80,000 acres of solar development by 2030 (Colorado Energy Office, 2023) and similar expansion occurring across western states, evidence-based guidelines for minimizing negative impacts while potentially enhancing ecosystem services are urgently needed. Our findings provide essential data for developing best practices that could transform solar installations from potential ecological liabilities into opportunities for biodiversity conservation and ecosystem service provision in agricultural landscapes. As the energy transition accelerates to meet growing electricity demand and climate goals, ensuring that renewable energy infrastructure supports rather than undermines biodiversity represents one of the key sustainability challenges of our time.

4.5.1 Enhanced Plant Diversity but Diminished Arthropod Communities

Our results reveal an ecological paradox that challenges assumptions about habitat-arthropod relationships: despite enhanced plant species richness, diversity, and cover across solar microclimate positions, both flying and ground-dwelling arthropod communities showed consistent reductions in abundance. Flying arthropods decreased by 48% and ground-dwelling arthropods by 27% in solar arrays compared to paired control sites. This decoupling of plant diversity from arthropod abundance is particularly unexpected given that three of our nine control sites were dominated by crops and litter with minimal plant diversity, while seven of our nine solar sites supported diverse perennial grassland communities with substantially greater structural complexity.

The magnitude and consistency of arthropod reductions across diverse functional groups—from a 74% reduction in Coleoptera to 50% in pollinators—cannot be explained by habitat degradation. Traditional ecological theory predicts that increased plant species richness

and structural diversity should support greater arthropod abundance through enhanced resource availability and niche partitioning (Haddad et al., 2009; Scherber et al., 2010). Our control sites, managed identically to pre-solar installation conditions, provide the critical baseline demonstrating that either infrastructure itself or solar management by mowing or grazing, rather than vegetation changes, drives arthropod decline. This finding contrasts with studies like Walston et al. (2023) that documented 20-fold increases in native bees at restored solar sites, but critically, their study lacked true controls and was designed to understand the effect of habitat restoration on arthropod abundance over time within two solar sites. Thus, Walston et al. (2023) demonstrates that habitat restoration within solar sites can indeed be effective, however our work further informs solar habitat restoration by addressing the effect of solar infrastructure itself and showing that restoration efforts need to be effective enough that they overcome the negative effect of solar infrastructure on arthropod communities. Our findings partially align with those of Jeal et al. (2019), who studied a concentrating solar power facility in South Africa and found that while total abundance and order richness of both ground dwelling and flying arthropods did not differ significantly between solar facilities and adjacent rangelands, community composition differed significantly between habitats. Similarly, Hamřík et al. (2025) documented that solar parks in Hungary provide heterogeneous habitats for winter-active ground-dwelling arthropods, though their study focused on comparing solar parks broadly to other habitat types rather than pre-installation controls. In contrast to our mostly rural grassland sites, Armstrong et al. (2021) found positive effects of ground-mounted solar arrays in urban parking lots, where vegetated solar canopies supported 40% greater arthropod abundance than non-vegetated canopies. However, this urban study compared different management strategies within solar installations

rather than comparing solar sites to true controls, and the baseline habitat (impervious parking lots) differs fundamentally from the productive grasslands in our study.

The responses among arthropod functional groups provide possible mechanistic insights. Coleoptera showed the most severe reduction (74% in flying, 71% in ground-dwelling), though the underlying mechanisms remain uncertain. Multiple factors could explain these reductions. Polarized light pollution from solar panels may trigger maladaptive behaviors in polarotactic insects, as Horváth et al. (2009) demonstrated that reflective surfaces can produce artificial polarized light signatures interfering with habitat selection and orientation. However, research on aerial electroreception in arthropods (England et al., 2025) suggest an additional mechanism. Many insects detect electric fields through electrostatic deflection of mechanosensory setae, which they use for navigation, foraging, and predator detection (Clarke et al., 2013; Sutton et al., 2016; England & Robert, 2024). Solar arrays generate and concentrate electric fields through photovoltaic conversion, potentially disrupting these natural electrical cues and creating electromagnetic "noise" that interferes with insect sensory systems. The flying arthropods showing the strongest reductions—Coleoptera and Pollinators (Hymenoptera/Lepidoptera)—are known to possess mechanosensory structures capable of electroreception, suggesting infrastructure-level sensory disruption beyond simple habitat quality changes.

Physical visual obstruction by solar infrastructure may provide an additional mechanism for reduced pollinator abundance. Flower discovery by pollinators relies heavily on visual detection at distances ranging from meters to tens of meters (Dafni et al., 2017), with detection distance determined by flower size, color contrast, and shape (Dafni et al., 2017). The evolutionary premium placed on visual conspicuousness—manifested in showy petals, bright colors, and prominent displays—reflects the critical importance of long-distance visual

detectability for plant-pollinator interactions (Borges et al., 2003). Solar panels create physical barriers that fragment visual fields and obstruct sight lines between pollinators and flowers, analogous to how buildings significantly impede pollinator movement in urban environments despite similar visitation rates to adjacent flowers (Williams et al., 2025). This visual disruption may be particularly detrimental in grasslands, where the low vegetation structure typically provides unobstructed visual access across the landscape. The arrays of vertical and tilting panels create a novel, visually complex environment more similar to forest edges or urban matrices than the open landscapes pollinators evolved to navigate. In forest understories where visibility is naturally limited, plants compensate through enhanced visual signals or alternative sensory modalities like strong fragrances (Lindh, 2005); however, the rapid anthropogenic installation of solar infrastructure provides insufficient time for such evolutionary responses in grassland plant-arthropod systems.

While the mechanisms discussed above may explain reductions in flying arthropods, the 27% reduction in ground-dwelling arthropods suggests additional or alternative drivers. Ground-dwelling arthropods are less likely to be affected by polarized light pollution or visual obstruction of flight paths, pointing toward substrate-level changes as potential mechanisms. Solar arrays in our study sites were subject to regular mowing or grazing to maintain vegetation height, potentially increasing soil compaction through repeated machinery passes or concentrated livestock activity in addition to the likely soil compacting effects of heavy machinery used for installation of solar infrastructure. Compaction can dramatically alter ground-dwelling arthropod communities; for example, Pauli et al. (2012) found that ants (Hymenoptera) were significantly more abundant in compacted agricultural soils compared to less disturbed systems. In our study, we observed a non-significant increase in ground-dwelling Hymenoptera in solar arrays, which

aligns with their association with compacted conditions and may represent one of the few arthropod groups tolerant of or favored by the altered substrate conditions beneath solar infrastructure.

Beyond infrastructure-level effects, differences in management intensity between solar sites and controls may contribute to arthropod reductions. Solar facilities in our study were mowed or grazed more frequently than control sites to maintain vegetation at appropriate heights for solar panel function and site access. This increased frequency of aboveground disturbance could directly reduce arthropod populations through mortality during disturbance events and by limiting habitat structure recovery between disturbances. The combined effects of physical disturbance, potential substrate compaction, and infrastructure-level impacts (electromagnetic interference, visual obstruction, polarized light) may act synergistically to suppress arthropod communities in solar arrays despite enhanced plant community metrics.

4.5.2 Plant Community Composition Reflects Site History and Solar Effects

The substantial increases in plant species richness, diversity, and cover across all solar positions demonstrate clear vegetation benefits, but the community composition of our paired control sites reveal how the starting point of an ecosystem that is converted to solar energy plays an important role in structuring the post conversion community. The site-specific response patterns—from dramatic compositional shifts at cropland conversion sites to minimal changes at sites with established perennial vegetation—underscore that solar development outcomes depend critically on baseline conditions. This heterogeneity in response, with seven of nine sites showing significant compositional changes, suggests that generalizations about solar impacts on vegetation must account for land use history. The persistence of pre-existing vegetation communities despite altered environmental conditions indicates that priority effects and dispersal

limitation may in some cases be stronger constraints than the abiotic changes induced by solar infrastructure.

4.5.3 Belowground Responses: Subtle Changes with Long-term Implications

The root mass and soil property patterns revealed unexpected belowground dynamics that merit attention. While no significant differences in root mass emerged between individual microclimate pairs, the trend toward reduced mass under panels ($p = 0.063$) combined with reduced plant cover suggests reduced belowground C inputs. The 2.9-fold greater root mass in shallow (0-15 cm) versus deep (15-30 cm) soil across all treatments indicates that solar installations maintain typical grassland rooting patterns despite altered surface conditions.

More concerning are the SOC and N patterns. Control areas maintained 5% higher SOC stocks and 10% higher N stocks than panel-influenced positions, despite the enhanced plant diversity and a shift toward perennial dominated communities in solar areas. Combined with 7% higher bulk density in solar areas—possibly indicating a legacy of compaction from construction—these results suggest that land use conversion to solar energy is likely to cause modest soil degradation within 5 - 8 years. Depth stratification patterns (65% more SOC in surface soils) remained consistent across treatments, indicating that solar infrastructure doesn't fundamentally alter vertical carbon distribution but may reduce overall storage capacity.

Installation of solar arrays resulted in increased soil bulk density. Increased bulk density can reduce water infiltration, limit root penetration, and alter microbial communities (Nawaz et al., 2013). These results highlight the importance of low-impact installation practices. For example, our recent research at another site suggested that installation is possible without any negative impacts on soil structure (Toy et al., 2025). The reduced SOC and nitrogen stocks in solar areas, despite greater plant diversity, suggest altered nutrient cycling that could affect long-

term site productivity. These findings contrast with modeling studies suggesting solar installations could enhance soil carbon (Moore-O'Leary et al., 2017) and highlight the importance of empirical validation.

4.5.4 Implications for Solar Development in Working Landscapes

Our findings necessitate reconsideration of how solar installations affect biodiversity in agricultural settings. While plant communities clearly benefit from reduced tillage intensity and elimination of crop monocultures, the consistent negative responses of arthropod communities reveal hidden ecological costs. The 50% reduction in pollinators has immediate implications for ecosystem services, as adjacent agricultural lands may depend on wild pollinator populations for crop production (Garibaldi et al., 2013). Similarly, reductions in predatory arthropods could compromise biological pest control, potentially increasing pesticide requirements in surrounding farmland.

The disconnect between plant and arthropod responses suggests that solar installations create novel ecosystems with altered trophic relationships. Enhanced plant resources that cannot be fully exploited by arthropod consumers may affect nutrient cycling, decomposition rates, and energy flow through food webs. These systemic changes could cascade to affect birds, small mammals, and other vertebrates dependent on arthropod prey, though such effects remain unquantified.

From a land use planning perspective, our results support strategic siting of solar installations on already-degraded lands where biodiversity baselines are low, rather than converting functional agricultural or natural areas where existing ecological communities may be disrupted. The consistent arthropod reductions across sites, despite varying baseline conditions, suggest that infrastructure impacts are relatively universal, making site selection critical for

minimizing net biodiversity loss. Importantly, we did not quantify floral resources and the potential impacts of vegetation management, such as mowing or grazing, on arthropod diversity.

4.5.5 Management Recommendations and Research Priorities

Our findings indicate that the management regimes at the sites we observed enhanced plant diversity but failed to support expected arthropod communities. This suggests that active interventions targeting infrastructure impacts, in addition to vegetation management, may be necessary. Potential strategies include installing anti-reflective strips on panels to reduce polarized light pollution (Horváth et al., 2010), creating refuge areas bordering solar sites where arthropods can establish source populations, or modifying panel spacing and orientation to minimize the footprint of deterrent effects.

The variable responses between taxa provide guidance for targeted conservation efforts. Social insects and generalists appear most resilient to solar infrastructure, suggesting management should focus on supporting vulnerable groups like solitary bees, predators, and specialists reliant on specific host plants. Habitat restoration efforts in solar arrays must be well planned out and effective in order to compensate for negative effects of solar infrastructure.

Critical research needs include identifying the specific mechanisms of arthropod deterrence to develop targeted mitigation strategies. Key questions include: To what extent is management such as mowing driving the trend compared to solar infrastructure? Is this finding unique to semi-arid systems in Colorado or do similar changes occur in other climates? What is the relative importance of polarized light, electromagnetic fields, visual disruption, and altered microclimate in deterring different arthropod groups? Do dynamic shading patterns from tracking systems affect arthropods differently than static arrays? Can arthropod communities adapt to solar infrastructure over longer timescales, or do these installations create persistent

ecological traps? Long-term studies tracking community assembly and ecosystem functioning over the 25-30 year lifespan of solar installations are essential for understanding whether early impacts attenuate or persist.

4.6 Conclusions

Our comprehensive assessment of ecological responses to solar energy development in semi-arid grasslands reveals complex trade-offs that challenge prevailing narratives about renewable energy and biodiversity co-benefits. The enhanced plant diversity coupled with diminished arthropod abundance represents an ecological surprise that highlights the importance of multi-taxa assessments in novel ecosystems. While solar installations can catalyze vegetation recovery in agricultural landscapes, they simultaneously created barriers to arthropod colonization that enhanced habitat resources did not overcome.

These findings have important implications for the sustainable expansion of solar energy infrastructure. As development accelerates to meet climate goals, our results underscore that solar installations are not ecologically neutral, even when they enhance certain metrics like plant diversity. The path toward truly sustainable solar development requires honest acknowledgment of these trade-offs, strategic siting to minimize impacts on functional ecosystems, and continued research to develop evidence-based mitigation strategies. Only through comprehensive understanding of both benefits and costs can we ensure that climate change mitigation through renewable energy does not inadvertently exacerbate the biodiversity crisis.

4.7 Tables

Table 4.1. Solar, management, and soil information for all of the sites included in the study.

Site ID	Solar Age (Years)	Location (County)	Current Management	Control Management	Irrigation Pre-Solar?	Irrigation Post Solar?	Soil Types
1	8	Boulder	Improved pasture seeding, sheep grazing	Annual Crop	Yes	No	Nunn clay loam, Wiley-Colby complex
2	8	Weld	Improved pasture seeding, mowing	Annual Crop	Yes	No	Kim loam
3	8	Weld	Native seeding, mowing	Annual Crop	No	No	Colby loam, Colby-Adena loams
4	8	Weld	Native seeding, mowing	Disturbed Land	No	No	Osgood Sand, Valent Sand
5	8	Jefferson	Native interseeding, mowing	Disturbed Land	No	No	Nunn clay loam, Renohill loam
6	7	Weld	Mowing	Disturbed Land	No	No	Altvan loam, Dacono clay loam
7	5	Boulder	Sheep Grazing	Improved Pasture	Yes	Yes	Valmont clay loam, Nunn clay loam
8	5	Larimer	Native seeding, mowing	Improved Pasture	Yes	No	Renohill clay loam, Midway clay loam
9	8	Weld	Native seeding, mowing	Native Rangeland	No	No	Valent Sand, Vona loamy sand

Table 4.2. Statistical significance of solar/microclimate, season, and site effects on aboveground variables. P-values from Type III ANOVA tests (fixed effects) and likelihood ratio tests (random effect). Models were linear mixed effects models with solar/microclimate (Control, Open, Under, East Edge, West Edge for plant community variables; Solar vs Control for arthropod variables) and season as fixed effects, and site as a random effect. All arthropod abundance values were log-transformed. Significance levels: *** p < 0.001, ** p < 0.01, * p < 0.05, . p < 0.1.

Response Variable	Solar/Microclimate	Season	Solar/Microclimate × Season	Site (Random Effect)
Total Vegetation Cover	<0.001***	0.484	0.994	<0.001***
Vegetation Species Richness	<0.001***	0.009**	0.765	<0.001***
Vegetation Shannon Diversity	<0.001***	0.052.	0.665	<0.001***
Flying Arthropod Abundance	<0.001***	0.102	0.579	<0.001***
Ground-Dwelling Arthropod Abundance	0.004**	0.022*	0.363	<0.001***

Table 4.3. Statistical significance of microclimate, depth, and site effects on belowground variables.** P-values from Type III ANOVA tests (fixed effects) and likelihood ratio tests (random effect). Models were linear mixed effects models with solar/microclimate (Control, Open, Under, East Edge, West Edge) and depth (0-15 cm, 15-30 cm) as fixed effects, and site as a random effect. Bulk density models used untransformed data; soil organic carbon used cube-root transformation; nitrogen stock and root mass used log transformation. Random effect p-values test whether including site as a random effect significantly improves model fit. Significance levels: *** p < 0.001, ** p < 0.01, * p < 0.05, . p < 0.1.

Response Variable	Solar/Microclimate	Depth	Solar/Microclimate × Depth	Site (Random Effect)
Bulk Density	<0.001***	0.006**	0.646	<0.001***
Soil Organic Carbon Stock	0.006**	<0.001***	0.735	<0.001***
Nitrogen Stock	0.025*	<0.001***	0.357	<0.001***
Root Mass	0.047*	<0.001***	0.538	<0.001***

4.8 Figures

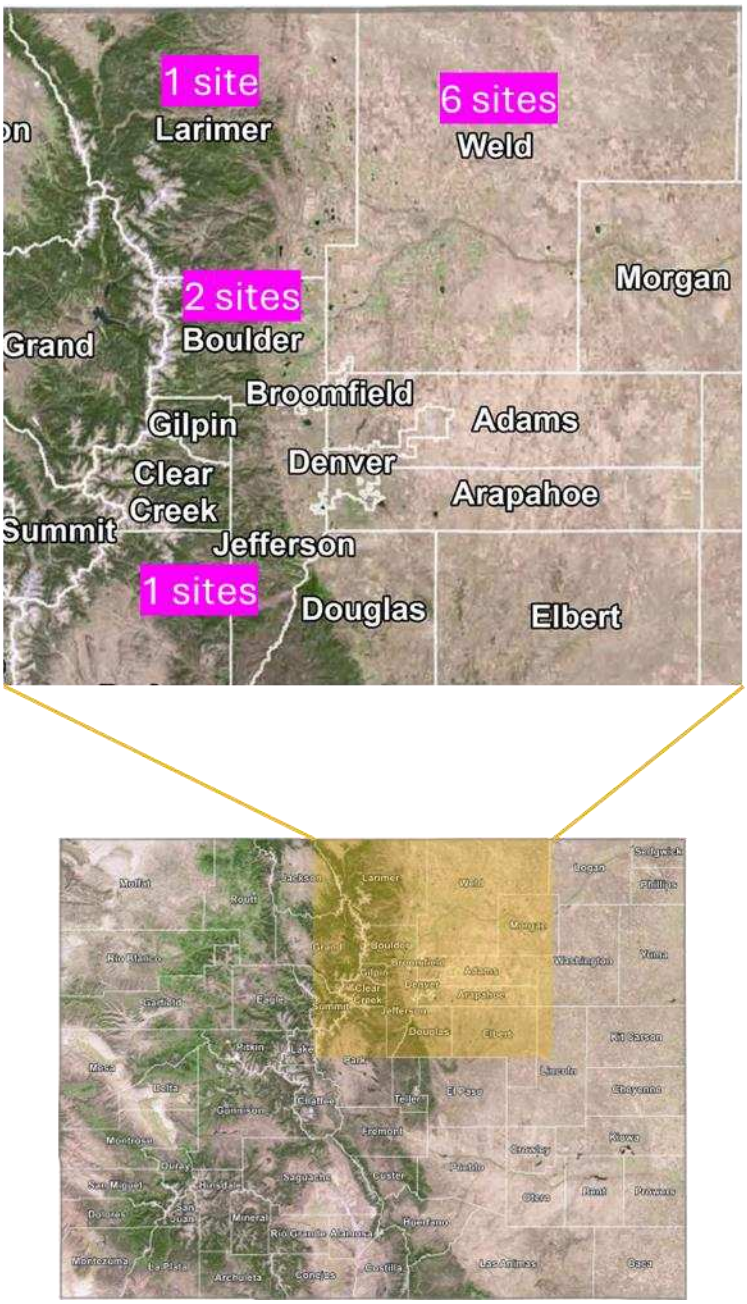

Figure 4.1. Map of Colorado, US (below) with zoomed in study map highlighting the counties where our study sites were located.

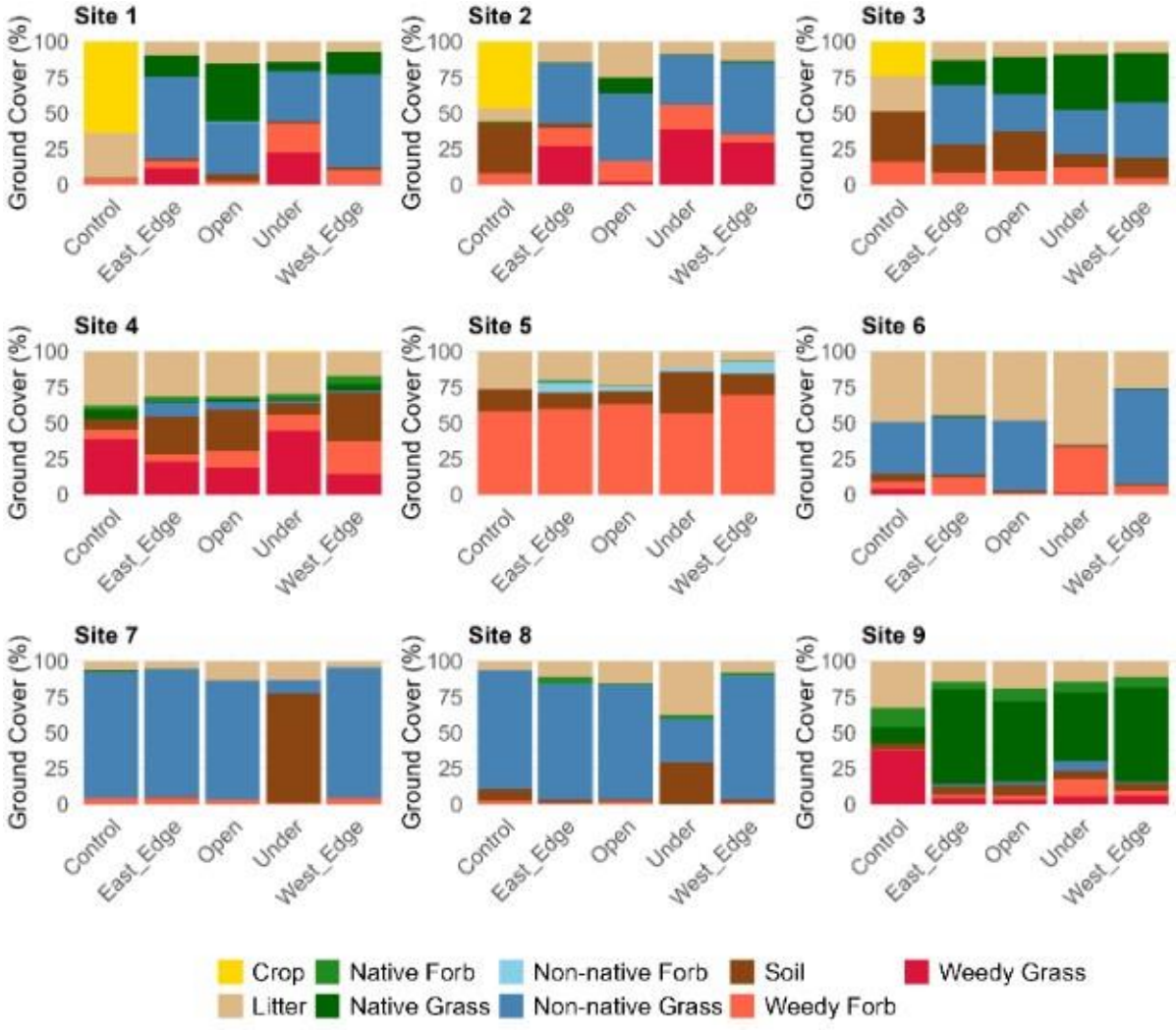

Figure 4.2. Comprehensive ground cover composition across nine agrivoltaic sites and microclimate positions. Stacked bars show mean proportional coverage (%) of functional groups including vegetation (crops, native and non-native forbs and grasses, weedy species), bare soil, and litter across 324 transects sampled in 2024. Each panel represents one site with five microclimate positions: Control (adjacent baseline proxy) and four positions within solar arrays (East Edge, Open, Under, West Edge). Functional groups were classified based on species origin (native, non-native, weed, crop) and growth form (forb, grass), with soil and litter included as non-vegetative ground cover components. Data represent comprehensive ground cover assessment where all components sum to 100% within each microclimate position.

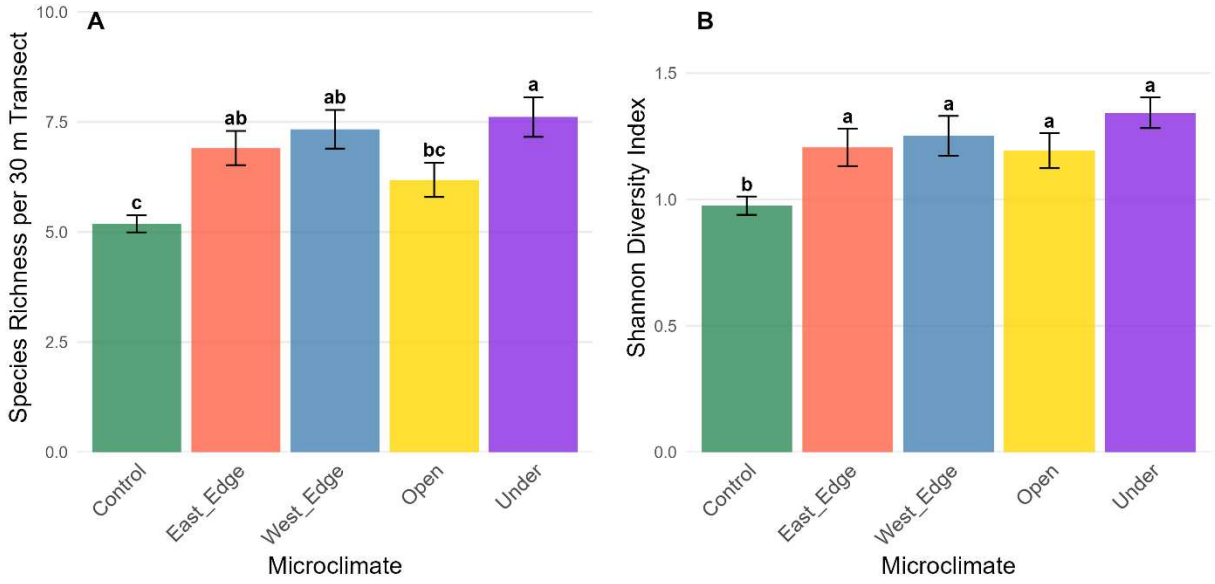

Figure 4.3. Plant diversity responses to agrivoltaic microclimate positions across nine solar installations in Colorado. (A) Species richness and (B) Shannon diversity index (mean ± SE) for control areas and four microclimate positions within solar arrays (n = 108 transects for Control; n = 54 for each solar position). Bars represent means across all sites and seasons with error bars showing standard error. Letters above bars indicate compact letter display (CLD) groups from Tukey's HSD post-hoc comparisons; means sharing the same letter are not significantly different ($\alpha = 0.05$). Mixed-effects models included microclimate and season as fixed effects with site as a random effect. Control areas represent adjacent fields used as proxies for baseline samples, while solar areas include East Edge, West Edge, Open, and Under microclimates.

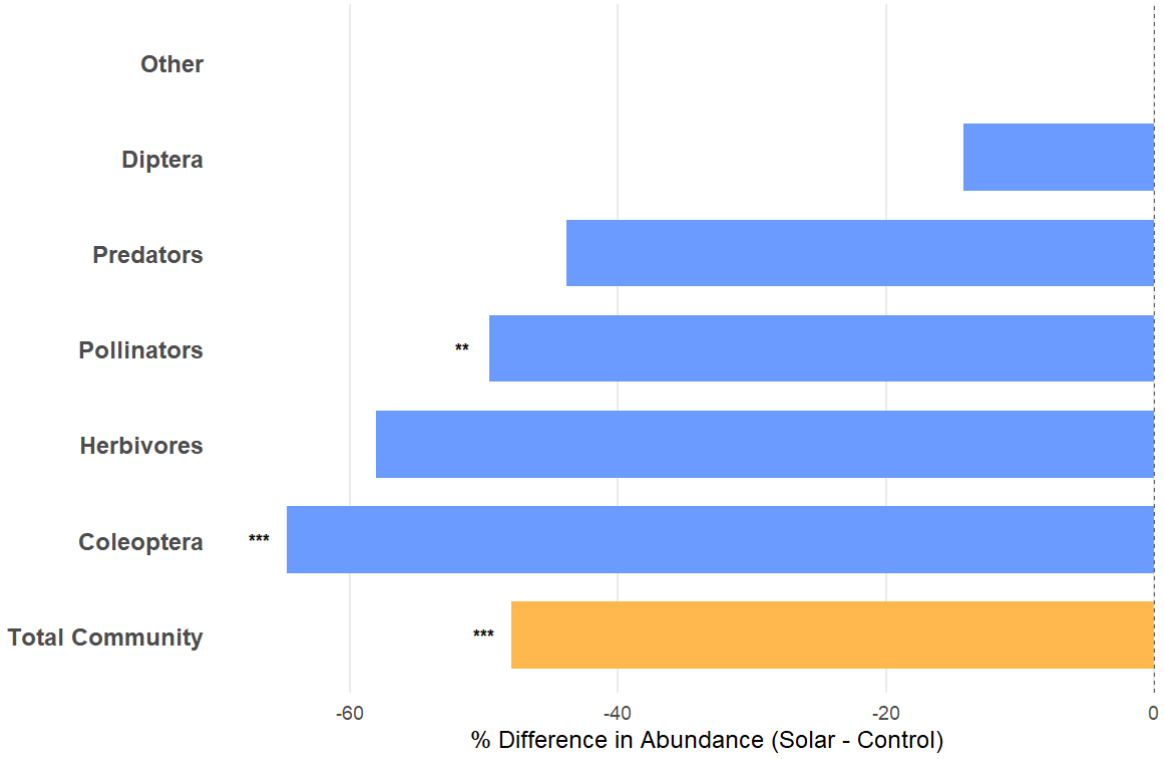

Figure 4.4. Percent difference in flying arthropod abundance between solar arrays and control areas averaged across three time points and organized by functional groups and the total community. Bars represent the measured mean percent difference calculated as (Solar - Control)/Control × 100, where negative values indicate reduced abundance in solar arrays relative to controls. Functional groups (blue bars) are ordered by effect magnitude, with the overall community response (orange bar) shown separately to distinguish between group-level and community-level analyses. Asterisks denote statistical significance based on linear mixed-effects models (*$p < 0.05$, **$p < 0.01$, ***$p < 0.001$). All functional groups showed reduced abundance in solar arrays, with Coleoptera experiencing the greatest reduction and Diptera the smallest. The total arthropod community showed a significant 48% reduction in solar arrays ($p < 0.001$), indicating consistent negative impacts across multiple taxonomic and functional levels.

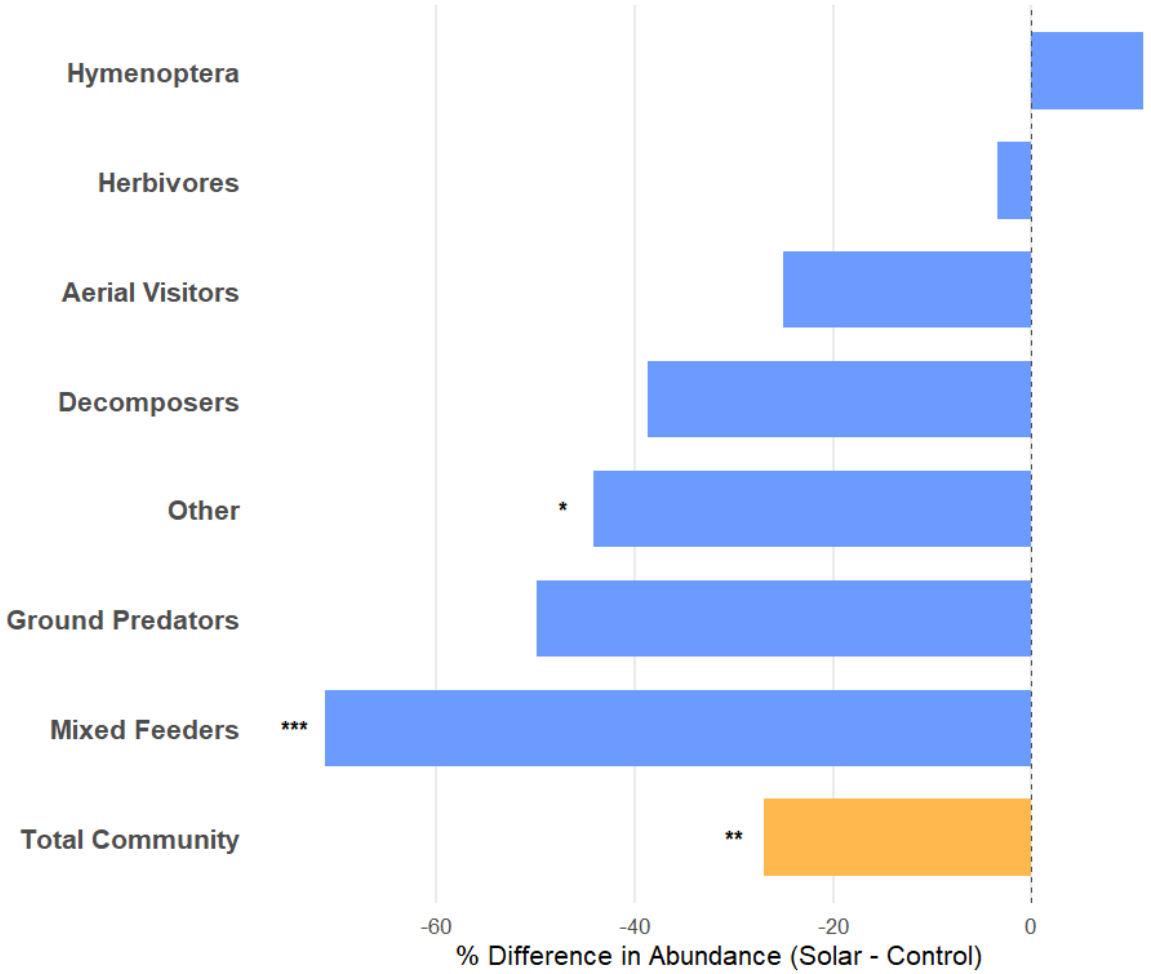

Figure 4.5. Percent difference in ground-dwelling arthropod abundance between solar arrays and control areas by functional group and the total community. Bars represent the measured mean percent difference calculated as (Solar - Control)/Control × 100, where negative values indicate reduced abundance in solar arrays relative to controls. Functional groups (blue bars) are ordered by effect magnitude, with the overall community response (orange bar) shown separately to distinguish between group-level and community-level analyses. Asterisks denote statistical significance based on linear mixed-effects models that account for site pairing and seasonal variation (*$p < 0.05$, **$p < 0.01$, **$p < 0.001$).

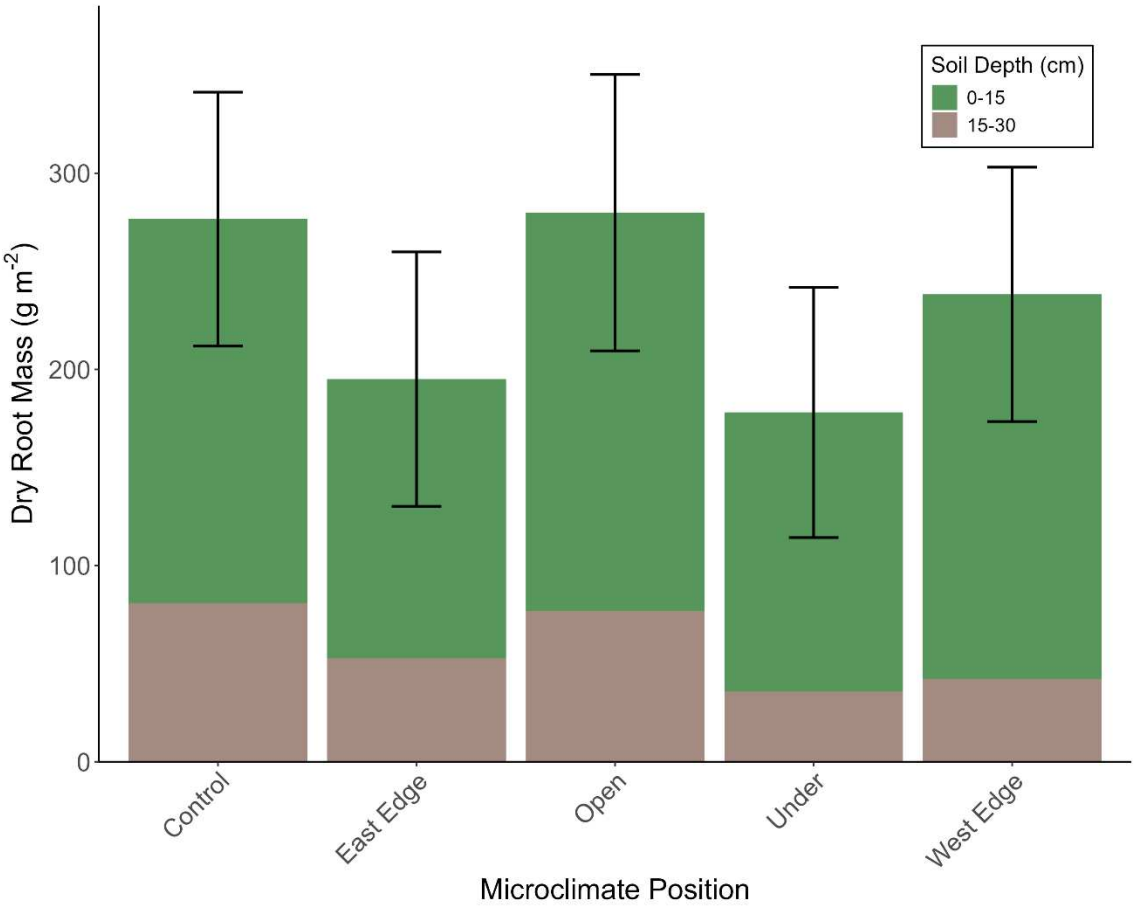

Figure 4.6. Effects of microclimate position and soil depth on dry root mass in grassland ecosystems beneath solar arrays. Showing mean root mass (± SE) for five positions relative to solar panels: Control (reference areas), Open, Under, East Edge, and West Edge (solar areas). Green bars represent shallow soils (0-15 cm) and brown bars deeper soils (15-30 cm). CLD letters were omitted because there were no significant differences between microclimates, only depths.

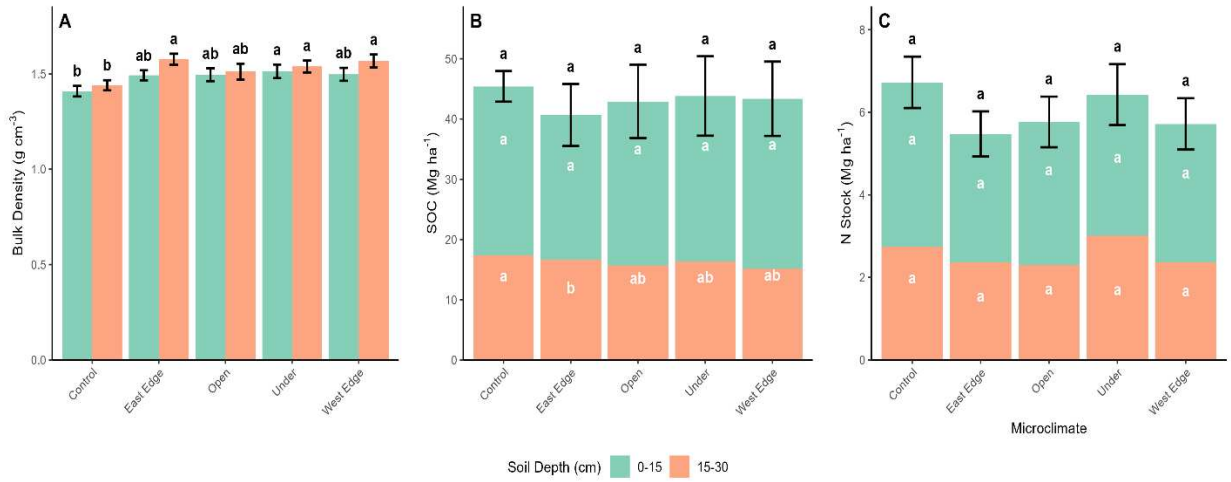

Figure 4.7. Soil properties by microclimate position and soil depth. (A) Bulk density shown as side-by-side bars for 0-15 cm (teal) and 15-30 cm (orange) depth intervals. (B) Soil organic carbon (SOC) stock and (C) nitrogen stock shown as stacked bars, where bar height represents the total stock across the 0-30 cm soil profile. Error bars represent standard error of the mean for individual depths (Panel A) or total profile stocks (Panels B and C). Compact letter displays indicate significant differences from Tukey's HSD post-hoc tests ($\alpha = 0.05$): in Panel A, black letters above bars compare microclimates within each depth; in Panels B and C, white letters within bar segments compare microclimates within each depth, while black letters above bars compare total profile stocks among microclimates. Groups sharing a letter are not significantly different. Note that bulk density (Panel A) is displayed with side-by-side bars because bulk density values at different depths are independent measurements and do not sum meaningfully, whereas SOC and N stocks (Panels B and C) are displayed as stacked bars because they represent cumulative nutrient pools across the soil profile.

LITERATURE CITED

Adeh, E. H., Selker, J. S., & Higgins, C. W. (2018). Remarkable agrivoltaic influence on soil moisture, micrometeorology and water-use efficiency. *PLOS ONE*, 13(11), e0203256.

Andersen, A. N. (2019). Responses of ant communities to disturbance: Five principles for understanding the disturbance dynamics of a globally dominant faunal group. *Journal of Animal Ecology*, 88(3), 350-362.

Armstrong, A., Ostle, N. J., & Whitaker, J. (2016). Solar park microclimate and vegetation management effects on grassland carbon cycling. *Environmental Research Letters*, 11(7), 074016.

Armstrong, J. H., Kulikowski, A. J., & Philpott, S. M. (2021). Urban renewable energy and ecosystems: integrating vegetation with ground-mounted solar arrays increases arthropod abundance of key functional groups. *Urban Ecosystems*, 24, 621-631.

Badelt, O., Sutter, L., Entling, M. H., & Albrecht, M. (2025). Mixed-habitat solar farms support three times more birds than intensive agriculture. *Bird Study*, 72(1), 45-58.

Bakker, J. D., & Wilson, S. D. (2004). Using ecological restoration to constrain biological invasion. *Journal of Applied Ecology*, 41(6), 1058-1064.

Barré, K., Baudouin, A., Froidevaux, J. S., Chartendrault, V., & Kerbiriou, C. (2024). Insectivorous bats alter their flight and feeding behaviour at ground-mounted solar farms. *Journal of Applied Ecology*, 61(2), 328-339.

Barron-Gafford, G. A., Pavao-Zuckerman, M. A., Minor, R. L., Sutter, L. F., Barnett-Moreno, I., Blackett, D. T., Thompson, M., Dimond, K., Gerlak, A. K., Nabhan, G. P., & Macknick, J. E. (2019). Agrivoltaics provide mutual benefits across the food–energy–water nexus in drylands. *Nature Sustainability*, 2(9), 848-855.

Bennun, L., van Bochove, J., Ng, C., Fletcher, C., Wilson, D., Phair, N., & Carbone, G. (2023). Existing evidence on the effects of photovoltaic panels on biodiversity: A systematic map with critical appraisal of study validity. *Environmental Evidence*, 12, 22.

Borges, R. M., Gowda, V., & Zacharias, M. (2003). Butterfly pollination and high-contrast visual signals in a low-density distylous plant. *Oecologia*, 136, 571–573.

Clarke, D., Whitney, H., Sutton, G., & Robert, D. (2013). Detection and learning of floral electric fields by bumblebees. *Science*, 340, 66–69.

Colorado Energy Office. (2023). *Colorado renewable energy outlook: Solar development projections 2030*. Colorado Energy Office, Denver, CO.

Dafni, A., Potts, S. G., Michalski, S., & Kevan, P. G. (2017). Factors determining visual detection distance to real flowers by bumble bees. *Journal of Pollination Ecology*, 20(1), 1–12.

DOE (U.S. Department of Energy). (2021). *Solar Futures Study*. Office of Energy Efficiency and Renewable Energy, Washington, DC. DOE/EE-2310.

Elamri, Y., Cheviron, B., Lopez, J. M., Dejean, C., & Belaud, G. (2018). Water budget and crop modelling for agrivoltaic systems: Application to irrigated lettuces. *Agricultural Water Management*, 208, 440-453.

England, S. J., & Robert, D. (2024). Prey can detect predators via electroreception in air. *Proceedings of the National Academy of Sciences of the United States of America*, 121, e2322674121.

England, S. J., Palmer, R. A., O'Reilly, L. J., Chenchiah, I. V., & Robert, D. (2025). Electroreception in treehoppers: How extreme morphologies can increase electrical sensitivity. *Proceedings of the National Academy of Sciences of the United States of America*, 122(30), e2505253122.

Garibaldi, L. A., Steffan-Dewenter, I., Winfree, R., Aizen, M. A., Bommarco, R., Cunningham, S. A., Kremen, C., Carvalheiro, L. G., Harder, L. D., Afik, O., & Klein, A. M. (2013). Wild pollinators enhance fruit set of crops regardless of honey bee abundance. *Science*, 339(6127), 1608-1611.

Haddad, N. M., Crutsinger, G. M., Gross, K., Haarstad, J., Knops, J. M., & Tilman, D. (2009). Plant species loss decreases arthropod diversity and shifts trophic structure. *Ecology Letters*, 12(10), 1029-1039.

Hamřík, T., Szabó, M. Z., Gallé-Szpisjak, N., Michalko, R., Tölgyesi, C., Torma, A., & Gallé, R. (2025). Solar parks provide heterogeneous habitats for winter-active ground-dwelling predatory arthropods. *Ecological Entomology*, 1-15.

Hernandez, R. R., Easter, S. B., Murphy-Mariscal, M. L., Maestre, F. T., Tavassoli, M., Allen, E. B., Barrows, C. W., Belnap, J., Ochoa-Hueso, R., Ravi, S., & Allen, M. F. (2014). Environmental impacts of utility-scale solar energy. *Renewable and Sustainable Energy Reviews*, 29, 766-779.

Horváth, G., Blahó, M., Egri, Á., Kriska, G., Seres, I., & Robertson, B. (2010). Reducing the maladaptive attractiveness of solar panels to polarotactic insects. *Conservation Biology*, 24(6), 1644-1653.

Horváth, G., Kriska, G., Malik, P., & Robertson, B. (2009). Polarized light pollution: A new kind of ecological photopollution. *Frontiers in Ecology and the Environment*, 7(6), 317-325.

IEA (International Energy Agency). (2024). *Renewables 2024: Analysis and forecast to 2029*. IEA, Paris.

IPCC (Intergovernmental Panel on Climate Change). (2014). *Climate Change 2014: Mitigation of Climate Change. Working Group III Contribution to the Fifth Assessment Report*. Cambridge University Press, Cambridge, UK.

IRENA (International Renewable Energy Agency). (2023). *Renewable capacity statistics 2023*. IRENA, Abu Dhabi.

Jeal, C., Perold, V., Seymour, C. L., Ralston-Paton, S., & Ryan, P. G. (2019). Utility-scale solar energy facilities – Effects on invertebrates in an arid environment. *Journal of Arid Environments*, 168, 1-8.

Kannenberg, S. A., Sturchio, M. A., Venturas, M. D., & Knapp, A. K. (2023). Grassland carbon-water cycling is minimally impacted by a photovoltaic array. *Communications Earth & Environment*, 4(1), 238.

Lambert, Q., Bischoff, A., Cueff, S., Cluchier, A., & Gros, R. (2021). Effects of solar parks on soil quality, microclimate, CO2 effluxes, and vegetation under a Mediterranean climate. *Land Degradation & Development*, 32(18), 5190-5202.

Lambert, Q., Gros, R., & Bischoff, A. (2022). Ecological restoration of solar park plant communities and the effect of solar panels. *Ecological Engineering*, 182, 106722.

Li, Y., Armstrong, A., Simmons, C., Krasner, N. Z., & Hernandez, R. R. (2025). Ecological impacts of single-axis photovoltaic solar energy with periodic mowing on microclimate and vegetation. *Frontiers in Sustainability*, 6, 1497256.

Lindh, B. C. (2005). Effects of conifer basal area on understory herb presence, abundance, and flowering in a second-growth Douglas-fir forest. *Canadian Journal of Forest Research*, 35(4), 938–948.

Liu, Y., Zhang, R. Q., Huang, Z., Cheng, Z., López-Vicente, M., Ma, X. R., & Wu, G. L. (2019). Solar photovoltaic panels significantly promote vegetation recovery by modifying the soil surface microhabitats in an arid sandy ecosystem. *Land Degradation & Development*, 30(18), 2177-2186.

Lovich, J. E., & Ennen, J. R. (2011). Wildlife conservation and solar energy development in the desert southwest, United States. *BioScience*, 61(12), 982-992.

Marrou, H., Guilioni, L., Dufour, L., Dupraz, C., & Wery, J. (2013). Microclimate under agrivoltaic systems: Is crop growth rate affected in the partial shade of solar panels? *Agricultural and Forest Meteorology*, 177, 117-132.

Moore-O'Leary, K. A., Hernandez, R. R., Johnston, D. S., Abella, S. R., Tanner, K. E., Swanson, A. C., Kreitler, J., & Lovich, J. E. (2017). Sustainability of utility-scale solar energy – Critical ecological concepts. *Frontiers in Ecology and the Environment*, 15(7), 385-394.

Moreira, E. F., Santos, R. L. dos, Penna, U. L., Angel-Coca, C., & Boscolo, D. (2020). Does landscape context affect pollination-related functional diversity and richness of understory

flowers in forest fragments of Atlantic Rainforest in southeastern Brazil? *Ecological Processes*, 9, 63.

Nawaz, M. F., Bourrié, G., & Trolard, F. (2013). Soil compaction impact and modelling. A review. *Agronomy for Sustainable Development*, 33(2), 291-309.

Rousseau, L., Fonte, S. J., Téllez, O., van der Hoek, R., & Lavelle, P. (2012). Soil macrofauna as indicators of soil quality and land use impacts in smallholder agroecosystems of western Nicaragua. *Ecological Indicators*, 27, 71-82.

Scherber, C., Eisenhauer, N., Weisser, W. W., Schmid, B., Voigt, W., Fischer, M., Schulze, E. D., Roscher, C., Weigelt, A., Allan, E., & Tscharntke, T. (2010). Bottom-up effects of plant diversity on multitrophic interactions in a biodiversity experiment. *Nature*, 468(7323), 553-556.

Sturchio, M. A., & Knapp, A. K. (2023). Ecovoltaic principles for a more sustainable, ecologically informed solar energy future. *Nature Ecology & Evolution*, 7(11), 1746-1749.

Sturchio, M. A., Macknick, J. E., Barron-Gafford, G. A., Chen, A., Alderfer, C., Condon, K., Hajek, O. L., Miller, B., Pauletto, B., Siggers, J. A., & Knapp, A. K. (2022). Grassland productivity responds unexpectedly to dynamic light and soil water environments induced by photovoltaic arrays. *Ecosphere*, 13(12), e4334.

Sutton, G. P., Clarke, D., Morley, E. L., & Robert, D. (2016). Mechanosensory hairs in bumblebees (*Bombus terrestris*) detect weak electric fields. *Proceedings of the National Academy of Sciences of the United States of America*, 113, 7261–7265.

Szabo, B., Szabó, A., Végvári, Z., & Barta, Z. (2024). Small-scale photovoltaic installations enhance bird diversity in Central European agricultural landscapes. *Renewable Energy*, 218, 119234.

Tinsley, E., Froidevaux, J. S., Zsebők, S., Szabadi, K. L., & Jones, G. (2023). Renewable energies and biodiversity: Impact of ground-mounted solar photovoltaic sites on bat activity. *Journal of Applied Ecology*, 60(11), 2365-2376.

Toy, C., Heider-Kuhn, N., Schipanski, M. (2025). Impact of solar energy infrastructure and ecovoltaic management on semi-arid grassland carbon cycling. *Environmental Research Communications,* 7, 105005. https://doi.org10.1088/2515-7620/ae0b1d

USDA (United States Department of Agriculture). (2023). *Land use and solar development: Agricultural impacts and opportunities*. Economic Research Service Report No. 315. USDA, Washington, DC.

Walston, L. J., Li, Y., Hartmann, H. M., Macknick, J., Hanson, A., Nootenboom, C., Lonsdorf, E., & Hellmann, J. (2022). Modeling the ecosystem services of native vegetation management practices at solar energy facilities in the Midwestern United States. *Ecosystem Services*, 56, 101456.

Walston, L. J., Hartmann, H. M., Fox, L., Macknick, J., McCall, J., Janski, J., & Jenkins, L. (2023). If you build it, will they come? Insect community responses to habitat establishment at solar energy facilities in Minnesota, USA. *Environmental Research Letters*, 19(1), 014053

Williams, N. M., Mola, J. M., Stuligross, C., Harrison, T., Page, M. L., Brennan, R. M., Roswell, M., Rundlöf, M., Saunders, M. E., Grab, H., Szendrei, Z., Albrecht, M., Guzman, L. M., Gut, L., Isaacs, R., & Blitzer, E. J. (2025). Bee-mediated pollen transport across five urban landscape features: Buildings are important barriers. *Ecology and Evolution*, 15, e70794.

CHAPTER 5: CONCLUSION

This dissertation provides comprehensive evidence that solar energy infrastructure creates novel ecosystems in semi-arid grasslands, characterized by predictable spatial heterogeneity, spatially reorganized ecosystem service provision, and unexpected decoupling between plant and arthropod community responses. Across three complementary studies examining multiple scales and ecological components within solar facilities between 0 - 8 years of age, patterns emerged that both challenge and refine our understanding of agrivoltaic system ecology.

5.1 Spatial Heterogeneity as a Driver of Ecosystem Service Provision

The most consistent finding across all studies is that single-axis tracking solar arrays create distinct microclimate zones—open areas between panels, directly beneath panels, and eastern/western edges—each with a unique combination of abiotic conditions that optimize different ecosystem services. This variance of ecosystem services within these microclimates aligns with ecosystem service bundle theory (Raudsepp-Hearne et al., 2010), demonstrating that services show non-random associations within the solar landscape. Open areas supported 2.7× more floral resources and maintained the highest aboveground productivity, functioning as pollinator resource hotspots. Conversely, under-panel areas demonstrated 25% greater surface soil carbon stocks despite 31% lower biomass production, likely through reduced decomposition rates.

This spatial complementarity within solar installations differs fundamentally from traditional agricultural systems where trade-offs often require landscape-level segregation of functions (Bennett et al., 2009). The fine-scale environmental gradients enable different services to be optimized in different zones within single fields. No individual microclimate or

management strategy optimized all services simultaneously—pasture maximized forage quality and productivity, native plantings supported 4.1-fold more floral resources, and balanced natives achieved the highest soil carbon stocks. This finding held true across all metrics examined, from carbon cycling to pollination support to forage production.

5.2 Carbon Cycling Dynamics Under Altered Environmental Conditions

The carbon cycling responses revealed complex interactions between solar infrastructure, microclimate, and precipitation variability. The Under microclimate, experiencing both the most intensive shading and effectively no direct precipitation inputs, showed the lowest above and belowground net primary productivity. However, this same microclimate maintained the highest standing root biomass and soil organic carbon stocks three years after installation, demonstrating that reduced decomposition can compensate for reduced productivity in maintaining soil carbon. Particularly notable was the altered root distribution beneath panels, with approximately 50% of root production allocated to each depth increment (0-15 cm and 15-30 cm) compared to the typical 70-30 distribution in open areas. This deeper rooting pattern, potentially enhancing subsoil carbon inputs, aligns with proposed mechanisms for enhancing soil carbon sequestration in grassland ecosystems (Kell, 2011; Lorenz & Lal, 2005). The response varied with precipitation: during the wettest year, the Open microclimate had significantly higher belowground productivity, while during the driest year, the Under microclimate showed the most severe reductions, suggesting that benefits of panel shelter are contingent on minimum water availability thresholds.

These patterns highlight the complex interplay between solar panel microclimates, precipitation variability, and grassland carbon dynamics, extending recent work suggesting minimal impacts on carbon cycling when properly designed (Kannenberg et al., 2023).

Importantly, low-impact installation methods that preserved vegetation and minimized disturbance appeared crucial for maintaining soil carbon stocks, as construction-related bulk density increases could otherwise compromise long-term carbon storage capacity.

5.3 The Paradox of Enhanced Plant Communities with Diminished Arthropod Communities

Perhaps the most unexpected and concerning finding was the consistent decoupling of plant and arthropod responses across nine solar installations. Despite 19-47% increases in plant species richness and 21-37% increases in Shannon diversity—with the strongest improvements at sites converted from crop monocultures—arthropod communities showed universal negative responses. Flying arthropod abundance decreased by 48% and ground-dwelling arthropods by 27%, with pollinators and beetles experiencing 50% and 74% reductions respectively.

This paradox cannot be explained by habitat degradation alone, as solar sites often supported more diverse perennial plant communities with higher cover than controls. The consistency across functional groups suggests infrastructure and/or management deterrent effects beyond habitat quality changes. Multiple mechanisms may contribute: polarized light pollution from panels may trigger maladaptive behaviors in polarotactic insects (Horváth et al., 2009), electromagnetic fields may disrupt electroreception used for navigation and foraging (England & Robert, 2024; Clarke et al., 2013), physical panels may obstruct visual detection of floral resources critical for pollinator foraging (Dafni et al., 2017), soil compaction may inhibit the movement of ground dwelling organisms, and disturbance from mowing or grazing may result in direct mortality in addition to reducing structural complexity of vegetation.

These findings contrast with studies documenting increased pollinator abundance at restored solar sites (Walston et al., 2023), but critically, those studies lacked proper controls. Our

paired design isolates infrastructure effects from habitat management, revealing that while habitat restoration within solar sites can increase arthropod abundance over time, it must overcome substantial negative effects of the infrastructure itself.

5.4 Vegetation Dynamics: Legacy Effects and Management Limitations

Vegetation responses were strongly mediated by pre-existing conditions and legacy effects. The dominance of non-native rhizomatous grasses (75-86% cover) across native seeding treatments demonstrates the powerful role of priority effects in constraining community assembly, consistent with restoration ecology literature showing resistance of established perennial grasses to displacement (Bakker & Wilson, 2004; Grman et al., 2013). Native species achieved only 0.1-5.8% cover despite intensive site preparation and seeding efforts.

Management interventions showed limited efficacy in overcoming these constraints. Irrigation increased aboveground productivity by 11% and forage quality by 16% but failed to enhance soil carbon stocks and actually reduced floral resources by 40%. The microclimate × irrigation interactions revealed that supplemental water only benefited the driest under-panel zones, suggesting targeted rather than blanket applications may be more effective. These findings align with semi-arid system ecology where water limitation typically constrains productivity (Sturchio & Knapp, 2023), but demonstrate that infrastructure-induced heterogeneity fundamentally alters resource limitation patterns.

5.5 Implications for Agrivoltaic Design and Management

These findings necessitate consideration of agrivoltaic systems as integrated food-energy-water (FEW) nexus interventions rather than simply renewable energy installations that happen to occur on agricultural land. In semi-arid systems where water availability mediates both food production and ecosystem functioning, our results reveal that optimizing energy infrastructure

inevitably restructures the spatial distribution and management requirements for the other two nexus components. The microclimate-specific patterns we documented—with Under areas experiencing 26-51% moisture reductions, West Edge positions concentrating water at 9-20% above ambient, and irrigation effects ranging from 43% productivity gains to 40% pollinator resource losses depending on location—demonstrate that FEW trade-offs operate at fine spatial scales within solar landscapes.

Water emerged as the key variable mediating both energy-food relationships (through infrastructure-induced productivity gradients) and energy-water relationships (through precipitation redistribution). However, the consistent 50% pollinator reduction despite enhanced plant communities reveals a critical failure in assumed FEW synergies: infrastructure designed to optimize energy production created conditions that degraded supporting services essential for landscape-scale food security, regardless of local habitat improvements. Understanding these interconnected trade-offs is essential for developing management strategies that maintain landscape functionality rather than inadvertently shifting environmental costs across nexus components.

Thus, we must reconsider agrivoltaic systems as multifunctional landscapes. Rather than viewing spatial heterogeneity as a management challenge, our results suggest embracing microclimate diversity as an organizing principle for landscape-level multifunctionality. The consistent spatial patterns across treatments indicate that panel design parameters—height, spacing, tracking systems—are likely just as important as vegetation management for determining ecosystem service outcomes.

For pollinator conservation and agricultural pest control, the 50% reduction in pollinators and substantial decreases in predatory arthropods have immediate implications for ecosystem

service provision to surrounding agricultural lands (Garibaldi et al., 2013). These impacts persisted despite improved vegetation communities at solar sites, suggesting a need for infrastructure modifications such as anti-reflective coatings to reduce polarized light pollution (Horváth et al., 2010) or design changes to minimize electromagnetic interference, depending on the primary mechanism(s) responsible for arthropod deterrence.

The superior performance of established pasture over native treatments for forage production (27% higher digestibility, 45% greater biomass, 43% higher crude protein) highlights tensions between ecological restoration goals and agricultural production. However, the spatial reorganization of forage quality—with enhanced protein beneath panels despite reduced biomass—mirrors silvopastoral systems and suggests opportunities for strategic grazing management (Jose, 2009).

5.6 Site Selection and Land Use Planning Considerations

Our results support strategic siting of solar installations based on baseline ecological conditions. The dramatic vegetation improvements at sites converted from annual crop production demonstrate clear plant biodiversity benefits when baseline conditions are poor. Conversely, sites with established perennial vegetation showed minimal change despite altered environmental conditions and interventions attempting to introduce new native species, suggesting high-quality grasslands, native and non-native, should be preserved for their existing ecological value.

The consistent arthropod reductions across all sites, regardless of baseline conditions, indicate that infrastructure impacts are relatively universal. This makes thoughtful site selection critical for minimizing net biodiversity loss at landscape scales. Priority should be given to

already-degraded lands, abandoned agricultural fields, or areas with compromised ecological function where solar development might provide net benefits through vegetation restoration.

5.7 Research Priorities and Future Directions

This dissertation identifies several critical research needs rooted in our findings. Long-term studies tracking ecosystem responses over the 25-30 year lifespan of solar installations are essential for understanding whether the patterns we observed—particularly the decoupling of plant and arthropod responses—persist or change as communities adapt. The three-year timeframe of our experimental work and 5-8 year post-installation assessments provide important baselines but cannot capture long-term trajectories.

Mechanistic studies identifying specific arthropod deterrent effects could enable targeted mitigation strategies. Understanding the relative importance of polarized light, electromagnetic fields, and visual obstruction for different taxa would inform infrastructure modifications. Further work is also necessary to more thoroughly isolate the effects of vegetation management. Similarly, research examining how different array configurations—fixed versus tracking, varying heights and row spacing—affect both the magnitude and spatial distribution of ecological impacts could identify designs minimizing trade-offs.

The role of precipitation variability in mediating solar impacts, particularly evident in our carbon cycling results, suggests climate change may alter the costs and benefits of agrivoltaic systems. Research across precipitation gradients and drought cycles would improve predictions of system performance under future climate scenarios.

5.8 Concluding Thoughts

This dissertation demonstrates that agrivoltaic systems in semi-arid grasslands create complex, novel ecosystems that neither uniformly benefit nor harm ecological functioning. Solar

infrastructure reorganizes rather than reduces ecosystem services, creating predictable spatial patterns of winners and losers across multiple trophic levels. While certain services like plant diversity and spatial heterogeneity are enhanced, others like arthropod habitat and possibly soil carbon sequestration are compromised.

The path toward responsible solar development requires honest acknowledgment of these trade-offs. The evidence does not support viewing agrivoltaic systems as perfect solutions that optimize all ecosystem services simultaneously. However, their capacity to maintain landscape-level functionality through spatial complementarity, combined with the urgent need for renewable energy deployment, suggests they remain valuable components of sustainable land-use strategies.

As we navigate the dual crises of climate change and biodiversity loss, this research provides essential evidence that renewable energy infrastructure has complex, context-dependent ecological effects requiring careful consideration in planning and policy. The transition to renewable energy is necessary and inevitable; our responsibility is ensuring it occurs in ways that minimize ecological harm while recognizing and working within the constraints that solar infrastructure imposes on ecosystem functioning. Only through continued research, adaptive management, and realistic expectations can agrivoltaic systems contribute to both climate mitigation and ecological sustainability in our rapidly changing world.

LITERATURE CITED

Bakker, J. D., & Wilson, S. D. (2004). Using ecological restoration to constrain biological invasion. Journal of Applied Ecology, 41(6), 1058–1064.

Bennett, E. M., Peterson, G. D., & Gordon, L. J. (2009). Understanding relationships among multiple ecosystem services. Ecology Letters, 12(12), 1394–1404.

Clarke, D., Whitney, H., Sutton, G., & Robert, D. (2013). Detection and learning of floral electric fields by bumblebees. Science, 340, 66–69.

Dafni, A., Potts, S. G., Michalski, S., & Kevan, P. G. (2017). Factors determining visual detection distance to real flowers by bumble bees. Journal of Pollination Ecology, 20(1), 1–12.

England, S. J., & Robert, D. (2024). Prey can detect predators via electroreception in air. Proceedings of the National Academy of Sciences of the United States of America, 121, e2322674121.

Garibaldi, L. A., Steffan-Dewenter, I., Winfree, R., Aizen, M. A., Bommarco, R., Cunningham, S. A., Kremen, C., Carvalheiro, L. G., Harder, L. D., Afik, O., & Klein, A. M. (2013). Wild pollinators enhance fruit set of crops regardless of honey bee abundance. Science, 339(6127), 1608–1611.

Grman, E., Bassett, T., & Brudvig, L. A. (2013). Confronting contingency in restoration: Management and site history determine outcomes of assembling prairies, but site characteristics and landscape context have little effect. Journal of Applied Ecology, 50(5), 1234–1243.

Horváth, G., Blahó, M., Egri, Á., Kriska, G., Seres, I., & Robertson, B. (2010). Reducing the maladaptive attractiveness of solar panels to polarotactic insects. Conservation Biology, 24(6), 1644–1653.

Horváth, G., Kriska, G., Malik, P., & Robertson, B. (2009). Polarized light pollution: A new kind of ecological photopollution. Frontiers in Ecology and the Environment, 7(6), 317–325.

Jose, S. (2009). Agroforestry for ecosystem services and environmental benefits: An overview. Agroforestry Systems, 76(1), 1–10.

Kannenberg, S. A., Sturchio, M. A., Venturas, M. D., & Knapp, A. K. (2023). Grassland carbon-water cycling is minimally impacted by a photovoltaic array. Communications Earth & Environment, 4(1), 238.

Kell, D. B. (2011). Breeding crop plants with deep roots: their role in sustainable carbon, nutrient and water sequestration. Annals of Botany, 108(3), 407–418.

Lorenz, K., & Lal, R. (2005). The Depth Distribution of Soil Organic Carbon in Relation to Land Use and Management and the Potential of Carbon Sequestration in Subsoil Horizons. Advances in Agronomy, 88, 35–66.

Raudsepp-Hearne, C., Peterson, G. D., & Bennett, E. M. (2010). Ecosystem service bundles for analyzing tradeoffs in diverse landscapes. Proceedings of the National Academy of Sciences, 107(11), 5242–5247.

Sturchio, M. A., & Knapp, A. K. (2023). Ecovoltaic principles for a more sustainable, ecologically informed solar energy future. Nature Ecology & Evolution, 7(11), 1746–1749.

Walston, L. J., Hartmann, H. M., Fox, L., Macknick, J., McCall, J., Janski, J., & Jenkins, L. (2023). If you build it, will they come? Insect community responses to habitat establishment at solar energy facilities in Minnesota, USA. Environmental Research Letters, 19(1), 014053.